De Novo Design of Bioactive Protein Switches, and Applications Thereof

Robert Andrew Langan

A dissertation

submitted in partial fulfillment of the

requirements for the degree of

Doctor of Philosophy

University of Washington

2019

Reading Committee:

David Baker, Chair

Justin Kollman

Jesse Zalatan

Program Authorized to Offer Degree:

Biochemistry

University of Washington

Abstract

De Novo Design of Bioactive Protein Switches, and Applications Thereof

Robert Andrew Langan

Chair of the Supervisory Committee:
David Baker
Department of Biochemistry

Allosteric regulation of protein function is widespread in biology, but challenging for *de novo* protein design as it requires explicit design of multiple states with comparable free energies. We explore the possibility of *de novo* designing switchable protein systems through modulation of competing inter and intra-molecular interactions. We design a static, five-helix "Cage" with a single interface that can interact either intra-molecularly with a terminal "Latch" helix or inter-molecularly with a peptide "Key". Encoded on the Latch are functional motifs for binding, degradation, or nuclear export that function only when the Key displaces the Latch from the Cage. We describe orthogonal Cage-Key systems that function in vitro, in yeast and in mammalian cells with up to 300-fold activation of function by Key. The design of switchable protein function controlled by induced conformational change is a milestone for *de novo* protein design and opens up new avenues for synthetic biology and cellular engineering.

TABLE OF CONTENTS

LIST OF FIGURES

LIST OF TABLES

ACKNOWLEDGEMENTS

Nothing in the world operates in a vacuum. Scientific progress is no different. Although working on academic projects can feel isolating, it is undeniable the affect that friends, family, and coworkers have on the progress we have made as a scientific community.

I am fortunate to have entered the University of Washington in 2014 with an astounding group of fellow graduate students in the Biochemistry and BPSD (Biological Physics, Structure, and Design) programs. Thank you in particular to Domnita Rusnac, Eleanor Vane, Lexi Walls, Rachel Hutto, Gülsima Usluer for all the comradery throughout my graduate school work. Together, we've been through happy hours after classes and commiserating over starting thesis work in the second year to celebrating papers published and major milestones. I can truly say I could not have completed my graduate work without you. It's truly special to find a group of friends that support you unconditionally in the good times and the bad. You are and will forever be my best friends. In addition, Sean Gillespie, Sean Gagnon, and Sami Naboulsi I consider as part of our graduate school cohort as they've been just as vital in keeping me sane throughout the pandemonium. And thanks to the rest of my cohort for support in our first year and continued comradery: Andrew Borst, Rose King, Tamuka Chidyausiku, Audrey Davis, Christina Faller, and Robin Kirkpatrick.

The Baker Lab is an incredibly special place to do research, and I am grateful for the amazing scientists that I've been able to work with. First, David Baker has cultivated an extremely collaborative research environment and did a great job ensuring my project was going in the right direction and teaching me how to think about problems in protein engineering. Second, my close mentor and good friend Scott Boyken. Scott guided my day to day research and was a fantastic mentor. Not only is he a spectacular scientist in his own right, but he was instrumental in guiding my PhD research in the direction it went. As one of the co-creators of LOCKR I am looking forward to working with him in the future. In addition, I want to specifically mention Marc Lajoie for his work on advancing LOCKR and also serving as a role model for how to do good science. A special shout out to Team LOCKR (Ryan Kibler, Nick Woodall, Jilliane Bruffey, and Alfredo Quijano Rubio) and Team Helical Bundle (Zibo Chen, Sherry Bermeo, Basile Wicky, Ajasja, and Tim Huddy) for day to day advice and moral support. I cannot list every single member of the lab for their help and support, but I want to specifically

thank Jorge Fallas for being one of my best friends and for many nights at Madison Pub talking life and science. I also need to thank the following from the IPD for their friendship and support: George Ueda, Cameron Chow, Anindya Roy, Karla-Luise Herpoldt, Michelle Masunaga, Benja Basanta, Ian Haydon, Brooke Fiala, Lauren Carter, Matt Bick, Brian Weitzner, Nihal Korkmaz, and everyone else in the Baker Lab, King Lab, and IPD.

To bring home the point that science does not happen in a vacuum, I would like to thank my scientific collaborators and the support structure at UW that has supported this work. First, Hana El-Samad and her lab at UCSF was helpful for testing degronLOCKR in cells. Andrew Ng was a great collaborator and I'm happy to have him as a co-first author on the seminal LOCKR paper – as well as his coworkers Alex Westbrook, Galen Dods, and Taylor Nguyen . In addition, I'd like to thank John Dueber and Jen Samson for testing my LOCKR designs in cells. My committee has helped me develop this project over the past three years and I'd like to thank Frank DiMaio, Phil Bradley, Justin Kollman, Mike Regnier, and Jesse Zalatan for their input. Thanks to Jesse and his lab as well (Robin Kirkpatrick and Kieran Lewis) for collaborating on using LOCKR in yeast for genetic modifications. Finally, I'd like to thank Erin Kirchner and the BPSD Program for their organization and support through my time here at UW. Honestly, a lot of science would not happen without Erin behind the scenes making sure the grad students get their ducks in a row.

Apart from all the scientific support and collaboration I've encountered during my graduate career, I'd like to thank my support structures in the city of Seattle. Specifically, the Seattle queer community has been extremely supportive and has allowed me an outlet separate from my work life. I'd like to thank Alex Porter for supporting me through parts of my graduate career and helping me develop a perspective for technology development. The friends I've met through UW queer grad student groups and around the city have also been incredibly helpful in keeping me sane through the past five years: Aaron Vetter, Albert Chae, Grant Dailey, Dean Allsopp, Earnest Watts, and Dayne Kirk Cunard. I would be remiss to not mention Jorge Fallas and Cameron Chow again, for not only being my best friends as coworkers but also as fellow members of the queer community (along with Anindya Roy and other queer members of the IPD).

Finally, none of this would be even possible without the support of my family for the past 27 years. Cathi Langan and Jeff Langan raised me and my brother, Jeff, as a critical thinker, to ask

questions, and with compassion. They are both brilliant people themselves and acted as role models for creative thinking and scientific inquiry. Without them, not only would I not exist, but I would not have grown into my love for science, developed creative, critical, thought processes, nor had the support to move 3000 miles from home for graduate school.

To everyone listed above, I send my most sincere gratitude.

DEDICATION

I dedicate this work to queer and questioning youth interested in studying a STEM field, but feel excluded due to their gender identity or sexuality.

Representation matters.

It gets better.

INTRODUCTION

There has been considerable progress in the *de novo* design of stable protein structures based on the principle that proteins fold to their lowest free energy state. These efforts have focused on maximizing the free energy gap between the desired folded structure and all other structures, and have resulted in a wide range of stable proteins which exclusively populate the designed state[1–4]. Designing proteins that can switch conformations is more challenging, as multiple states must have sufficiently low free energies to be populated relative to the unfolded state, and the free energy differences between the states must be small enough that the state occupancies can be toggled by an external input[5,6]. Recent advances in designing systems with multiple states include a transmembrane ion transporter[7] and Gβ1 variants that dynamically exchange between two related conformations[8]; however, a method for the *de novo* design of a modular, tunable protein system that switches conformational state in the presence of an external input has not yet been achieved.

We set out to design *de novo* switchable protein systems guided by the following general considerations. First, programming free energy differences between two states is more straightforward in a system governed by inter- and intra-molecular competition at the same site rather than allosteric activation at distant sites[9–11] because many of the individual interactions can be similar if not identical, leading to cancellation of errors. This is because a change in the design will impact both states similarly, allowing more predictable design principles. Second, a stable protein framework with an extended binding surface available for the competing interactions is more programmable and less likely to engage in off-target interactions than a framework that only becomes ordered upon binding[12,13]. These features are described by the abstract system depicted in Figure 1a, which undergoes thermodynamically-driven switching between a binding competent and a binding incompetent state. A Latch (blue) contains a peptide sequence (orange) that can bind a Target (yellow) unless blocked by intramolecular interactions to a Cage (cyan); a Key (green) that binds more tightly to the Cage outcompetes the Latch, allowing the peptide to bind the Target. The behavior of such a system is governed by the binding equilibrium constants for the individual subreactions (Figure 1a): K_{open}, the dissociation of Latch from Cage; K_{LT}, the binding of Latch to Target; and K_{CK}, the binding of Key to

Cage. Solving this set of equations (Figure 1b; Appendix A) shows that when the Latch-Cage interaction is too weak (red and orange curves), the system binds Target in the presence of little to no Key and the fold induction by Key is low, while when the Latch-Cage interaction is too strong (purple curve), the system only partially binds Target even at high Key concentrations. The Latch-Cage interaction affinity that gives optimal switching (Figure 1b, blue curve *left*, green curve *right*) is a function of the Latch-Target binding affinity. We used this model to guide design of switchable, functional, protein systems.

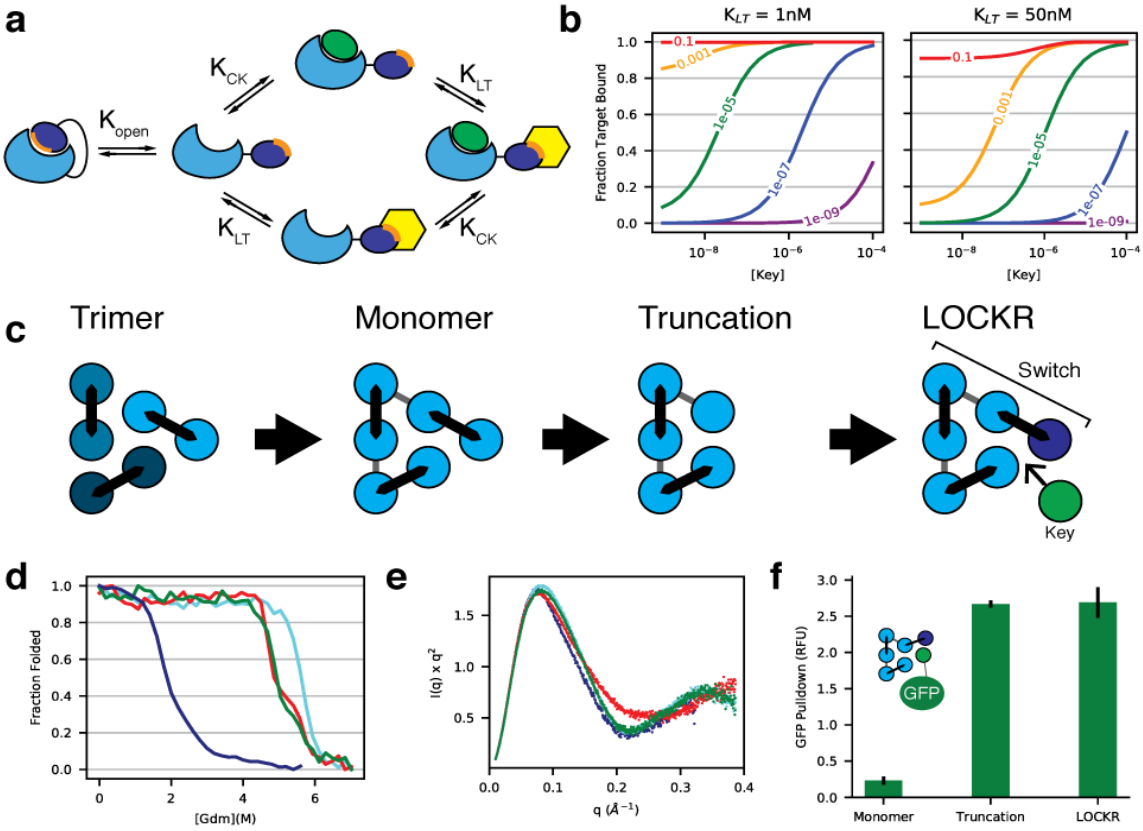

Figure 1 - Design of the LOCKR Switchable System

a, Design concept. The Switch, composed of a Cage (cyan) and Latch (blue), is in equilibrium between open and closed states. Binding of Key (green) stabilizes the open state, promoting binding of Latch to Target (yellow). b, Solutions of the model in (a) for different values of K_{LT} and K_{open} (indicated on binding curves) with K_{CK} fixed at 1 nM. c, Conversion of homotrimer 5L6HC3 to monomeric five- and six-helix frameworks by loop closure. In LOCKR (right), the double mutant V217S/I232S reduces binding affinity of Latch for Cage, allowing it to be displaced by Key. d, Guanidinium chloride denaturation of trimer (dark blue), monomer (cyan), truncated five-helix framework (red), and LOCKR (green) monitoring mean residue ellipticity (MRE) at 222 nm. e, Small-angle x-ray scattering (SAXS) Kratky plots for the monomeric frameworks are similar to that of the input trimer, with the greatest deviation for the five-helix framework. Colors continued from (d). f, Key binds to the truncation and LOCKR (V217S/I232S), but not the six-helix monomer. Free GFP-Key was added to monomeric frameworks immobilized onto a plate via a hexahistidine tag; after washing, binding was measured by GFP fluorescence (n=3, error bars indicate standard deviation).

[1] DEVELOPMENT OF A *DE NOVO* PROTEIN SWITCH

LOCKR DESIGN

To physically implement the switchable system of Figure 1a, we chose structural features amenable to tuning the affinities of the Cage-Latch and Cage-Key interactions over a wide dynamic range. Alpha helices have advantages over beta strands in that inter-helical interfaces are dominated by sidechain-sidechain interactions, which can be more readily tuned than the backbone hydrogen bonding interactions between beta strands[14]. To allow fine control over the specificity and relative affinities of the Cage-Latch and Cage-Key interactions, we chose to design interfaces containing buried hydrogen bond networks. As illustrated by Watson-Crick base pairing, considerable alterations of specificity can be obtained with relatively minor changes in the positions of hydrogen bond donors and acceptors[15]. We selected as a starting point a designed homo-trimer of -helical hairpins with hydrogen bond network-mediated subunit-subunit interaction specificity (5L6HC3_1[15]; PDB ID: 5IZS). By designing short unstructured loops connecting the subunits, we generated monomeric protein frameworks with five or six helices and 40 residues per helix (Figure 1c). In the five-helix framework, there is an open binding site for a sixth helix added in trans, whereas this site is filled by a sixth helix in cis in the six-helix framework.

The five helix (Cage) and six helix (Cage plus Latch) designs were soluble when recombinantly expressed in *E. coli*; the purified proteins were largely monomeric by size-exclusion chromatography (Extended Data 1), and very stable, remaining folded up to 5 M guanidine hydrochloride (Figure 1d). Small-angle x-ray scattering (SAXS) spectra of the connected designs are similar to that of the starting trimer and indicative of a well folded protein[16] (Figure 1e, Table 1; the greater deviations for the five helix design likely reflects the loss of a helix), suggesting that the structure is not altered by the loops. The five-helix framework, but not the six-helix framework, binds to the sixth helix fused to GFP in a pull-down assay (Figure 1f); the latter result is expected since if the interfaces are otherwise identical and the connecting linker unstrained, the intramolecular interaction should outcompete its intermolecular counterpart because of the reduced entropic cost of formation of intramolecular interactions. To enable the Key to outcompete the Latch, we tuned K_{open} by incorporating

mutations in the Latch that weaken its interaction with the Cage: large hydrophobics to alanine or serine, and alanine residues to larger hydrophobics or serine[17–19]. A Cage-Latch framework with two mutations in the Latch, V223S and I238S, bound Key nearly as strongly as the five-helix Cage without the Latch (Figure 1f, Extended Data 2); the two serines likely weaken the Cage-Latch interaction by decreasing the helical propensity of the Latch and increasing the cost of desolvating the Latch when it binds the Cage. In the absence of the Key, the Latch is bound to the Cage as in the original monomer (their SAXS spectra are nearly identical and closely match those of the design models; Figure 1e, Extended Data 1), but the guanidine hydrochloride denaturation midpoint and $\Delta G_{folding}$ are more similar to the truncated five helix design indicating the mutations are destabilizing (Figure 1d,e; Extended Data 1). We call such Cage-Latch frameworks switches, and the Switch-Key pair LOCKR for Latching Orthogonal Cage-Key pRoteins for the remainder of this dissertation.

[2] DESIGNING BIOACTIVE PROTEIN SWITCHES

The ability to design function into *de novo* switches is the main utility of the LOCKR platform. Shown in Chapter 1, we have designed a prototypical Cage:Key system illustrating that there is a combination of parameters K_{open} and K_{CK} where the Switch remains well folded (i.e. closed) but still able to bind Key. Here, I describe methods for designing generic functional sequence into LOCKR-type switches and several instances of such. We are able to successfully control protein-protein interactions, protein degradation, protein localization, and various short peptides of use in biotechnology.

INITIAL DESIGN METHODS

Models of functional LOCKRs were made by grafting bioactive sequences (candidates below) onto the latch. This design was performed using RosettaScripts with the input file `thread_relax.xml` (See Code Availability). A bash script, `thread_switch.sh` (See Code Availability), applied the design XML at every helical register on the latch by passing script variables, sequence and threading position, into the XML. The protocol uses two Rosetta movers, SimpleThreadingMover to change the amino acid sequence on the latch, and FastRelax with default settings to find the lowest energy structure given the mutations from the previous mover. Designs were selected by eye in PyMol 2.0 along with the following quantitative criteria. High quality grafts had important binding residues interacting with the cage and occluded the target as determined by crystal structure, if available (PDB ID: 2VM6 for Bim:Bcl2). As a secondary consideration, good designs minimized the number of buried unsatisfied hydrogen bonding residues. In limited cases for caging the cODC degron in orthogonal LOCKR switches, a designed hydrogen bonding network residue was opted for over a functional residue at the first or last residue to maintain the integrity of the hydrogen bond patterning, which impacts K_{open} if that hydrogen bond is satisfied or not.

LOCKR INDUCIBLE BIM-BCL2 BINDING

To install function into the initial LOCKR design, we selected the Bim-Bcl2 interaction central to apoptosis as a model system, and sought to cage Bim such that binding to Bcl2 only occurred

in the presence of Key. We chose to incorporate two Bim-related sequences into the switch: the eight Bim residues which interact with Bcl2[20] and a peptide from a larger designed Bcl2 binding protein[21], to explore the effect of changes in K_{open} and K_{LT} (the two embedded sequences make different interactions with the Cage and bind Bcl2 with different affinities). The two sequences were embedded in the Latch by sampling different helical registers such that residues involved in binding to Bcl2 are sequestered in the Cage-Latch interface (Extended Data 3), optimizing for the burial of hydrophobic residues and surface exposure of polar residues. These initial designs either bound Bcl2 in the absence of Key, or were not inducible (Extended Data 4). The range of accessible K_{open} and K_{CK} values were evidently not matched to K_{LT} as the Key induced response was far from the ideal curves in Figure 1b.

We reasoned that a wider range of K_{open} and K_{CK} values could be accessed by lengthening the helices in the Cage to provide more accessible interaction surface area. Extending the Cage:Latch interface could then increase the interaction affinity[18] (decrease K_{open}) to make the system more "off" in absence of Key, and extending the Key to increase affinity for the Cage could allow it to better outcompete the Latch once K_{open} is appropriately tuned (decrease K_{CK} relative to K_{open}), making the system more inducible. Taking advantage of the modular nature of *de novo* parametric helical bundles[2,22,23], the Cage, Latch and Key were each extended by 5, 9 or 18 residues. To enable the Key to outcompete the Latch, the latter was truncated by four to nine residues to generate a range of K_{open} values (Extended Data 4; this creates a "toehold" on the Cage that contributes to binding of the Key but not Latch, enabling the former to outcompete the latter). Both the full length Bim containing Latch and the truncated versions were fully off in the absence of Key (no binding to Bcl2 was observed, left bars in Figure 2b). The most strongly inducible binding (Figure 2b, right bar in right panel) was observed with the system with 18-residue extensions of the Cage and the Key, and a 9-residue shorter Latch that leaves an exposed 9-residue toehold on the Cage (the Key does not interact directly with Bcl2 (Extended Data 4) meaning signal shown is from Switch activation alone). This extended design with toehold exhibits an approximately 40-fold activation on addition of Key in biolayer interferometry experiments (Figure 2c), comparable to or better than many naturally occurring protein interaction induced switches[24–26].

According to the model in Figure 1a, the range of Key concentrations over which BimLOCKR is activated should be controllable by tuning K_{CK} by altering the length of the Key. A lower

affinity of Key for Cage (higher K_{CK}) requires that more Key must be added for activation to occur. Biolayer interferometry experiments in which different length Keys were titrated against fixed concentrations of Bcl2 and BimSwitch demonstrate that the LOCKR system can indeed be tuned in this way (Figure 2d). With Bcl2 present on the sensor tip, and BimSwitch at 250 nM, no binding to the sensor was observed in the absence of Key. As Keys of different length were titrated into the solution (Key concentration on x axis), BimSwitch activated and bound to Bcl2 on the sensor (binding signal on y axis). The concentration at which activation occurred differs dramatically for the different length Keys: a 40 residue Key provided no activation (pale green), a 45 residue Key activated with an EC_{50} of 230 +/- 58 nM (green), and the full length 58 residue Key activated with an EC_{50} of 27.0 +/- 2.8 nM (dark green, Figure 2c,d). As expected from the model in Figure 1a, the equilibria involved in activation are indeed sensitive to small changes in binding free energy (Figure 2d).

To examine the function of BimLOCKR over a range of K_{LT} , we

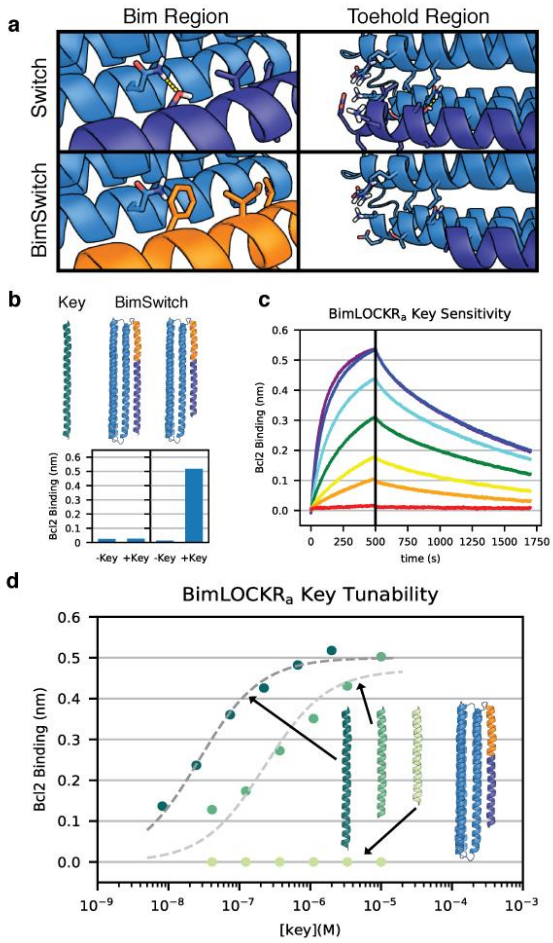

Figure 2 - BimLOCKR Design and Activation

a, Following incorporation of the BIM peptide into the LOCKR Latch, the Latch-Cage binding free energy was reduced by introducing sub-optimal interactions (left, removal of a buried hydrogen bond) and by truncating the Latch, leaving exposed hydrophobic residues in the Cage available for Key binding (right). **b,** Bio-layer interferometry measurement of BimLOCKR (250 nM) binding to immobilized BCL2 in the presence and absence of 5 µM key. In the lengthened BimLOCKR constructs, Bim is tightly caged in the absence of Key; introduction of the toehold (right) allows key to outcompete latch leading to activation of switch and BCL2 binding. **c,** Bio-layer interferometry measurement of kinetics of key-dependent binding of BimLOCKR to Bcl2. Purple is 3 µM Key, then a three fold dilution of the Key through blue, cyan, green, yellow, and orange; BimLOCKR is at 250 nM in all cases. Red line is 250 nM BimLOCKR without Key. with 250 nM BimLOCKR. **d,** Bcl2 binding by BimLOCKR as a function of key concentration. Bio-layer interferometry association traces similar to those on the left in panel c for the different length Keys were fit to obtain predicted equilibrium sensor responses (y-axis in d).

studied Key induced binding to Bcl2 and its homologs BclB and Bak, which bind Bim with K_ds of 0.17 nM (Bcl2)[21], 20 nM (BclB)[21], and 500 nM (Bak; Extended Data 7). Bio-layer interferometry experiments were performed with different Bcl2 homologs immobilized on the tip, and BimLOCKR with and without Key in solution. Consistent with the Figure 1a model, activation of BclB binding requires higher Key concentrations than activation of Bcl2 binding while Bak does not activate in this range of Key concentrations. The formal symmetry of the Figure 1a model with regard to Key and Target is observed experimentally: when the Key is immobilized on the tip, binding of the switch to the tip is activated by addition of Target just as binding of the Switch to Target is activated by addition of Key (Extended data 5).

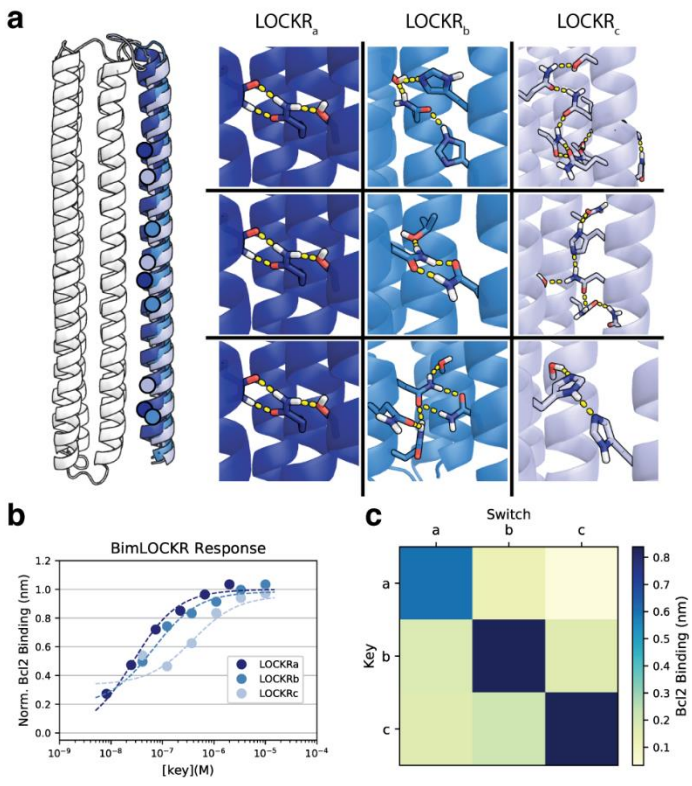

Figure 3 - Design and validation of orthogonal BimLOCKR

a, Left: LOCKR in cartoon representation. Cage in white with three different Latches and hydrogen bond networks marked by colored circles. Right: Design models of hydrogen-bond networks across the orthogonal LOCKR interfaces corresponding to the colored circles on the left. **b,** Binding of different BimSwitch designs to Bcl2 in response to cognate Key, measured by biolayer interferometry (Octet) and normalized to the computed R_{max}. **c,** Binding response to Bcl2 from biolayer interferometry experiments for each switch at 250 nM against each Key at 5 μM; average of two replicates.

To enable independent caging and specific unlocking of different protein functions in the same compartment, we next sought to create orthogonal Switch-Key pairs by incorporating different hydrogen bond networks at the Cage-Latch/Key interface. Alternative backbone conformations for the Latch/Key helix were generated by parametrically sampling the distance from the center of the bundle, helical phase, and z-offset relative to the five helix Cage. New hydrogen bond networks were designed using HBNet[15] to span the interface between the new sixth helix and the five helix Cage with all buried polar atoms participating in hydrogen bonds; the remaining

interface around the networks was subjected to full sequence and sidechain rotamer optimization using Rosetta design[27,28]. Five well-packed and sequence-dissimilar designs with all buried polar atoms participating in hydrogen bonds (Extended Data 6,7; Appendix A) were selected for Bim switch assays. BimLOCKR$_b$ and BimLOCKR$_c$ show 22-fold and 8-fold activation with their cognate Keys and a nine residue toehold on the Latch (Figure 3a,b). The three LOCKR systems are orthogonal: each switch is activated only by its cognate Key at concentrations up to 5 μM (Figure 3c), illustrating the power and consistency (3 of 6 designs were successful) of the buried hydrogen bond network approach to achieving specificity.

LOCKR INDUCIBLE PROTEIN DEGRADATION

To assess the functionality of LOCKR in live cells, we next chose to cage the cODC degron, a ubiquitin-independent degradation signal from the C-terminus of murine ornithine decarboxylase[29], with the goal of making degradation of the switch, and any protein fused to it, inducible by Key. The caging strategy employed for Bim was used to embed three variants of cODC into Switch$_a$: the wild-type sequence, wild-type with a proline removed (since proline destabilizes alpha helices), and the dipeptide sequence CA, believed to be the minimal functional residues of the degron (Extended Data 8). We tested each switch variant in budding yeast *S. cerevisiae*, using a dual inducible system[30] to independently titrate the concentration of the switch with a yellow fluorescent protein (YFP) N-terminal fusion and the Key with a blue fluorescent protein (BFP) C-terminal fusion (Figure 4a). To assess the dynamic range of switch activation we titrated in different amounts of Key using a range of progesterone (Pg) concentrations at a fixed amount of YFP-degronSwitch$_a$ (at a single concentration of estradiol (E2)) and measured steady-state fluorescence using flow cytometry. Key induced degradation observed for these initial constructs was dependent on the presence of the cODC degron in the switch, and was not observed when YFP was fused to either BimSwitch$_a$ or Switch$_a$ (Extended Data 9). In order to optimize the amount of inducible degradation, we varied the switch toehold length to tune K_{open}. The switch with the largest dynamic range was the proline-removed cODC and a 12-residue toehold (hereafter referred to as degronSwitch$_a$). Using this variant, YFP fluorescence fused to degronSwitch$_a$ was reduced up to 73% upon full induction of Key$_a$ (Extended Data 10).

We explored the dynamic range of degronLOCKR$_a$ at different concentrations of YFP-degronSwitch$_a$ and Key$_a$-BFP for two different Key lengths (Figure 4b) by testing the full range of E2 and Pg combinations. The extent of Key$_a$-induced degradation of degronSwitch$_a$ varied as a function of the concentration of both proteins. Key$_a$ fluorescence was stable as a function of degronSwitch$_a$ concentration (Extended Data 11), suggesting the Key is not co-degraded with the degronSwitch. With a truncated Key$_a$ (43 residues versus 55 residues), the same dynamic range of switch activation was observed, but a higher Key concentration was required for maximal activation (Figure 4c). This is similar to the behavior observed with BimLOCKR (Figure 2d), and suggests our model of Cage/Key interaction holds true within living cells. To assess the dynamics of degronLOCKR$_a$ activation, we used an automated flow cytometry platform to measure YFP fluorescence as a function of time. Cells were grown at a constant concentration of E2 until YFP-degronSwitch$_a$ reached steady-state and then induced with Pg to activate production of Key$_a$-BFP. We found that the half-life for active degronLOCKR$_a$ in yeast is 24 minutes (see Appendix A), which is very similar to the reported half life of 11-30 minutes for the constitutive cODC degron [29].

To evaluate degronLOCKR function in mammalian cells, we fused the degronSwitch to mCherry, expressed it in human HEK293T cells, and measured its fluorescence in the presence and absence of Key. Using the degronSwitch with a 9- or 12-residue toehold, induced degradation of mCherry was observed in less than 50% of the cells (Extended Data 12). We hypothesized that this behavior was due to aggregation of the degronSwitch (Extended Data 1a), which could result from unintended interactions between repeated sections of sequence in the design that came from the original homo-trimer. Indeed, an asymmetrized degronSwitch (see Appendix A) with an 8-residue toehold, upon induction of key, was degraded in 90% of the cells with a reduction in mean mCherry fluorescence intensity of over 300 fold (Figure 4e).

We next sought to enhance the functionality of degronLOCKR to trigger orthogonal degradation of different proteins in the same cell by installing the proline-removed cODC degron in LOCKR$_b$, LOCKR$_c$, and LOCKR$_d$. In yeast, we constitutively expressed each orthogonal switch variant fused to YFP (Extended Data 13) and measured the degradation of YFP with constitutive expression of each Key variant fused to cyan fluorescent protein (CFP). DegronLOCKR$_a$ and degronLOCKR$_c$ were strongly activated by their cognate Keys, but not by each other's Key (other constructs did not activate; Extended Data 14). To test the orthogonality

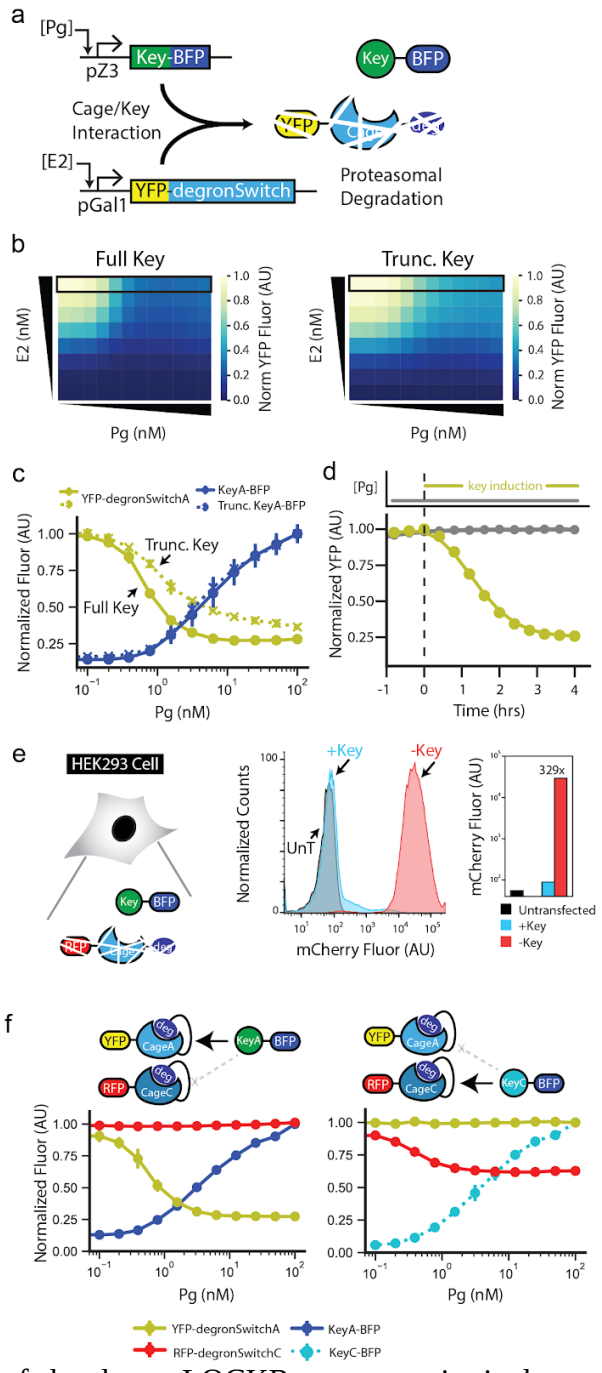

Figure 4 - Testing degronLOCKR function in live cells

a, Schematic of dual inducible system used in *S. cerevisiae* to test functionality of degronLOCKR. Progesterone (Pg) induces production of Key-BFP, and estradiol (E2) induces production of YFP-degronSwitch. **b,** Heatmaps of YFP fluorescence as a function of E2 (0-50 nM) and Pg (0-100 nM) for full length Key (left) and a Key that was truncated by 12 residues (right) as measured by flow cytometry. **c,** Line plot comparing the fluorescence of the YFP-degronSwitch$_a$ and Key$_a$-BFP at a max dose of E2 (black rectangle in (b) as a function of Pg induction. YFP fluorescence was normalized to the no Pg value and BFP fluorescence was normalized to the maximum Pg value. Error bars represent s.d. of three biological replicates. **d,** Dynamic measurements of active degronLOCKR using an automated flow cytometry platform. E2 was induced to activate expression of YFP-degronSwitch$_a$, and Pg was induced at t_{4hrs} to activate expression of Key$_a$-BFP. Measurements were taken every 24 minutes. **e,** DegronLOCKR functionality in HEK293T cells. mCherry was fused to an asymmetrized degronSwitch and expressed in HEK293T cells with and without key. Fluorescence was measured using flow cytometry and the histogram shows reduction in mCherry expression in the presence of key. The geometric mean of mCherry expression is plotted for untransfected cells (UnT), cells expressing key-BFP, and cells expressing BFP. **f,** Coexpression of orthogonal LOCKRs in the same cell. YFP-degronSwitch$_a$ and RFP-degronSwitch$_c$ were expressed using constitutive promoters and either Key$_a$-BFP (left) or Key$_c$-BFP (right) were expressed using the pZ3 inducible promoter. Normalized fluorescence of YFP-degronSwitch$_a$, RFP-degronSwitch$_c$ and either Key$_a$-BFP or Key$_c$-BFP are plotted as a function of Pg induction. Error bars represent s.d. of biological replicates.

of the degronLOCKRs, we constitutively coexpressed degronLOCKR$_a$ and degronLOCKR$_c$ in the same cell fused to YFP and red fluorescent protein (RFP), respectively, and used the Pg inducible system to titrate expression of each Key variant in separate strains. Expression of Key$_a$ led to selective degradation of YFP but not RFP, and expression of Key$_c$ led to selective degradation of RFP but not YFP (Figure 4f). This demonstrates that the dual degronLOCKR system can function orthogonally and simultaneously in living cells.

LOCKR INDUCIBLE NUCLEAR EXPORT

Dynamic shuttling of transcription factors and kinases in and out of the nucleus plays an essential role in cellular function. To investigate the possibility of inducible control over nuclear localization, we caged a nuclear export sequence (NES[31]) in $Switch_a$ with the same strategy used for Bim and cODC, and fused the resulting $nesSwitch_a$ to YFP with a strong nuclear localization sequence[32]. RFP-histone fusion (HTA2) was constitutively expressed in the same yeast cells to act as a nuclear marker (Figure 5a). To test the switching capability of $nesLOCKR_a$, we compared YFP localization with and without Key expression. YFP was found to co-localize with RFP in the nucleus in the absence of Key_a-BFP (Figure 5b, left). When NLS-YFP-$nesSwitch_a$ was coexpressed with Key_a-BFP the YFP fluorescence appeared more cytosolic, indicating uncaging of the nuclear export signal (Figure 5b, right). Observed YFP punctae in the cytosol are likely due to aggregation since coexpression of YFP-$nesSwitch_a$ without a NLS and Key_a-BFP results in a similar pattern (Extended Data 17a, b). Uncaging of the NES is independent of the presence of a NLS on Key_a-BFP (Extended Data 17c, d); the mechanism for maintaining nesLOCKR outside of the nucleus may be a combination of nuclear export from the nucleus and capture of either newly translated NLS-YFP-$nesSwitch_a$ or residual NLS-YFP-$nesSwitch_a$ by Key in the cytosol (Key_a-BFP is always observed to colocalize with YFP-$nesSwitch_a$ (Extended Data 17)).

Next, we used nesLOCKR to control localization of SynTF. We hypothesized that activation of nesLOCKR would lead to a reduction in output of the pSynTF promoter since SynTF needs to be localized to the nucleus to activate transcription. Using the dual induction system (Figure 5c), we expressed different concentrations of SynTF-RFP-$nesSwitch_a$ and Key_a-BFP in the same cell as a pSynTF-YFP reporter, and measured the steady-state fluorescence using flow cytometry (Figure 5d). Induction of the Key at 31.25 nM E2 caused a 33% decrease in YFP signal, indicating successful activation of nesLOCKR and exclusion of SynTF from the nucleus (Figure 5e). Together, these results demonstrate our ability to cage different functional peptide motifs in live cells, highlighting the modularity and utility of LOCKR.

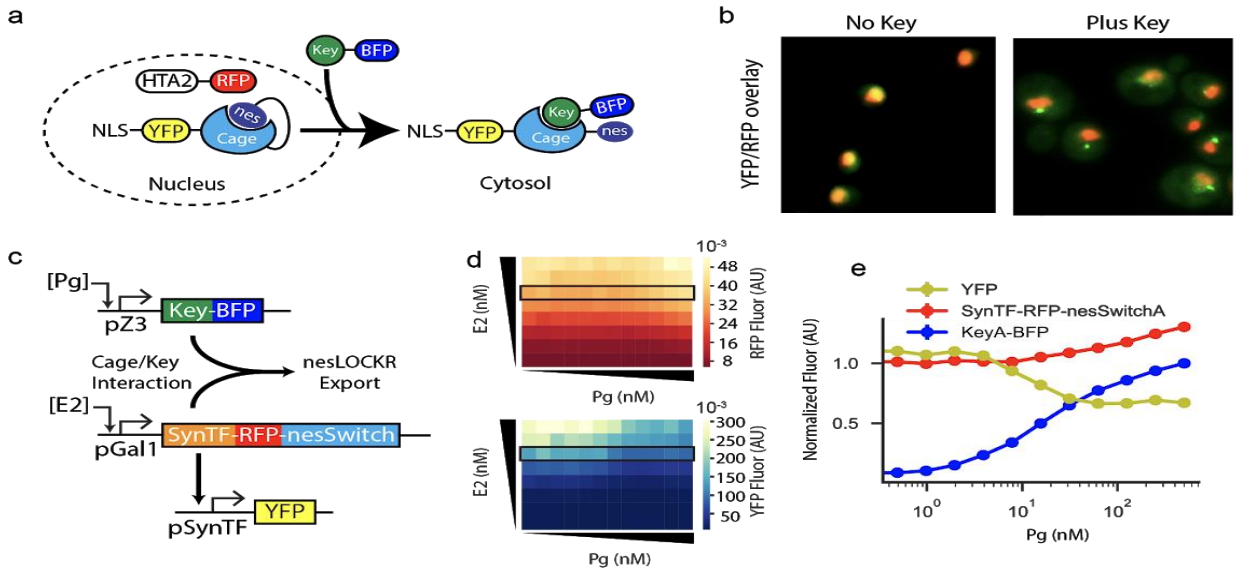

Figure 5 - Controlling protein localization in yeast using nesLOCKR

a,) Schematic of Key-induced nuclear export of NLS-YFP-nesSwitch$_a$. The nucleus is marked by the histone HTA2-RFP. **b,** Fluorescence microscopy showing (left) co-localization of NLS-YFP-nesSwitch$_a$ with nuclear HTA2-RFP fluorescence when no Key$_a$-BFP is expressed, compared to (right) a more diffuse NLS-YFP-nesSwitch$_a$ fluorescent signal observed outside of the nucleus when Key$_a$-BFP is expressed. **c,** Schematic of dual induction assay to determine the effect of nesLOCKR$_a$ on a synthetic transcription factor (SynTF). Pg induces expression of Key$_a$-BFP, and E2 induces expression of SynTF-RFP-nesSwitch$_a$ fusion. The pSynTF promoter is activated by SynTF and expresses YFP. **d,** Heatmaps of YFP and RFP fluorescence as a function of E2 (0-125 nM) and Pg (0-500 nM) measured by flow cytometry. **e,** Line plot comparing the fluorescence of YFP, SynTF-RFP-nesSwitch$_a$ and Key$_a$-BFP at 31.25 nM E2 (black rectangle in 6d) as a function of Pg induction. YFP and RFP fluorescence was normalized to the no Pg value, and BFP fluorescence was normalized to the maximum Pg value. Error bars represent s.d. of three biological replicates.

LOCKR INDUCIBLE STREPTAGII BINDING

We next sought to design a LOCKR switch based purely upon protein-protein interactions where that interaction does not have bioactivity, as in the Bim:Bcl2 case. To this end, we chose the StrepTagII protein purification tag. StrepTagII binds to streptavidin, streptactin, and monoclonal antibodies designed to bind it[33]. This choice presents a unique design challenge because the sequence (Table 2) contains a proline, which is highly disfavored in alpha-helical proteins[34]. Following the same design protocol described in "Initial Design Methods", seven potential grafting positions were considered. (Figure 6a) One such graft started in the loop preceding the Latch helix and a glycine added before the StrepTagII sequence with the hypothesis that the helical propensity of the rest of the latch, and the flexibility from the glycine,

would adequately cage the StrepTagII binding to an antibody target. All sequences designed are found in

Table 3.

To test the success of strepLOCKR designs, an antibody target was used from Genscript against the StrepTagII sequence. Bio-layer interferometry experiments were set up with the antibody immobilized on the BLI tip and the switch and/or key in solution. All designed Switches showed binding to the antibody in the absence of Key. (Figure 6b) However, when the most caged variant was challenged for Key activation, it showed an increase in binding signal to the target antibody. (Figure 6c) What this indicates is that K_{open} is tuned such that the open state is overpopulated which allows target to bind in the absence of Key. This is likely due to the proline destabilizing the helix as previously described. No further design was considered due to focus on more promising targets.

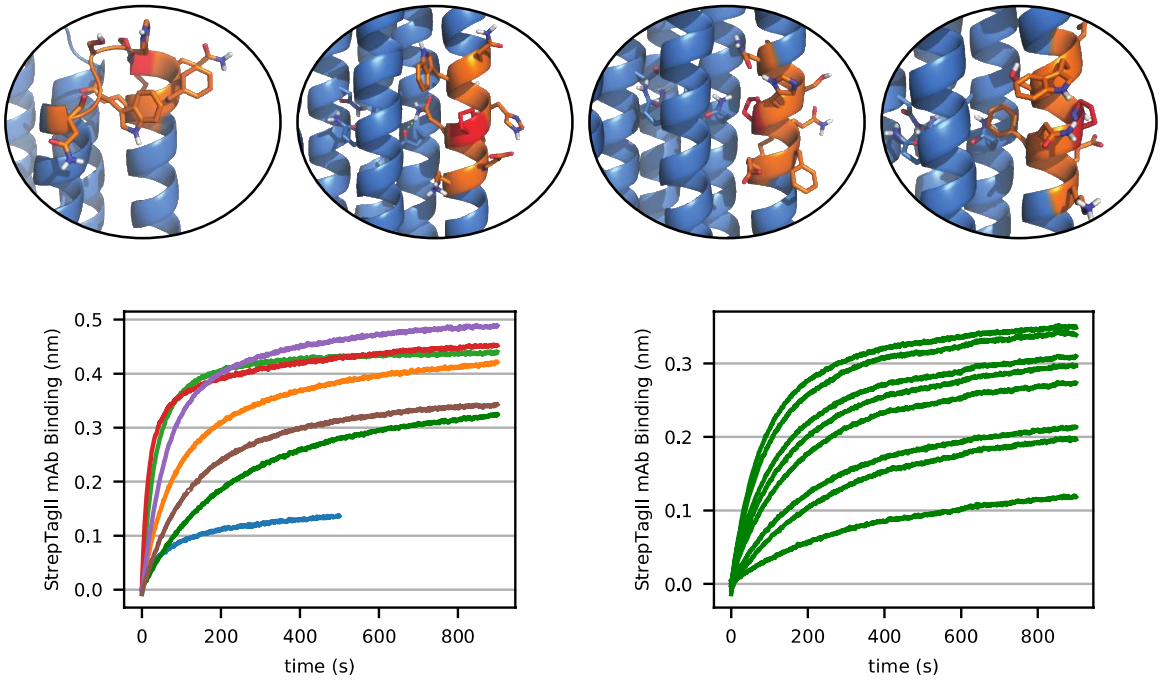

Figure 6 – strepLOCKR Design and Activation

a) Four exemplary threads of StrepTagII onto $Switch_a$. The switch scaffold is colored in sky-blue color with the StrepTagII sequence in orange in stick representation. The proline is colored in red. In order, these threads begin at positions 299, 312, 320, and 329. Hydrogen bonds to the hydrogen bond networks in the cage (shown in blue stick representation) are present only in the 312 thread and denoted by a yellow dashed line. **b)** BioLayer Interferometry timecourse data showing association phase of all tested strepSwitches without Key added. Different designs are in different colors, with 299 shown in red, 312 in green, 320 in blue, and 329 in purple. Concentration of Switch in this assay is 500nM. **c)** strepSwitch 312 at 100nM was challenged with Key from 2 μM down to 2.7 nM by three-fold dilution. The lowest curve shows 100 nM Swich without Key.

The failure of these strepLOCKR switches then elucidates strategies for future designers to utilize functional sequences that are more destabilizing. For instance, the StrepTagII sequence also contains large aromatic residues that have polar atoms (tryptophan and histidine). It would be instructive to design new LOCKR Switches that have hydrogen bond networks that contain these residues such that the grafting can accommodate these residues. Furthermore, more study must be done to determine the best way to graft a sequence with proline. Addition of glycine to kink the helix is one other strategy. Overall the design of Switches to cage the StrepTagII sequence has provided insight into the LOCKR design process that I utilize to create the following design methods and functional LOCKR Switches below.

GRAFTSWITCHMOVER FOR FUNCTIONAL LOCKR DESIGN

To streamline design of functional LOCKR proteins, I wrote a Rosetta Mover which automates the manually intensive aspects of selecting functional Switch designs. This allows design of function to happen in the same protocol as structure design in combination with standard helical bundle design protocols[15]. The workflow of this Mover is outlined in Figure 7. The protocol requires the user define key parameters, the two requirements being one or more sequences to graft onto the switch and of those sequences, which residues are important to be buried. While burial importance depends on a case by case basis, generally important residues are hydrophobic and contribute to the activity of the bioactive peptide. The protocol begins by identifying the residues that are designable (Figure 7a). Default behavior is to identify the C-terminal helix by the DSSP algorithm[35]; the user is able to override this to identify the N-terminal helix, specify start and end residues, or define a ResidueSelector that returns the set of designable residues. Any way the set of residues is defined, the Mover will detect where the given sequence can fit in that set even if it is discontinuous. It will also find compatible positions for more than one defined sequence that results in non-overlapping grafts. The user can define if the sequences are grafted in a particular order or not, which is useful for the following designs in this dissertation.

Then, for each position or set of positions identified in step 6a, the mover performs a two step process to identify if the positions successfully bury the important residues defined by the user. The first step illustrated in Figure 7b does the mutations at one position (or set of positions) identified in step 6a using the SimpleThreadingMover, a module part of the Rosetta suite. This step uses a soft score function and will repack the neighboring residues. The user may define

that the Mover not repack the neighbors as well as define TaskOperations that restricts the repacking to certain residues. The second step illustrated in Figure 7c uses the user defined "important residues" and the NeighborsByDistanceCalculator (also built into Rosetta) to determine how buried the important residues are. If the average degree of these residues is less than six (6) the Mover rejects the thread and continues with the next potential position(s) found in step 6a.

Once all the acceptable grafts are identified, Rosetta will then perform a minimization and repack of the grafted areas and its neighbors (Figure 7d). This is done with a user defined score function, or the default score function used in the given Rosetta trajectory. Due to the output of multiple structures the built-in MulitplePoseMover can collect all the output and perform downstream design and filtering. In this way, the design process from backbone to functional LOCKR system is streamlined.

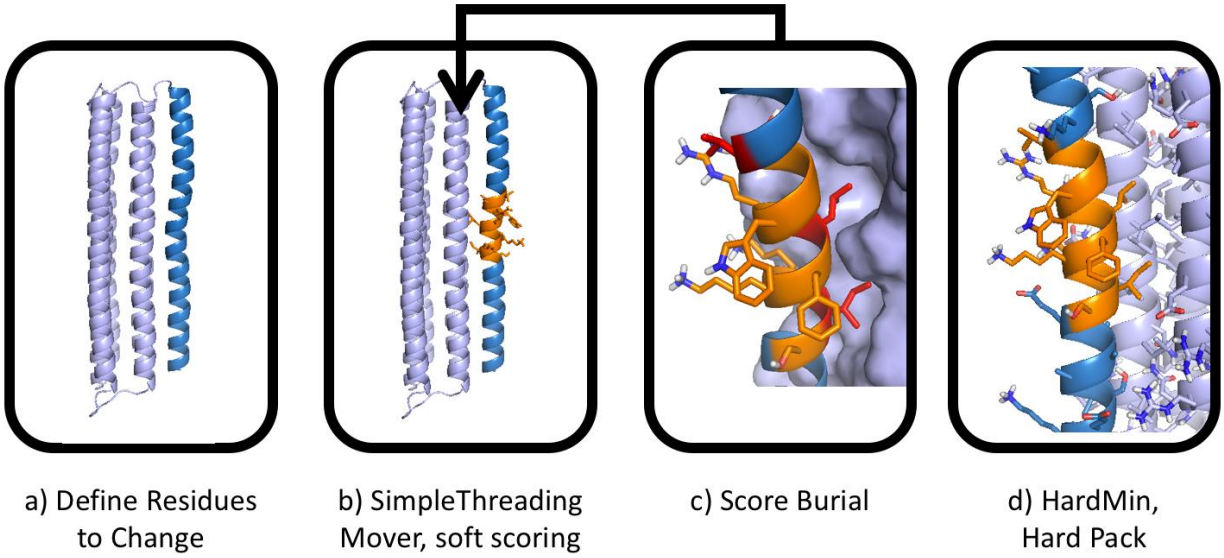

Figure 7 – GraftSwitchMover Workflow

a) The mover starts by the user defining the designable residues, in this example highlighted in darker blue. This can be a continuous selection or discontinuous. **b**) For every possible position selected in a) the Mover threads the defined sequence(s) using a soft scorefunction. The orange cartoon and sticks represents the threaded sequence. **c**) At each position the Mover scores the user-defined important residues for burial, here depicted in red. If the average degree is less than the desired cutoff the design is thrown out. **d**) Once all positions are tried, all that pass the burial cutoff score are minimized and repacked using a hard scorefunction.

LOCKR Inducible Post-Translational Modification

A common theme in biological protein systems are covalent modifications made to the protein after translation. These modifications include proteolysis, phosphorylation, ubiquitinylation, conjugation to other proteins, and a host of other molecular modifications to standard protein biochemistry[36]. Modification is also associated with functional modulation, where a protein may be active or inactive depending on modification state. Furthermore, there are structural rearrangements that happen to cause the functional changes and depending on the modification this functional change can be irreversible. Here, I've explored the possibility of designing LOCKR switches that undergo post-translational modifications once activated. Also, I discuss the future where LOCKR may be activated in a key-independent manner by such modifications.

spyLOCKR and tevLOCKR

Common in biotechnological research are enzymes that act on proteins *in vitro* to add or remove domains to recombinant protein. Therefore, I sought to install these functions into LOCKR to explore the utility of the system in biotechnological and synthetic biology systems. TEV protease is commonly used to cleave protein purification tags off recombinant proteins, through recognition of a simple octa-peptide motif (`ENLYFQGS`)[37]. Cleavage occurs between the glutamine and glycine residues for an irreversible modification of the protein backbone. Another system utilized in biotechnology labs is the SpyTag-SpyCatcher covalent interaction. The SpyCatcher protein is reengineered from bacterial adhesions to form an iso-peptide bond to the glutamate residue in the SpyTag sequence (`AHIVMVDAYKPTK`)[38]. Using this tag, any two proteins can be conjugated via a covalent bond. Both tags are used in cellular engineering and in laboratory biotechnology[39–41] which makes them promising targets for LOCKR based control.

Utilizing the Rosetta Mover referenced above, TEV protease site and SpyTag were independently grafted onto the asymmetrized $Switch_a$ (See Code Availability for RosettaScripts). Two each of the resulting tevSwitch and spySwitch designed proteins were purified and assayed for function. All switches express as a monomer by Size Exclusion Chromatography but display different ability to cage the SpyTag or TEV protease sequence. The SDS-PAGE gels in Figure 8 demonstrate the result of overnight incubation of Switch and either TEV or SpyCatcher in 25mM Tris (pH 8.0) with 50mM NaCl, with or without 10 μM Key. For the spyLOCKR designs, the

two designs differ in threading position by 11 residues, or approximately three helical turns. Both spyLOCKR$_2$ and spyLOCKR$_8$ hold SpyTag in a conjugation incompetent conformation as evidenced in Figure 8a, each lane without the key present. However, spyLOCKR$_8$ is more activated upon addition of key. (Figure 8a) In Figure 8b the tevLOCKR designs show a similar trend. The tevLOCKR$_1$ and tevLOCKR$_6$ are both able to prevent cleavage in the absence of key; tevLOCKR$_6$ is the only design that shows cleavage upon addition of the key (shown by a shift in the band labeled "tevLOCKR cleaved"; Figure 8b).

I reasoned that combining the SpyTag and TEV protease site on a latch would be useful in downstream applications, for instance as a means to conjugate two protein domains through SpyTag and remove the latch via TEV protease once activated. GraftSwitchMover was used to simultaneously design LOCKR switches that contain the TEV protease site and SpyTag, in that order, on the Latch. Because two functional peptides may destabilize the Latch more than one (therefore impacting K_{open}) I used the shortened asymmetric scaffold described above, as well as

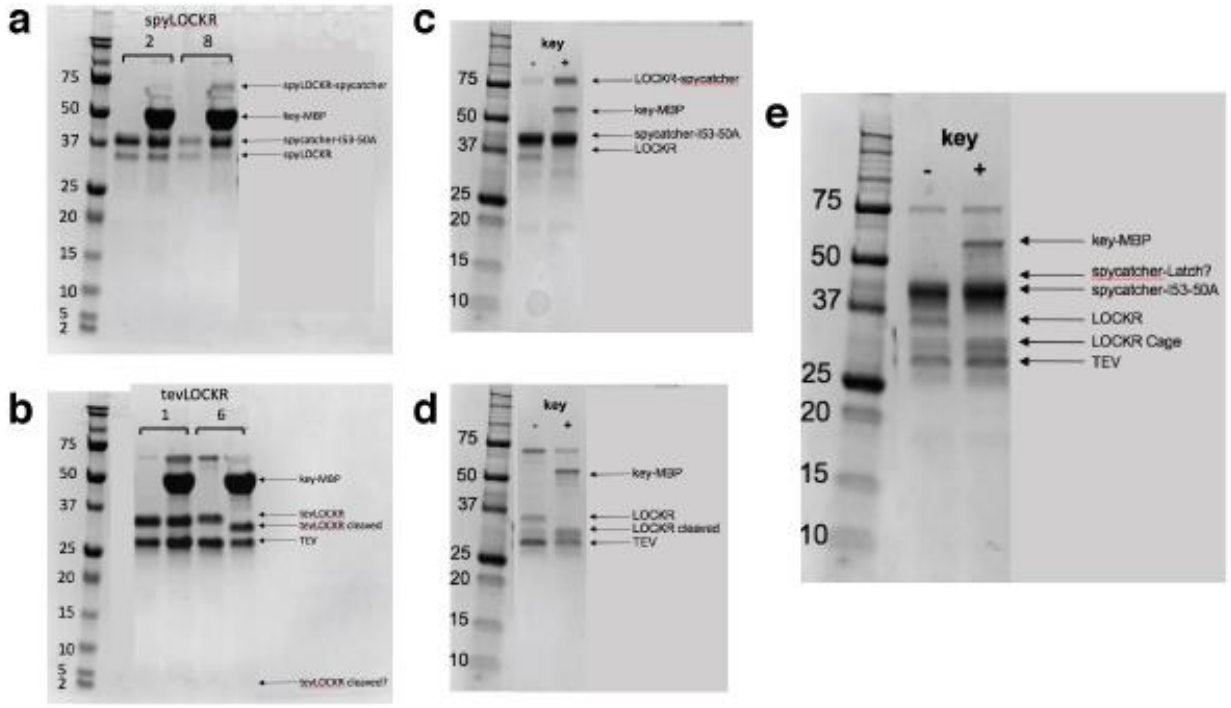

Figure 8 – Designing SpyTag and TEV protease site into LOCKR

a,b) SDS-PAGE of spyLOCKR and tevLOCKR designs, respectively, with or without key. All designed species labeled on the left. **c-e)** SDS-PAGE of tev-spyLOCKR$_{63}$ against SpyCatcher alone (c) TEV alone (d) or both in combination (e), with or without Key.

the asymmetric scaffold with helices as long as the original proof-of-concept BimLOCKR. I selected five designs based on similarity to tevLOCKR$_6$ and spyLOCKR$_8$ and minimizing the number of unstatisfied hydrogen bonds along the Cage:Latch interface. Figure 8c-e depicts the result from tev-spyLOCKR$_{63}$ where it is capable of suitably caging both TEV protease site and SpyTag, and capable of activation by Key to allow both conjugation to SpyTag and cleavage by TEV protease – alone and in combination. Figure 8c shows tev-spyLOCKR$_{63}$ challenged against SpyCatcher alone, with or without key. The conjugation product in the second lane is labeled "LOCKR-SpyCatcher" at 70kDa. Figure 8d shows challenge against TEV protease alone and shows a shift from 32.7kDa to 30kDa in the presence of Key. Finally, Figure 8e shows challenge against both targets. We do not see increased leakiness (first lane) despite two targets being present. Further, we see a disappearance of the 32.7kDa band signifying TEV cleavage and increased density above SpyCatcher alone. (Figure 8e) These results represent the first successful dual-function LOCKR system.

LOCKR Inducible Light-Based Assays

We see from the results above that LOCKR is able to control protein-protein interactions (BimLOCKR, strepLOCKR), and the catalytic activity that accompanies that (degronLOCKR, spyLOCKR, tevLOCKR). The readout for these interactions involves destruction of the sample (SDS-PAGE) or immobilization of one of the components (BioLayer Interferometry). It would be instructive to design LOCKR systems where all three components can be varied dynamically to more accurately observe the landscape of parameters outlined in Figure 1a and the kinetics of the interactions simultaneously. Using LOCKR inducible light-based readout is one method to achieve this goal; here, I describe the design and validation of LOCKR switches to control reconstitution of split luciferase where the readout here is luminescence only in the presence of Key. I then continue to describe the design of LOCKR switches capable of modulating FRET signal upon the conformational change. The benefit of such is that the three thermodynamic parameters in Figure 1a are completely independent from the FRET readout allowing the ability to probe any generic LOCKR system that fits the requirements of the FRET system.

lucLOCKR

To utilize luminescence as the readout for LOCKR activation, we turned to the NanoBiT split luciferase system[42]. This system uses the NanoLuc® Luciferase which catalyzes the breakdown of Furimazine in the presence of oxygen to release carbon dioxide and light. This luciferase is split at residue 157 and several short peptides that mimic the C-terminus of the luciferase bind at various affinities to the Nluc to allow catalysis. One such peptide, `VSGWRLFKKIS`, binds with 0.7 nM affinity[42] to activate catalysis and is a great candidate for grafting onto the LOCKR switch Latch. Grafting was performed per previously described protocols and two switches were selected for testing: lucLOCKR$_1$ and lucLOCKR$_3$.

Each luciferase switch was challenged against the Nluc in an endpoint assay taken 5 minutes after mixing, as well as over a timecourse where all LOCKR components were mixed with the NanoBiT reagents at the start of the assay. This setup allows control of the Switch, Key, and Target concentrations simultaneously and real time readouts, in contrast to BioLayer Interfereometry and SDS-PAGE assays where only one of the two advantages is disallowed by the protocol. For the data shown in Figure 9a-b, the Nluc Target is held constant at 50 nM while the Switch concentration varied by 10-fold dilution from 5μM to 5nM and the Key concentration was varied by 5-fold dilution from 25μM to 500nM with a no Key control. Based on these data, the two lucSwitches display

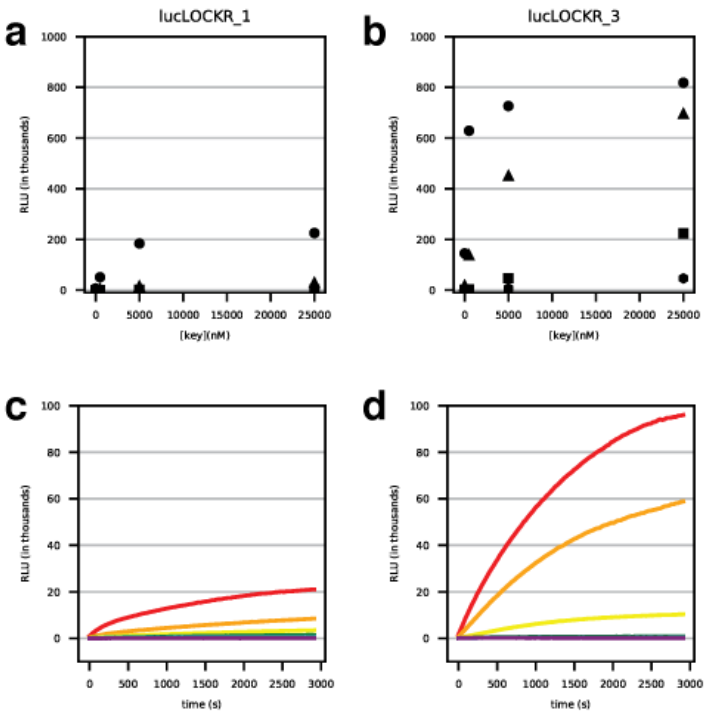

Figure 9 – Activation of lucLOCKR

a-b) Challenging Key (x-axis) against 50 nM Nluc at different concentrations of the Switch - 5μM in circles, 500nM in triangles, 50nM (1:1 with Target) in squares, and 5nM in hexagons. Shows average of two replicates, error bars show s.d. **c-d)** Kinetic measurement of lucLOCKR activation. Switch at 250nM (c; lucLOCKR$_1$) or 25nM (d; lucLOCKR$_3$) with Target at 50nM. Red line represents luminescence over time at 50 μM Key where each color lower represents a 5-fold dilution series. One replication.

differing sensitivity to Key. lucLOCKR$_1$ is less sensitive, implying that the threading of luciferase at that position is not as disruptive to the Latch:Cage interface, allowing K_{open} to remain biased towards the closed conformation. In Figure 9b we see that lucLOCKR$_3$ is leaker since the 5μM of Switch with no Key shows luciferase activity and the total activity as key is added begins to plateau at micromolar concentrations of Key. Figure 9c-d depict the kinetics of the same lucLOCKR designs when Key is added at t=0 sec. We see the same reduction in signal from lucLOCKR$_1$ even though it is 10-fold more concentrated than lucLOCKR$_3$. Further, we see that lucLOCKR$_3$ doesn't even show any activation until 2μM Key, which is consistent with Figure 9b, indicating that tuning the dynamic range of activation is possible by introducing mutations into the Latch to tune K_{open}. These data indicate that using lucLOCKR we can see a readout of over 600-fold from LOCKR switches *in vitro*.

These designs signal that lucLOCKR can be a powerful tool for biotechnological development and biosensor design. The NanoBiT system has other peptides that activate fluorescence at weaker affinities[42] which means K_{LT} can be acutely tuned along with K_{open} and K_{CK}. Using this strategy, depending on the application lucLOCKR can be tuned with fine control to the desired working concentrations of the system. Furthermore, NanoBiT works in live cells so this system can be used as a real-time readout of biological activity. Finally, the peptide with the lowest affinity requires co-localization to Nluc for luciferase activity, so if Nluc was fused to the Key then lucLOCKR can be used as a biosensor for the target. Contrary to traditional LOCKR assays where the Key activates Target binding, the model in Figure 1 is symmetrical such that Target can activate Key binding. In this way, a luciferase based biosensor could be designed such that the Latch encodes the low affinity NanoBiT sequence along side another binding peptide. Then, the biosensor Target would activate the Key-Nluc binding to the Cage and NanoBiT sequence to activate luminescence. This expands the utility of LOCKR from cellular engineering, as with degronLOCKR, to biosensor applications to detect molecules relevant for medical diagnosis or biochemical research.

fretLOCKR

We reason that LOCKR development would benefit from an assay where Switch activation was measured independent from Key or Target binding. Previous methods all require measurement resulting directly from Target binding, meaning that any change made to the Key

or Target binding will also change the mechanics of the assay used to measure it. Towards a solution to this problem, we turn to FRET where fluorescent proteins fused to either termini of the Switch are close enough for FRET in the closed state, but not in the open state. **Error! Reference source not found.** illustrates two such switches and the resulting spectra these proteins produce.

The first proof-of-concept fretLOCKR consists of the asymmetric Switch scaffold with mTurquoise2 and SYFP fused to the N- and C-terminii, respectively as illustrated in Figure 10a. This FRET pair has an R_0 of 58.5Å so the distance labeled in **Error! Reference source not found.**a should give a FRET signal. The emission wavescan in the absence of Key after excitation at 435nm (Figure 10b) shows an emission peak at 528nm characteristic of SYFP above the depicted mTurquoise2 spectrum. Furthermore, this peak begins to disappear upon addition of 300 μM Key (**Error! Reference source not found.**b). The ratio between the mTurquoise2 emission peak, 474nm, and the SYFP emission peak, 528nM, describes the extent of FRET in each reaction. Figure 10c shows the 5-fold dilution series of Key from 300 μM to 19.2 nM, where we see a gradient of response at higher Key concentrations.

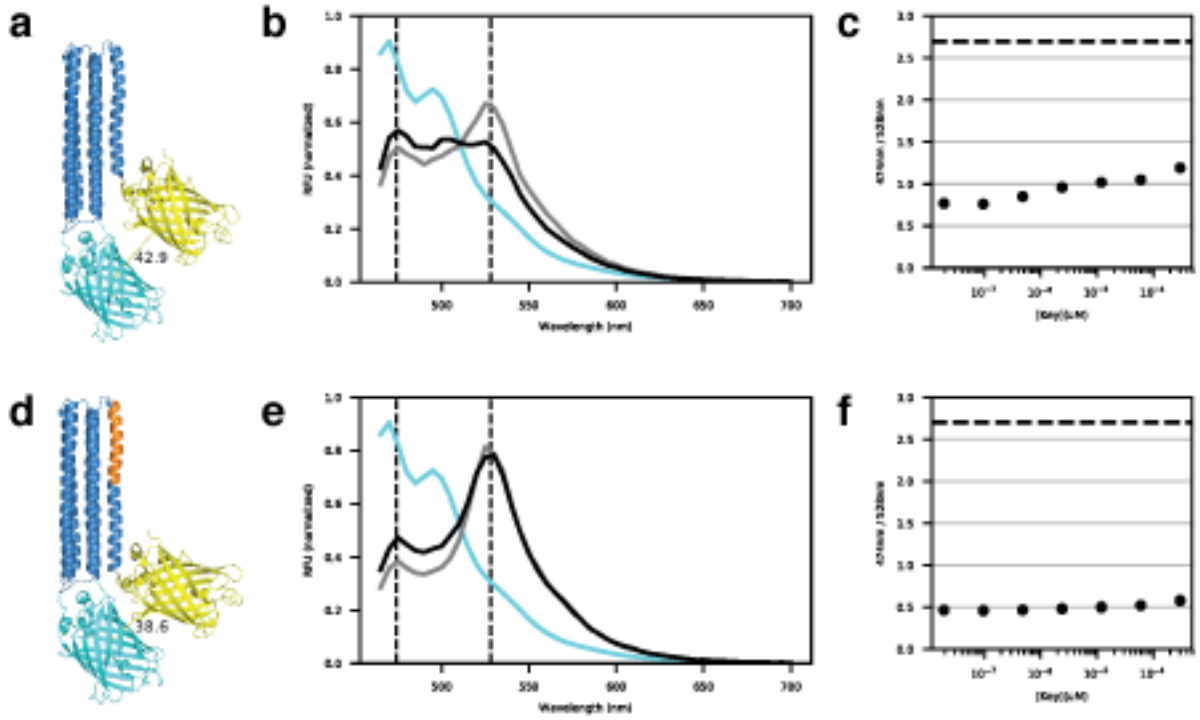

Figure 10 – fretLOCKR Activation

a) Model of $LOCKR_a$ fused to a fluorescent protein FRET pair. mTurquoise2 in cyan, SYFP in yellow with $Switch_a$ in sky-blue. **b)** Emission wavescan after excitation at 345nm. mTurquoise2 spectrum in cyan, with fretLOCKR no Key in grey, with 300 μM Key in black. **c)** Ratio of 427nm:530nm (vertical dashed lines in (b) plotted as a function of Key concentration. **d-f)** same plots as (a-c) for Bim-fretLOCKR where the Bim peptide is shown in orange in (d).

To fully probe the Switch, Key, and Target dynamics in this system, we then grafted Bim onto the fretSwitch in the same manner as subsection LOCKR Inducible Bim-Bcl2 Binding. This way, we should see enhanced Key binding in the presence of Bcl2 similar to Extended Data Figure 7. The model in Figure 10d shows Bim in orange and the FRET pair closet together due to removal of the toehold in Figure 10a. This coincides with a stronger peak at 528nm because FRET is stronger at closer distances. However, this switch shows only minor signs of activation, with no decrease in the 528nm peak but a slight increase in the 474nm mTurquoise2 emission peak. (Figure 10e) In the same Key titration schema as before, we see only modest increase of the 474/528 ratio at high micromolar concentrations of Key.

In this chapter, I outlined strategies for using the *de novo* proteins described in Chapter 1 as functional protein switches. Furthermore, I outlined two methods of design; one method is computationally intensive and yielded the first LOCKR prototypes while the second is inline with Rosetta protocols and streamlines the design of functional LOCKR switches. Utilizing these methods, and the scaffolds outlined in Chapter 1, I described the design and characterization of switches that control the following: Bim-Bcl2 interactions; cODC degron activity; StrepTagII binding a designed antibody; nuclear export; covalent modifications to the switch via TEV protease and SpyCatcher; luciferase activity; and FRET signal. In general, these methods can be used to design switches that cage generic biological function so long as the signal can fit in the Latch. Exploring the idea of caging other protein motifs, such as small molecule binding motifs or entire protein domains, would expand the technology.

[3] AND APPLICATIONS, THEREOF

The true test of a technology's modularity is its applicability to real world problems. The true purpose of entrepreneurial venture is to solve a problem, and through that lens I have developed the LOCKR platform. While the design of LOCKR is biochemically interesting, it also has applications ranging from performing rudimentary logic operations, to controlling aspects of biology automatically in synthetic biological circuits. These applications are also not strictly academic ventures, and hold promise in improving cell based therapies for cancer and gene therapy. Here, I will describe a few applications of the LOCKR technology to real problems in biochemistry and biotechnology. Many of these applications are undertaken by collaborators and as such I will not go into detail in this document.

Broadly, LOCKR is currently being expanded in functionality to act as biosensors, cage large protein domains, and respond to real biological signals. One promising applications is the utility of LOCKR as synthetic extracellular receptors to initiate an intracellular signaling event. As described in sub-sub section "lucLOCKR" the Target can be used to induce dimerization of the Switch and Key. Using this dimerization event on the extracellular side of the cell can induce dimerization of signaling domains on the intracellular side. Therefore, this strategy can allow a cell to respond with user-defined signaling modules to user-defined Targets in blood, organs, or even tumors. Development of this technology is very early and will be continued in industry upon completion of my PhD.

Throughout Chapters 1 and 2 I discuss at length the tunability of LOCKR. Several examples I show switches that are too leaky, and several that require high levels of Key to see any signal. This latter case is useful to solve the problem of performing rudimentary logic to target therapeutics and biological modulators. If a switch requires high amounts of Key to activate, that concentration can be achieved through adding large excess Key or by physically bringing the Switch and Key in proximity to each other. In this way, activation of the Switch acts as an AND sensor, where there is signal only when two markers are present in close proximity. This is useful in targeting ultra-specific cell types that express unique pairs of markers, such as immune cell subtypes or tumors. There is also utility in co-localizing the Switch and Key to two loci on DNA to more specifically target locations in the genome. I extend my appreciation to Marc

Lajoie for solving the problem of cell-type differentiation using LOCKRs described here. I would also like to recognize Robin Kirkpatrick and Jesse Zalatan for moving forward on targeting loci on DNA.

The modularity of LOCKR is highlighted in the synthetic biology applications of degronLOCKR. Working with the El-Samad lab at UCSF we have developed strategies for designing and refining degronLOCKR constructs to control biological function. In general, the following sections describe the utility of fusing degronLOCKR to various native proteins to degrade them dependent on Key expression at strategic times.

DEGRONLOCKR CONTROL OF GENE EXPRESSION IN LIVE CELLS

To implement LOCKR based control in cells, we sought to use degronLOCKR to modulate the intracellular concentration of a synthetic transcription factor and dCas9 in yeast. We first placed a zinc-finger based synthetic transcription factor (SynTF)[43] fused to both RFP and degronSwitch$_a$ under the control of the E2 inducible promoter, and Key$_a$-BFP-NLS under the control of the Pg inducible promoter. To monitor SynTF activity, we measured pSynTF-YFP fluorescence in the same cell (Figure 11a). An increase in expression of SynTF-RFP-degronSwitch$_a$ increased both RFP and YFP fluorescence, while an increase in Key expression decreased both outputs (Figure 11b). For example, at 31.25 nM E2 (Figure 11b), maximal Key induction caused a 61% reduction of RFP and 82% reduction of YFP (Figure 11c). Notably, degronLOCKR caused a graded change in YFP fluorescence as a function of Key concentration, which contrasts with the more digital behavior of transcription factors typically used in synthetic biology applications[44]. In addition, coupling the degronSwitch to the SynTF amplifies the fold change of degronLOCKR, illustrating the usefulness of this strategy to control transcription. To further establish degronLOCKR as a general method of transcriptional control, we next tested degradation of an activating dCas9-VP64 fusion[45]. dCas9 was targeted to the tet operator site of the pTet7x with a constitutively expressed sgRNA to induce expression of YFP (Figure 11d), and Key expression was titrated at different concentrations of dCas9 (Figure 11e). We observed a 78% reduction of RFP and 41% reduction of YFP upon induction of Key at 31.25 nM E2 (Figure 11f). Together, these results demonstrate the modularity and functionality of degronLOCKR for controlling the stability of proteins in live cells.

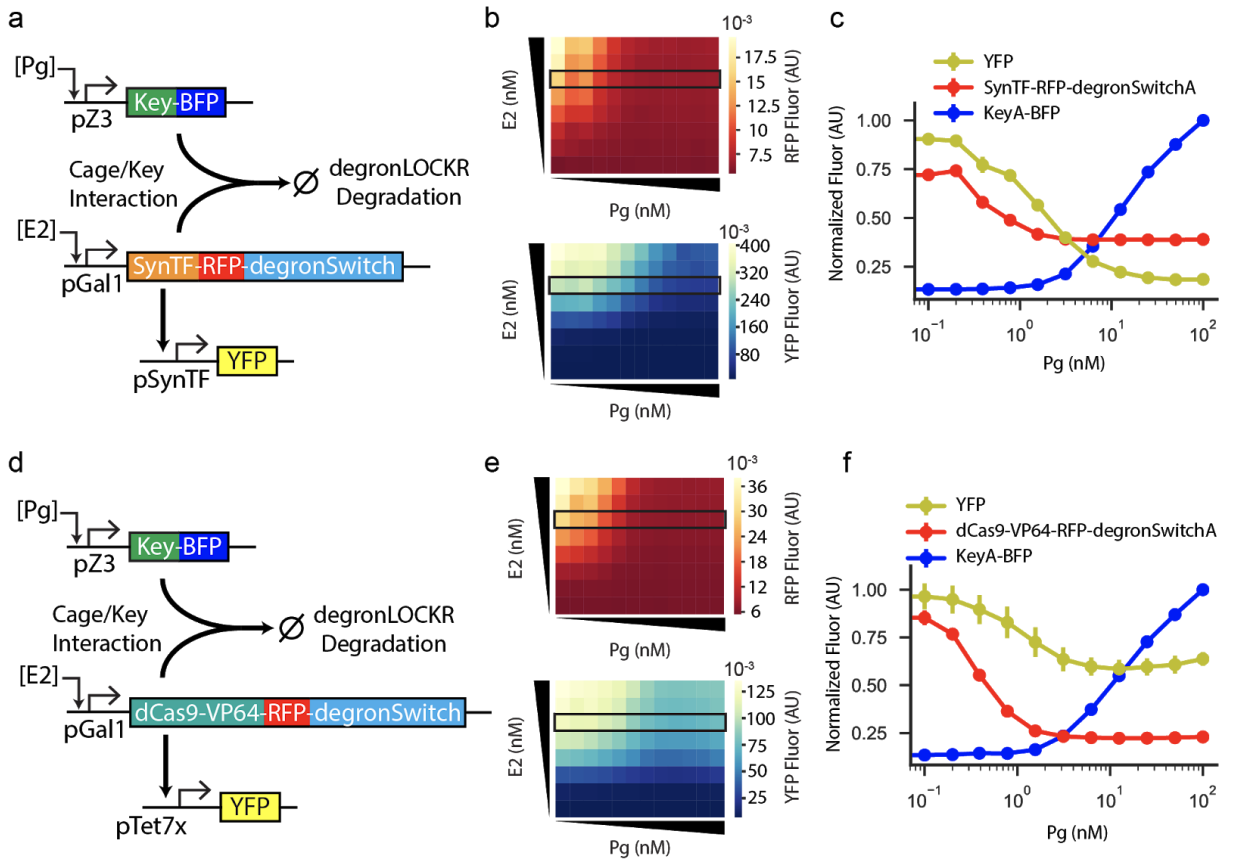

Figure 11 – Controlling gene expression using degronLOCKR

a, Schematic of dual induction assay to determine the effect of degronLOCKR$_a$ on a synthetic transcription factor (SynTF). Pg induces expression of Key$_a$-BFP, and E2 induces expression of SynTF-RFP-degronSwitch$_a$ fusion. The pSynTF promoter is activated by SynTF and expresses YFP. **b,** Heatmaps of YFP and RFP fluorescence as a function of E2 (0-125 nM) and Pg (0-100 nM) measured by flow cytometry. **c,** Line plot comparing the fluorescence of YFP, SynTF-RFP-degronSwitch$_a$ and Key$_a$-BFP at 31.25 nM E2 (black rectangle in 5b) as a function of Pg induction. YFP and RFP fluorescence was normalized to the no Pg value, and BFP fluorescence was normalized to the maximum Pg value. Error bars represent s.d. of three biological replicates. **d,** Schematic of dual induction assay to determine the effect of degronLOCKR$_a$ on a dCas9-VP64 targeted to the pTet7x promoter via a constitutively expressed sgRNA (not shown). Pg induces expression of Key$_a$-BFP, and E2 induces expression of dCas9-VP64-RFP-degronSwitch$_a$ fusion. The pTet7x promoter is activated by dCas9-VP64 and expresses YFP. **e,** Heatmaps of YFP and RFP fluorescence as a function of E2 (0-125 nM) and Pg (0-100 nM) measured by flow cytometry. **f,** Line plot comparing the fluorescence of YFP, dCas9-VP64-RFP-degronSwitch$_a$ and Key$_a$-BFP at 31.25 nM E2 (black rectangle in 5e) as a function of Pg induction. YFP and RFP fluorescence was normalized to the no Pg value, and BFP fluorescence was normalized to the maximum Pg value. Error bars represent s.d. of three biological replicates.

DEGRONLOCKR MEDIATED FEEDBACK

The previous section describes the utility of fusing degronLOCKR to synthetic transcription factors, and relies on addition of hormone to express the key to impart control. In collaboration with Andrew Ng and Hana El-Samad at UCSF we have utilized the tunability of degronLOCKR

to impart automated control of biological signaling. Previous efforts to engineer feedback have relied on using naturally occurring parts which suffer from the lack of modularity and tunability that LOCKR affords. Here, I'll summarize the use of degronLOCKR to impart feedback control on biological pathways in *S. cerevisiae*, and describe the role the tunability of degronLOCKR plays in designing feedback.

Collaborators at UCSF identified signaling proteins that activate upon addition of α-factor to yeast culture, and used degronLOCKR to control the activity of these proteins. By fusing degronLOCKR to the native copy of these signaling proteins, they identified the impact of fusing degronSwitch onto Ste20, Ste11, Fus3, and Ste12, which are well known to act as positive regulators in the α-factor pathway, therefore decrease pathway activity when degronLOCKR is activated (Extended Data Figure 18). Conversely, they discover that Fus3 acts as a negative regulator in the nucleus, therefore increases activity of the α-factor pathway when degraded in the nucleus. Studying this phenomenon is of interest for future work, and is allowed by the modularity of the degronLOCKR technology. To close the circuit, they engineer the α-factor pathway to express the Key. As a result, the more active the pathway the more Key is made which in turn degrades the regulators of the pathway. Using this strategy to degrade Ste12 they demonstrate that under higher α-factor load, the pathway is progressively less active as it imparts negative feedback upon itself. On the other hand, degrading the negative regulator Fus3 in the nucleus enhances activity of the α-factor pathway such that lower amounts of α-factor activate the pathway than in wild type. (Extended Data Figure 19) Their major contribution to the project is the strategy of fusing degronLOCKR to signaling proteins, as well as fully characterizing the operational properites of the degronLOCKR system (Extended Data Figure 20).

The design part of this project that I contributed to involves using the tunability of degronLOCKR to tune the extent of feedback on this yeast circuit. The process of tuning the feedback essentially means how strong the connection is from the process (pathway activity) to the controller (degronLOCKR activation) as diagrammed in Figure 12a. One strategy for achieving this include varying sensitivity of the Key promoter to pathway activity. A very sensitive promoter will strongly connect pathway activity with degradation shown in Figure 12b by the strong promoter resisting addition of Pg (as read out from reduced YFP expression in the synthetic system in Extended Data Figure 20) moreso than weaker promoters. The other strategy is to modulate the affinity of the Key for the Switch. The strongest key causes the most

degradation of the transcription factor under the least pathway activity, shown by lack of YFP expression under addition of Pg, and a weak key is only able to to induce modest feedback (Figure 12c). Applying the results from this synthetic circuit to the α-factor pathway, we are able to control the feedback on Ste12 by two knobs. Figure 12d outlines the strategy to combine promoter strength with Key strength to achieve tight control on biological feedback. As a result, Figure 12e shows that we can put the α-factor pathway under loose feedback (with weak promoter and weak Key) with only modest drop in YFP expression at high α-factor, while in the opposite scheme (strong promoter, strong Key) we completely ablate the response to α-factor. Figure 12e also demonstrates that this feedback acts on the timescale of a couple hours and is tunable to a range between these two extremes.

It is instructive to take these results and apply them to problems in cell based therapies. This proof of concept in yeast can be extended to human cells, though the biological problems become more complicated. The ability to engineer cells to dynamically respond to their environment is a large open problem in synthetic biology, and a problem that degronLOCKR is uniquely qualified to tackle.

CONCLUSIONS AND A LOOK FORWARD

The design of tunable and generalizable protein switches is a considerable advance for de novo protein design, which has focused largely on systems that have single stable states (the elegant designed membrane protein ROCKER is thought to alternate between two states, but there is no environmental trigger[7]). In the switchable LOCKR system described here, a designed key added in trans induces a large conformational change in a designed cage that unlocks protein function. We demonstrate the power and generality of LOCKR by caging several distinct functions: in vitro, the proapoptotic peptide Bim binding to Bcl2, StrepTag II binding, and a host of biotechnologically interesting peptides, and in cells, protein degradation mediated by the cODC degron, and protein localization via a nuclear export sequence. The modularity and hyperstability of de novo designed proteins enables tuning of switch activation over a broad dynamic range by modulating the strength of the competing Cage-Key and Cage-Latch interfaces. Moving forward, LOCKR provides a general approach for controlling function that should be applicable to a wide range of proteins and synthetic biology challenges.

It is instructive to compare LOCKR to regulatory systems in nature that utilize autoinhibition and attempts to co-opt those systems for engineered protein switches. Activation of the apoptosis cascade by the pro-apoptotic proteins Bak and Bax can be triggered by displacement of auto-inhibitory interactions[46], analogous to Key activation in LOCKR. Actin nucleation is modulated by N-WASP, which has an autoinhibited actin nucleating Arp2/3 binding domain that is released upon binding to the activators Cdc42 and PIP2. A number of proteins, including N-WASP, have been repurposed to control non-cognate functions in a switchable, inducible manner[47,48], but the LOCKR system has several advantages. First, LOCKR is a universal platform to cage and then activate at will functionalities ranging from inducible activation of high-affinity protein-protein interactions to controlled degradation to localization of an attached cargo. Second, for any functional modality, many cargos can be regulated: we have shown here how a transcription factor and hence gene expression can be efficiently modulated by LOCKR-gated degradation, but other cargoes including kinases and other enzymes can also be controlled in the same way. This should be contrasted to strategies that rely on repurposing of natural switches where the switching mechanism and tuning strategy are highly specialized to the output and ligand; the marginal cost of creating a new synthetic switch from natural parts can be high due to the need for extensive engineering. In contrast, altering the affinities of LOCKR components is tunable based on simple design principles that are general irrespective of the functional modality or application. Our use of a toehold for tuning the displacement of an alpha helix is reminiscent of DNA strand displacement technology in which a single strand can bind a single-stranded toehold of duplex DNA and displace the shorter of the two strands in the duplex[49,50]. Viewed in this light, LOCKR brings to proteins the modularity of DNA switching technology, with the advantages of tunability and flexibility over rewired natural protein systems, and ready interfacing with biological machinery over DNA nanotechnology. More generally, the domain of sophisticated environmentally sensitive and switchable function no longer belongs exclusively to naturally occurring proteins.

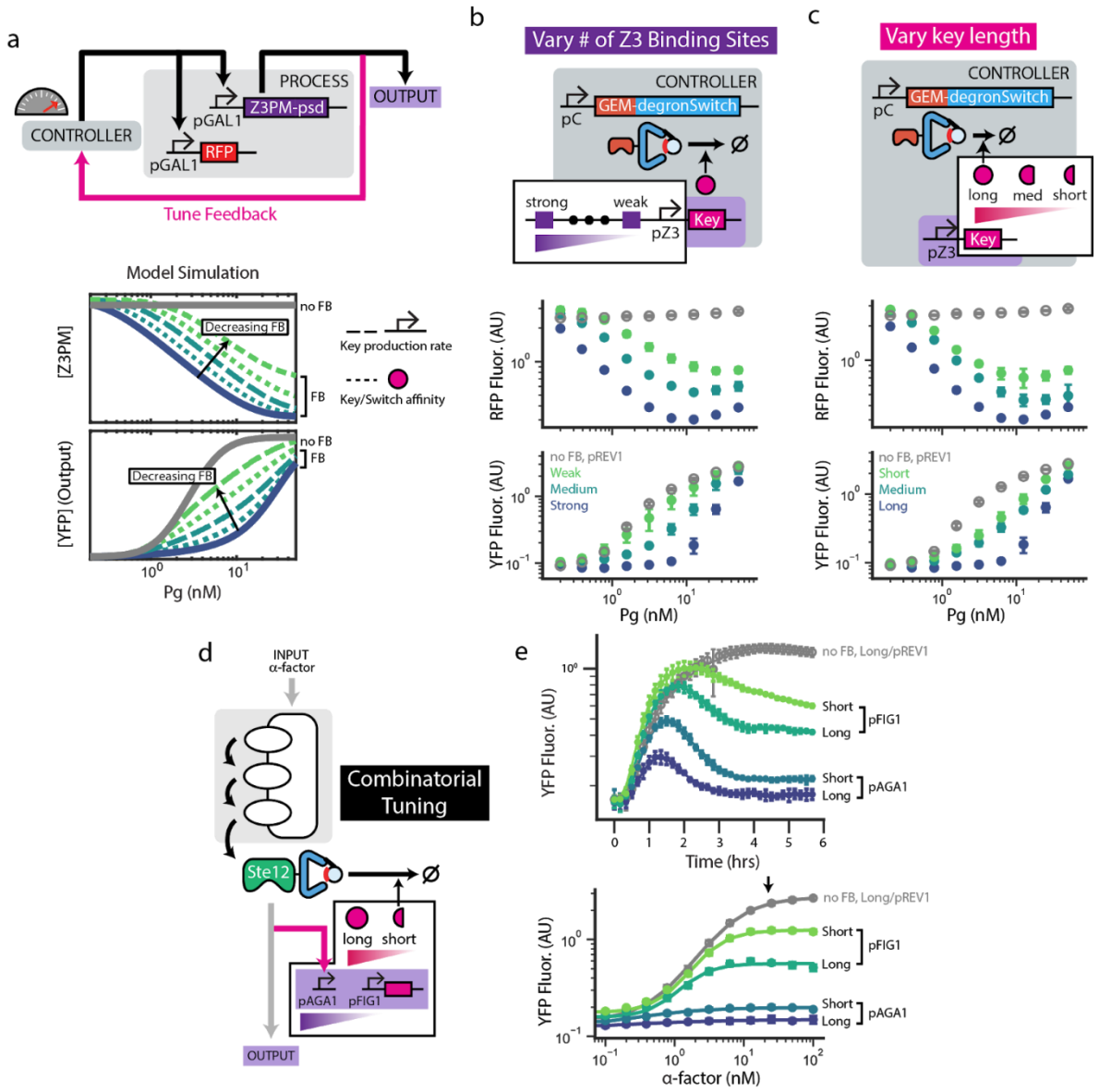

Figure 12 - degronLOCKR synthetic feedback strategy is predictably tunable

a) (Top) Exploring different methods to tune the feedback strength in the synthetic feedback circuit. (Bottom) Model simulation (see supplementary information) of circuit output and Z3PM as a function of Pg disturbance for decreasing key production rate or key/switch affinity. b & c) Experimental validation of tuning. **b)** (Top) Tuning feedback by varying the number of Z3 binding sites on pZ3 with the key at a fixed length. (Bottom) RFP and YFP fluorescence as a function of Pg for strong (pZ3-6x), medium (pZ3-4x), and weak (pZ3-3x) feedback strains versus no feedback (pREV1-key-CFP-NLS) strain. Points represent mean ± s.d. of three biological replicates. **c)** (Top) Tuning feedback by varying the length of the key with the strength of the feedback promoter fixed at pZ3-6x. (Bottom) RFP and YFP fluorescence as a function of Pg for long (55 aa), medium (51 aa), and short (43 aa) key feedback strains versus no feedback (pREV1-NLS-key-CFP) strain. Points represent mean ± s.d. of three biological replicates. **d)** Changing promoter strength and key length to tune feedback on the synthetic negative feedback loop in the mating pathway. pAGA1 is a stronger reporter of the mating pathway than pFIG1. **e)** (Top) Dynamic measurements of pAGA1-YFP-cODC for various feedback and no feedback strains following stimulation with 25nM α-factor. Solid line represents a moving average taken over three flow cytometry data points and points represent the mean ± s.d. of three biological replicates. (Bottom) α-factor dose response of feedback strains versus a no feedback (pREV1-NLS-key-CFP) strain. YFP fluorescence was measured using flow cytometry four hours after α-factor induction. Points represent the mean of three biological replicates and and error bars represent the standard error. Solid lines are a hill function fit to the data. The dose of α-factor used in the dynamic experiment (top) is indicated on the graph.

BIBLIOGRAPHY

1. Huang, P.-S., Boyken, S. E. & Baker, D. The coming of age of de novo protein design. *Nature* **537**, 320–327 (2016).

2. Huang, A. P., Oberdorfer, G., Xu, C., Pei, X. Y. & Brent, L. Title : High thermodynamic stability of parametrically designed helical bundles.

3. Brunette, T. J. *et al.* Exploring the repeat protein universe through computational protein design. *Nature* **528**, 580–584 (2015).

4. Rocklin, G. J. *et al.* Global analysis of protein folding using massively parallel design, synthesis, and testing. *Science (80-.).* **357**, 168–175 (2017).

5. Ambroggio, X. I. & Kuhlman, B. Design of protein conformational switches. *Curr. Opin. Struct. Biol.* **16**, 525–530 (2006).

6. Choi, J. H., Laurent, A. H., Hilser, V. J. & Ostermeier, M. Design of protein switches based on an ensemble model of allostery. 6968 (2015). doi:10.1038/ncomms7968

7. Joh, N. H. *et al.* De novo design of a transmembrane Zn^{2+}-transporting four-helix bundle. *Science (80-.).* **346**, 1520–1524 (2014).

8. Davey, J. A., Damry, A. M., Goto, N. K. & Chica, R. A. Rational design of proteins that exchange on functional timescales. *Nat. Chem. Biol.* **13**, 1280–1285 (2017).

9. Ha, J.-H. & Loh, S. N. Protein conformational switches: from nature to design. *Chemistry* **18**, 7984–99 (2012).

10. Liu, J. & Nussinov, R. Allostery: An Overview of Its History, Concepts, Methods, and Applications. *PLoS Comput. Biol.* **12**, e1004966 (2016).

11. Raman, S., Taylor, N., Genuth, N., Fields, S. & Church, G. M. Engineering allostery. *Trends Genet.* **30**, 521–528 (2014).

12. Perkins, J. R., Diboun, I., Dessailly, B. H., Lees, J. G. & Orengo, C. Transient protein-protein interactions: structural, functional, and network properties. *Structure* **18**, 1233–1243 (2010).

13. Singh, G. P., Ganapathi, M. & Dash, D. Role of intrinsic disorder in transient interactions of hub proteins. *Proteins* **66**, 761–765 (2007).

14. Dou, J. *et al.* De novo design of a fluorescence-activating $β$-barrel. *Nature* (2018).

15. Boyken, S. E. *et al.* De novo design of protein homo-oligomers with modular hydrogen-bond network–mediated specificity. *Science (80-.).* **352**, 680–687 (2016).

16. Dyer, K. N. *et al.* High-throughput {SAXS} for the characterization of biomolecules in solution: a practical approach. *Methods Mol. Biol.* **1091**, 245–258 (2014).

17. Fleming, P. J. & Rose, G. D. Do all backbone polar groups in proteins form hydrogen bonds? *Protein Sci.* **14**, 1911–1917 (2005).

18. Chothia, C. & Janin, J. Principles of protein--protein recognition. *Nature* **256**, 705 (1975).

19. Moreira, I. S., Fernandes, P. A. & Ramos, M. J. Hot spots---A review of the protein--protein interface determinant amino-acid residues. *Proteins: Struct. Funct. Bioinf.* **68**, 803–812 (2007).

20. Delgado-Soler, L., Pinto, M., Tanaka-Gil, K. & Rubio-Martinez, J. Molecular Determinants of {Bim(BH3}) Peptide Binding to {Pro-Survival} Proteins. *J. Chem. Inf. Model.* **52**, 2107–2118 (2012).

21. Berger, S. *et al.* Computationally designed high specificity inhibitors delineate the roles of {BCL2} family proteins in cancer. *Elife* **5**, (2016).

22. Grigoryan, G. & Degrado, W. F. Probing designability via a generalized model of helical bundle geometry. *J. Mol. Biol.* **405**, 1079–1100 (2011).

23. Crick, F. H. C. The Fourier transform of a coiled-coil. *Acta Crystallogr.* **6**, 685–689 (1953).

24. Ikeda, K., Watanabe, Y., Ohto, H. & Kawakami, K. Molecular interaction and synergistic activation of a promoter by Six, Eya, and Dach proteins mediated through {CREB} binding protein. *Mol. Cell. Biol.* **22**, 6759–6766 (2002).

25. Giesecke, A. V, Fang, R. & Joung, J. K. Synthetic protein-protein interaction domains created by shuffling {Cys2His2} zinc-fingers. *Mol. Syst. Biol.* **2**, 2006.2011 (2006).

26. Rehtanz, M., Schmidt, H.-M., Warthorst, U. & Steger, G. Direct interaction between nucleosome assembly protein 1 and the papillomavirus {E2} proteins involved in activation of transcription. *Mol. Cell. Biol.* **24**, 2153–2168 (2004).

27. Kuhlman, B. & Baker, D. Native protein sequences are close to optimal for their structures. *Proc. Natl. Acad. Sci. U. S. A.* **97**, 10383–10388 (2000).

28. Leaver-Fay, A. *et al.* Chapter nineteen - Rosetta3: An {Object-Oriented} Software Suite for the Simulation and Design of Macromolecules. in *Methods in Enzymology* (eds. Johnson, M. L. & Brand, L.) **487**, 545–574 (Academic Press, 2011).

29. Takeuchi, J., Chen, H., Hoyt, M. A. & Coffino, P. Structural elements of the ubiquitin-independent proteasome degron of ornithine decarboxylase. *Biochem. J* **410**, 401–407 (2008).

30. Aranda-D\'\iaz, A., Mace, K., Zuleta, I., Harrigan, P. & El-Samad, H. Robust Synthetic

Circuits for {Two-Dimensional} Control of Gene Expression in Yeast. *ACS Synth. Biol.* **6**, 545–554 (2017).

31. Güttler, T. *et al.* NES consensus redefined by structures of PKI-type and Rev-type nuclear export signals bound to CRM1. *Nat. Struct. Mol. Biol.* (2010). doi:10.1038/nsmb.1931

32. Kosugi, S. *et al.* Six classes of nuclear localization signals specific to different binding grooves of importinα. *J. Biol. Chem.* (2009). doi:10.1074/jbc.M807017200

33. Schmidt, T. G. M. & Skerra, A. The Strep-tag system for one-step purification and high-affinity detection or capturing of proteins. *Nat. Protoc.* (2007). doi:10.1038/nprot.2007.209

34. Pace, C. N. & Scholtz, J. M. A helix propensity scale based on experimental studies of peptides and proteins. *Biophys. J.* (1998).

35. Frishman, D. & Argos, P. Knowledge-based protein secondary structure assignment. (1995). doi:10.1002/prot.340230412

36. Mann, M. & Jensen, O. N. Proteomic analysis of post-translational modifications. *Nature Biotechnology* (2003). doi:10.1038/nbt0303-255

37. Kapust, R. B. *et al.* Tobacco etch virus protease: mechanism of autolysis and rational design of stable mutants with wild-type catalytic proficiency. *Protein Eng.* (2001).

38. Zakeri, B. *et al.* Peptide tag forming a rapid covalent bond to a protein, through engineering a bacterial adhesin. *Proc. Natl. Acad. Sci. U. S. A.* (2012). doi:10.1073/pnas.1115485109

39. Schoene, C., Fierer, J. O., Bennett, S. P. & Howarth, M. SpyTag/Spycatcher cyclization confers resilience to boiling on a mesophilic enzyme. *Angew. Chemie - Int. Ed.* (2014). doi:10.1002/anie.201402519

40. Gao, X., Fang, J., Xue, B., Fu, L. & Li, H. Engineering Protein Hydrogels Using SpyCatcher-SpyTag Chemistry. *Biomacromolecules* (2016). doi:10.1021/acs.biomac.6b00566

41. Nallamsetty, S. *et al.* Efficient site-specific processing of fusion proteins by tobacco vein mottling virus protease in vivo and in vitro. *Protein Expr. Purif.* (2004). doi:10.1016/j.pep.2004.08.016

42. Dixon, A. S. *et al.* NanoLuc Complementation Reporter Optimized for Accurate Measurement of Protein Interactions in Cells. *ACS Chem. Biol.* (2016). doi:10.1021/acschembio.5b00753

43. Khalil, A. S. *et al.* A synthetic biology framework for programming eukaryotic transcription functions. *Cell* (2012). doi:10.1016/j.cell.2012.05.045

44. Nielsen, A. A. K. *et al.* Genetic circuit design automation. *Science (80-.).* (2016). doi:10.1126/science.aac7341

45. Perez-Pinera, P. *et al.* RNA-guided gene activation by CRISPR-Cas9-based transcription factors. *Nat. Methods* (2013). doi:10.1038/nmeth.2600

46. Westphal, D., Dewson, G., Czabotar, P. E. & Kluck, R. M. Molecular biology of Bax and Bak activation and action. *Biochim. Biophys. Acta* **1813**, 521–531 (2011).

47. Dueber, J. E., Yeh, B. J., Bhattacharyya, R. P. & Lim, W. A. Rewiring cell signaling: the logic and plasticity of eukaryotic protein circuitry. *Curr. Opin. Struct. Biol.* **14**, 690–699 (2004).

48. Stein, V. & Alexandrov, K. Synthetic protein switches: design principles and applications. *Trends Biotechnol.* **33**, 101–110 (2015).

49. Zhang, D. Y. & Winfree, E. Control of {DNA} strand displacement kinetics using toehold exchange. *J. Am. Chem. Soc.* **131**, 17303–17314 (2009).

50. Linko, V. & Dietz, H. The enabled state of {DNA} nanotechnology. *Curr. Opin. Biotechnol.* **24**, 555–561 (2013).

APPENDIX A – METHODS

PCR mutagenesis and isothermal assembly

All primers for mutagenesis were ordered from Integrated DNA Technologies (IDT). Mutagenic primers were designed to anneal >18bp on either side of the site for mutagenesis with the desired mutation encoded in the primer. PCR was used to create fragments upstream and downstream of the mutation site with >20bp overlap with the desired pET vector. The resulting amplicons were isothermally assembled into either pET21b, pET28b, or pET29b restriction digested with XhoI and NdeI and transformed into chemically competent *E. coli* XL1-Blue cells. Monoclonal colonies were sequenced with Sanger sequencing. Sequence verified plasmid was purified using Qiagen miniprep kit and transformed into chemically competent *E. coli* BL21(DE3)Star, BL21(DE3)Star-pLysS cells (Invitrogen), or Lemo21(DE3) cells (NEB) for protein expression.

Synthetic gene construction

Synthetic genes were ordered from Genscript Inc. (Piscataway, NJ, USA) and delivered in pET 28b+, pET21b+, or pET29b+ *E. coli* expression vectors, inserted at the NdeI and XhoI sites of each vector. For pET28b+ constructs, synthesized DNA was cloned in frame with the N-terminal hexahistidine tag and thrombin cleavage site and a stop codon was added at the C-terminus. For pET21b+ constructs, a stop codon was added at the C-terminus such that the protein was expressed with no hexahistidine tag. For pET29b+ constructs, the synthesized DNA was cloned in frame with the C-terminal hexahistidine tag. Plasmids were transformed into chemically competent *E. coli* BL21(DE3)Star, BL21(DE3)Star-pLysS cells (Invitrogen), or Lemo21(DE3) cells (NEB) for protein expression.

Bacterial protein expression and purification

Starter cultures were grown in Lysogeny Broth (LB) or Terrific Broth II (TBII) overnight in the presence of 50 μg/mL carbenicillin (pET21b+) or 30 μg/mL (for LB) to 60 μg/mL (for TBII) kanamycin (pET28b+ and pET29b+). Starter cultures were used to inoculate 500 mL of Studier TBM-5052 autoinduction media containing antibiotic and grown at 37 ℃ for 24 hours. Cells were harvested by centrifugation at 4000 rcf for 20 minutes at 4 ℃ and resuspended in lysis

buffer (20 mM Tris, 300 mM NaCl, 20 mM Imidazole, pH 8.0 at room temperature), then lysed by microfluidization in the presence of 1 mM PMSF. Lysates were cleared by centrifugation at 24,000 rcf for at least 30 minutes at 4 ℃. Supernatant was applied to Ni-NTA (Qiagen) columns pre-equilibrated in lysis buffer. The column was washed twice with 15 column volumes (CV) of wash buffer (20 mM Tris, 300 mM NaCl, 40 mM Imidazole, pH 8.0 at room temperature), followed by 15 CV of high-salt wash buffer (20 mM Tris, 1 M NaCl, 40 mM Imidazole, pH 8.0 at room temperature) then 15 CV of wash buffer. Protein was eluted with 20 mM Tris, 300 mM NaCl, 250 mM Imidazole, pH 8.0 at room temperature. Proteins were further purified by gel filtration using FPLC and a Superdex™ 75 Increase 10/300 GL (GE) size exclusion column, pooling fractions containing monomeric protein.

Size-exclusion Chromatography, Multi-Angle Light Scattering (SEC-MALS)

SEC-MALS experiments used a Superdex™ 75 Increase 10/300 GL (GE) size exclusion column connected to a miniDAWN TREOS multi-angle static light scattering and an Optilab T-rEX (refractometer with EXtended range) detector (Wyatt Technology Corporation, Santa Barbara CA, USA). Protein samples were injected at concentrations of 3-5 mg/mL in TBS (pH 8.0). Data was analyzed using ASTRATM (Wyatt Technologies) software to estimate the weight average molar mass (Mw) of eluted species, as well as the number average molar mass (Mn) to assess monodispersity by polydispersity index (PDI) = Mw/Mn.

Circular dichroism (CD) measurements

CD wavelength scans (260 to 195 nm) and temperature melts (25 to 95 ℃) were measured using an AVIV model 420 CD spectrometer. Temperature melts monitored absorption signal at 222 nm and were carried out at a heating rate of 4 ℃/min. Protein samples were at 0.3 mg/mL in PBS pH 7.4 in a 0.1 cm cuvette. Guanidinium chloride (GdmCl) titrations were performed on the same spectrometer with an automated titration apparatus in PBS pH 7.4 at 25 ℃, monitored at 222 nm with protein sample at 0.03 mg/mL in a 1cm cuvette with stir bar. Each titration consisted of at least 40 evenly distributed concentration points with one minute mixing time for each step. Titrant solution consisted of the same concentration of protein in PBS + GdmCl. GdmCl concentration was determined by refractive index.

Small angle X-ray scattering (SAXS)

Samples were exchanged into SAXS buffer (20 mM Tris, 150 mM NaCl, 2% glycerol, pH 8.0 at room temperature) via gel filtration. Scattering measurements were performed at the SIBYLS 12.3.1 beamline at the Advanced Light Source. The X-ray wavelength (λ) was 1.27 Å and the sample-to-detector distance of the Mar165 detector was 1.5 m, corresponding to a scattering vector q ($q = 4\pi*\sin(\theta/\lambda)$ where 2θ is the scattering angle) range of 0.01 to 0.59 $Å^{-1}$. Data sets were collected using 34 0.2 second exposures over a period of 7 seconds at 11 keV with protein at a concentration of 6 mg/mL. Data were also collected at a concentration of 3 mg/mL to determine concentration-dependence; all presented data was collected at the higher concentration as no concentration-dependent aggregation was observed. Data from 32 exposures was averaged separately over the Gunier, Parod, and Wide-q regions depending on signal quality over each region and frame. The averages were analyzed using the *ScÅtter* software package to analyze data and report statistics (Extended Data Table 1). *FoXS* was used to compare design models to experimental scattering profiles and calculate quality of fit (*X*) values. The hexahistidine tags and thrombin cleavage sites on the N-termini of LOCKR proteins were modeled using Rosetta Remodel so that the design sequence matched that of the experimentally tested protein. To capture conformational flexibility of these residues, 100 independent models were generated, clustered, and the cluster center of the largest cluster was selected as a representative model for *FoXS* fitting without bias.

GFP pulldown assay

His-tagged LOCKR was expressed per the above protocol from pET28b+ while the Key was expressed fused to superfolder GFP (sfGFP) without a his-tag in pET21b+. The his-tagged LOCKR was purified to completion and dialyzed into TBS (20 mM Tris, 150 mM NaCl, pH 8.0 at room temperature); the Key-GFP remained as lysate for this assay. 100 μL LOCKR at >1 μM was applied to a 96-well black Pierce® Nickel Coated Plate (ThermoFisher) and incubated at room temperature for 1 hour. Sample was discarded from the plate and washed 3x with 200 μL TBST (TBS + 0.05% Tween-20). 100 μL of lysate containing Key-GFP was added to each well and incubated at room temperature for 1 hour. Sample was discarded from the plate and washed 3x with 200 μL TBST (TBS + 0.05% Tween-20). The plate was washed 1x with TBS, and 100 μL of TBS was added to each well. sfGFP fluorescence was measured on a Molecular Devices

SpectraMax M5 plate reader or BioTek Synergy Neo2 plate reader; fluorescence was measured at 485 nm excitation and 530 nm emission, with a bandwidth of 20 nm for excitation and emission.

Bio-Layer Interferometry (BLI)

BLI measurements were made on an Octet® RED96 System (ForteBio) with streptavidin (SA) coated biosensors and all analysis was performed within ForteBio Data Analysis Software version 9.0.0.10. Assays were performed with protein diluted into HBS-EP+ Buffer from GE (10 mM HEPES, 150 mM NaCl, 3 mM EDTA, 0.05% v/v Surfactant P20, 0.5% non-fat dry milk, pH 7.4 at room temperature). Biotinylated Bcl2 was loaded onto the SA tips to a threshold of 0.5 nm programmed into the machine's protocol. Baseline was obtained by dipping the loaded biosensors into HBS-EP+ buffer; association kinetics were observed by dipping into wells containing defined concentrations of LOCKR and Key, then dissociation kinetics were observed by dipping into the buffer used to obtain the baseline. Kinetic constants and response at equilibrium were computed by fitting a 1:1 binding model.

Construction of DNA circuits

Hierarchical golden gate assembly was used to assemble plasmids for yeast strain construction using the method in Lee et al.[42]. Individual parts had their BsaI, BsmBI, and NotI cut sites removed to facilitate downstream assembly and linearization. Parts were either generated via PCR or purchased as gBlocks from IDT. These parts were assembled into transcriptional units (promoter-gene-terminator) on cassette plasmids. These cassettes were then assembled together to form multi-gene plasmids for insertion into the yeast genome. All plasmids used for yeast integration are listed in Supplementary Table 1.

Yeast strains and growth media

The base *S. cerevisiae* strain used in all experiments was BY4741 (MATa his3Δ1 leu2Δ0 met15Δ0 ura3Δ0). All yeast cultures were grown in YPD media (10 g/L Bacto Yeast Extract, 20 g/L Bacto peptone, 20 g/L dextrose) or synthetic complete medium (SDC) (6.7 g/L Bacto-yeast nitrogen base without amino acids, 2 g/L complete supplement amino acid mix, 20 g/L dextrose). Selection of auxotrophic markers (URA3, LEU2, and/or HIS3) was performed on synthetic

complete medium with the appropriate dropout amino acid mix. All yeast strains used in this work are listed in Supplementary Table 2.

Estradiol and Progesterone induction

Yeast strains were grown overnight by picking a single colony from a plate into YPD media. Saturated culture was diluted 1:500 in fresh SDC and aliquoted into individual wells of a 2 mL 96 well storage block (Corning) for a three hour outgrowth at 30 ℃ and 900 RPM in a Multitron shaker (Infors HT). Estradiol (Sigma-Aldrich) and progesterone (Fisher Scientific) were prepared at a 10x concentration by making the appropriate dilutions into SDC from a 3.6 mM estradiol and 3.2 mM progesterone stock solution. After the three hour outgrowth, 50 µl of estradiol and progesterone inducer were added to the 96 well block in the appropriate combinations and the block was returned to the shaker.

Mammalian Cell Culture and Transfection

HEK293T cells were maintained in DMEM (Dulbecco's Modified Eagle Medium, Gibco) supplemented with 10% Fetal Calf Serum (SAFC) and passaged every ~3 days.

Transfections were done in triplicate, with Fugene HD (Promega), according to manufacturer's instructions.

Description of automated flow cytometry and continuous culture system

Hardware

We adapted an existing automated experimental platform [31] to perform variable concentration small molecule induction and long-term culturing. Yeast cultures were grown in 50 mL optically clear conical tubes (Falcon) that were held in eight custom temperature-controlled, magnetically stirred chambers. Liquid handling was accomplished using a 14 position stream selector (VICI Cheminert) and two syringe pumps (Cavro XCalibur Pump, TECAN) of a BD High-Throughput Sampler. Commands to the HTS were controlled using LABVIEW 2013. This setup allowed for periodic sampling and dilution of individual cultures. Each sampling period consisted of three main steps: 1) send sample to flow cytometer for measurement, 2) extract culture and send to waste, and 3) replenish culture with fresh media at desired hormone concentration. Each sampling period can be designated to either induce cultures to a new higher hormone

concentration or to maintain desired hormone concentration. A sampling frequency of 24 minutes and a dilution volume of 3 mL were used.

Yeast culture

Yeast strains were grown overnight by picking a single colony from a plate into YPD media. Saturated culture was diluted 1:200 into fresh SDC. Cultures were grown for 2 hours in glass tubes at 30C and 250RPM in a Innova 44 shaker (New Brunswick). Cultures were then diluted to 0.01 OD600 in fresh SDC and aliquoted into individual 50 mL optically clear conical tubes (Falcon) at a total volume of 30mL YPD. Another one hour outgrowth was performed in bioreactors with magnetically-controlled stir bars at 30C. All SDC media was supplemented with 5,000U/mL Penicillin Streptomycin (Thermo-Fisher).

Estradiol and progesterone induction to test degronLOCKR dynamics

A 1X concentration was determined by the highest desired hormone concentration at which to test strains (30 nM E2 and 50 nM Pg, respectively). A solution of E2 and SDC media was created at a 10X concentration to bring pre-induced cultures to a desired concentration in one sampling period. A second solution of Pg and SDC media was created at a 10X concentration to induce Key expression after degSwitch-YFP expression reached steady-state. SDC media was prepared at three different concentrations of hormone: (1) 10X E2/no Pg, (2) 1X E2/no Pg, (3) 1X E2/10X Pg, and (4) 1X E2/1X Pg. After a one hour outgrowth in bioreactors (t=-6 hr), the first induction was performed to achieve E2 concentration by extracting 3 mL from all cultures and replenishing with (1). After E2 induction, sampling proceeded as described above (see *Hardware)*. All sampling periods following the first induction time point included sending a sample to the cytometer for measurement, extracting 3 mL from all cultures, and replenishing cultures with (2). During the second induction time point (t=0 hr), cultures were induced with (3) to activate Key expression. This induction was followed by the same procedure as the first induction, except that hormone concentrations were maintained by (4). Controls (no activated Key expression) did not undergo a second induction and, instead, continued to be replenished by (2).

Flow cytometry

Yeast experiments

Analysis of fluorescent protein expression was performed using a BD LSRII flow cytometer (BD Biosciences) equipped with a high-throughput sampler. Yeast cultures were diluted in TE before running through the instrument to obtain an acceptable density of cells. YFP (Venus) fluorescence was measured using the FITC channel, RFP (mScarlet) was measured using the PE-Texas Red channel, and BFP (mTagBFP2) was measured using the DAPI channel. For steady-state measurements, 5,000-10,000 events were collected per sample. For dynamic measurements, 2,000-10,000 events were collected per sample. Fluorescence values were calculated as the height (H) measurement for the appropriate channel and normalized to cell size by dividing by side scatter (SSC-H). All analysis of yeast flow cytometry data was performed in Python 2.7 using the package FlowCytometryTools and custom scripts.

HEK293T experiments

Analysis of fluorescent protein expression was performed using a BD Fortessa flow cytometer (BD Biosciences) equipped with a high-throughput sampler. Cells were harvested and washed twice in PBS before running through the instrument in PBS+5% FBS. mCherry fluorescence was measured using the PE-CF594 channel and BFP (tagBFP) was measured using the BV 421 channel. 50,000 events were collected per sample. Live cells were gated according to FSC-A and SSC-A, and singlets were gated according to SSC-A and SSC-H. Analysis of HEK293T flow cytometry data was performed using FlowJo v10.

Fluorescence microscopy

Saturated culture was diluted 1:100 in fresh SC media followed by a 3 hour outgrowth at 30 ℃ with shaking at 700 RPM in a Multitron shaker (Infors HT). Estradiol (Sigma-Aldrich) and progesterone (Fisher Scientific) were prepared at a 20x concentration by making the appropriate dilutions into SC media from a 3.6 mM estradiol and 3.2 mM progesterone stock solution. Cells were induced with estradiol and/or progesterone at a final concentration of 200 μM and 250 μM, respectively. After 8 hours of growth, cells were resuspended in 1x PBS and imaged on a Zeiss Axio Observer Z1 microscope with X-Cite Series 120 fluorescent lamp and Hamamatsu Orca-Flash 4.0 Digital Camera.

Thermodynamic LOCKR Model

The thermodynamic model in Figure 1a, main text, illustrates three free parameters for five equillibrea; one that defines the equillibrium of latch opening, one that defines the dissociation constant of the key, and one that defines the dissociation constant of the target. These define three equations that relate the concentrations of all species (open or closed Switch, Key, Target, Switch:Key, Switch:Target, and Switch:Key:Target) at equilibrium.

(i) $K_{open} = [Switch_{open}] / [Switch_{closed}]$

(ii) $K_{CK} = [Switch_{open}][Key] / [Switch{:}\,Key] = [Switch{:}\,Target][Key]/[Switch{:}\,Key{:}\,Target]$

(iii) $K_{LT} = [Switch{:}\,Key][Target] / [Switch{:}\,Key{:}\,Target] = [Switch_{open}][Target] /[Switch{:}\,Target]$

The total amount of each component (Switch, Key, and Target) is also constant, as defined by experimental conditions, and constrains the values of each species at equilibrium. This introduces the following equations to the model.

(iv) $[Switch]_{total} = [Switch_{open}] + [Switch_{closed}] + [Switch{:}\,Key] + [Switch{:}\,Target] + [Switch{:}\,Key{:}\,Target]$

(v) $[Key]_{total} = [Key] + [Switch{:}\,Key] + [Switch{:}\,Key{:}\,Target]$

(vi) $[Target]_{total} = [Target] + [Switch{:}\,Target] + [Switch{:}\,Key{:}\,Target]$

These six equations were solved using the python module `sympy.nsolve()`\cite{10.7717/peerj-cs.103} to find the concentration of each species at equilibrium given the six constants (three equilibrium constants, three total concentrations). To compute fraction bound for relevant figures, the total concentration of Switch:Target and Switch:Key:Target was extracted from this solution, divided by the total Target present, and plotted for the corresponding figures. Code for this model is contained in `LOCKR.py`, see Code Availability.

Rosetta Design of Orthogonal LOCKRs

The XML `redesign_c_terminal_helix_parallel.xml` (See Code Availability) was used to redesign LOCKRa to orthogonal cage-key pairs using Rosetta \cite{rosetta} with scorefunction `beta_nov16`. We extracted a model of the five-helix cage from the $LOCKR_a$ model and used Rosetta's BundleGridSampler module to generate an ensemble of backbones for new latch geometries. The BundleGridSampler generates backbone geometry based on the Crick expression for a coiled-coil \cite{crick_1953,helical_bundle} and allows efficient, parallel sampling of a regular grid of coiled-coil expression parameter values, which correspond to a

continuum of peptide backbone conformations. For each parametrically-generated latch conformation sampled, the InterfaceByVector residue selector specified the interface of the cage and latch for design of hydrogen bonding networks (HBNet) \cite{hbnet} followed by Rosetta sidechain design. Residues on the cage not selected by the residue selector were held constant to their original LOCKR design residues. Hydrogen Bond networks were designed using HBNetStapleInterface on the residues selected at the interface. The output contained designs with two or three hydrogen bond networks which span the three helices that make up the interface. Downstream design and filtering was performed according to previous methods. \cite{hbnet}

Candidate orthogonal LOCKR designs were selected based on lacking unsatisfied buried hydrogen bonding residues, the count of alanine residues as a proxy for packing quality, and sequence dissimilarity as a metric to find most dissimilar polar/hydrophobic patterning, to select for orthogonality. Unsatisfied hydrogen bonding atoms were filtered out using the BuriedUnsatHbonds filter allowing no unsatisfied polar atoms according to the filter's metrics. Packing quality was determined by counting alanine residues at the interface because high alanine count means poor interdigitation of residues. A maximum of 15 alanine residues were allowed in the entire three helix interface. Pairwise sequence dissimilarity of every designed latch was scored with BLOSUM62 by aligning sequences using the Bio.pairwise2 package from BioPython \cite{biopython} as shown in `seq_alignment.py` (See Code Availability). Alignment was performed disallowing gaps within the sequence (using large opening and extension penalties) which is analogous to a structural alignment of two helices to find the most similar superposition based on hydrophobic-polar patterning. Each score was subtracted from the maximum score to convert scores into a distance metric; the most diverse sequences has the lowest BLOSUM62 score which converts to the largest distance. The resulting matrix is shown in Extended Data Figure 5. The sequences were then clustered using `HeirClust_fromRMSD.py` and clustered with a cutoff of 170 (horizontal line in Extended Data Figure 6), resulting in 13 clusters. The center of each cluster was picked by maximizing distance between the 13 centers selected. The 13 candidates were then filtered by eye in PyMol 2.0 for unsatisfied hydrogen bonding atoms and qualitative packing quality. The five best designs by these three metrics were ordered as $LOCKR_{b\text{-}f}$.

Further utilizing the Switch$_a$ scaffold in mammalian cells requires redesign to enhance stable expression. The Switch scaffold contains amino acid sequence repeats leftover from the original symmetric, homotrimeric design; the asymmetrized degronSwitch was designed using Rosetta\cite{rosetta} to identify asymmetric sequence changes in these repeated regions that are compatible with the Switch scaffold structure to maintain overall topology and packing interactions.

Calculation of degronLOCKR Half-Life

The half-life of degronLOCKR-induced degradation was calculated using two equations that model the system before and after key induction:

(vii) $\frac{dYFP_{caged}}{dt} = \alpha - (\gamma + \beta_{caged}) * YFP_{caged}$

(viii) $\frac{dYFP_{uncaged}}{dt} = \alpha - (\gamma + \beta_{uncaged}) * YFP_{uncaged}$

where α is the YFP production rate, γ is the dilution rate, β_{caged} is the caged degronLOCKR-mediated degradation rate (without key induction), and $\beta_{uncaged}$ is the uncaged degronLOCKR-mediated degradation rate (with key induction). We expect that $\beta_{uncaged}$ is a function of key concentration but here we will only consider the active degradation rate at steady-state for a single key concentration. We first calculated γ as a function of the measured growth rate and the dilution rate:

(ix) $\gamma = \frac{\ln 2}{T_d} + \frac{\frac{V_e}{V_t}}{T_s}$

where T_d is the doubling time of the culture, V_e is the volume removed during each sampling, V_t is the total volume in each bioreactor, and T_s is the sampling period. To solve for β_{caged} and α, we first found the solution to equation (vii):

(x) $YFP_{caged}(t) = \frac{\alpha}{\gamma + \beta_{caged}} * \left(1 - e^{-(\gamma+\beta_{caged})*t}\right)$

When $t = t_{rise} = \frac{1}{\gamma + \beta_{caged}}$:

(xi) $YFP_{caged}(t_{rise}) = YFP_{SS} * (1 - e^{-1}) = 0.63 * YFP_{SS}$

where $YFP_{SS} = \frac{\alpha}{\gamma + \beta_{caged}}$. We solved for β_{caged} by determining t_{rise}, which allowed allowed us to calculate α using the steady-state YFP expression measurement before key induction:

$$\alpha = YFP\_SS * (\gamma + \beta_{uncaged})$$

Using γ and α we were able to calculate β_{caged}. The degradation rate of the degronSwitch (β) is a function of key concentration, but to simplify our calculation we were only interested in determining uncaged degronLOCKR half-life at steady-state key concentration. Thus we determined $\beta_{uncaged}$ using the steady-state of equation (viii). The calculated half-life of uncaged degronLOCKR is equal to $\frac{\ln 2}{\beta_{uncaged}}$, or 24 minutes. The half-life of caged degronLOCKR, or $\frac{\ln 2}{\beta_{caged}}$, is equal to 310.6 minutes, indicating that uncaging of degronLOCKR upon key induction increases degradation by over 10-fold.

Structural visualization and figures

All structural images for figures were generated using PyMOL[43].

Code Availability

Python scripts, bash scripts, and Rosetta Design XMLs are available for download at https://github.com/BobbyLangan/DeNovoDesignofBioactiveProteinSwitches

APPENDIX B – EXTENDED DATA

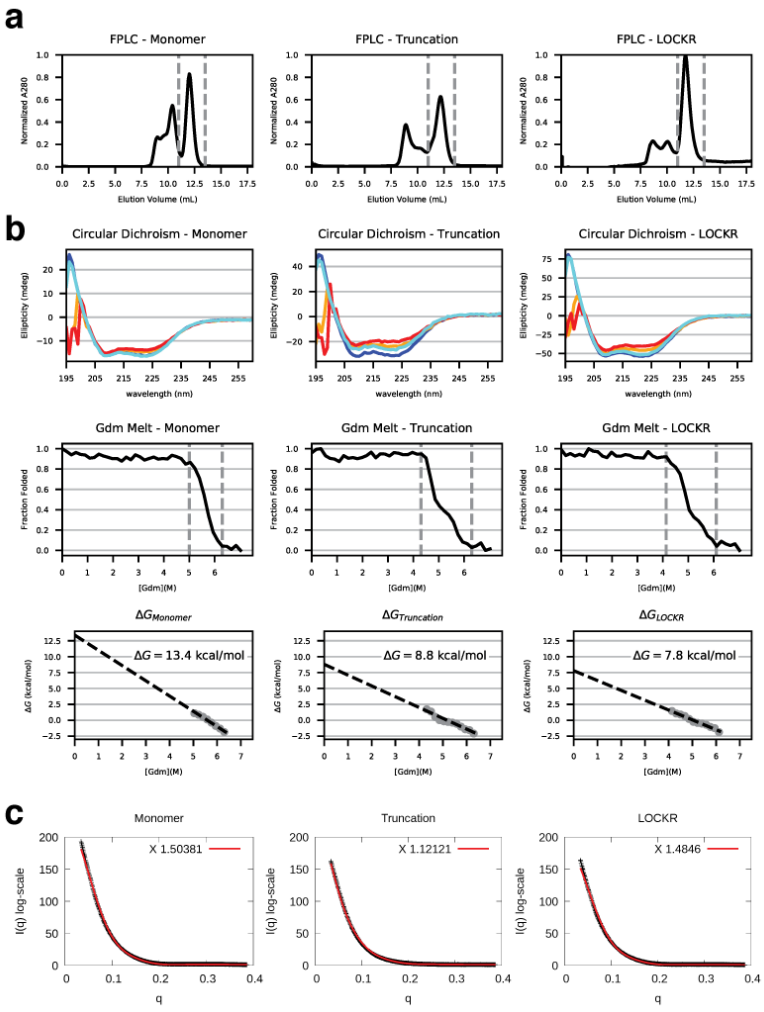

Extended Data Figure 1 – Biophysical characterization of LOCKR

Biophysical data from LOCKR design. a) Size Exclusion Chromatography for the Monomer, Truncation, and LOCKR designs on Superdex 75. Peaks indicated by vertical dashed lines represent monomeric protein used in downstream characterization and functional assays. b) Circular dichroism spectroscopy to determine protein stability upon heating and chemical denaturant, Guanidinium Chloride-HCl. Top row: full wavescan at 25°C (blue), 75°C (orange), 95°C (red), then cooled to 25°C (cyan). Middle row: guanidine melts also shown overlapped in Figure 1d. Bottom row: fraction folded was converted to equilibrium constant, then to $\Delta G_{unfolding}$ value. The linear unfolding region, marked by vertical lines in middle row, was fit to determine

the $\Delta G_{folding}$ for each design. c) SAXS spectra (black) referenced in Figure 1e fit to Rosetta design models (red) using FoXS with chi-values referenced in the upper right.

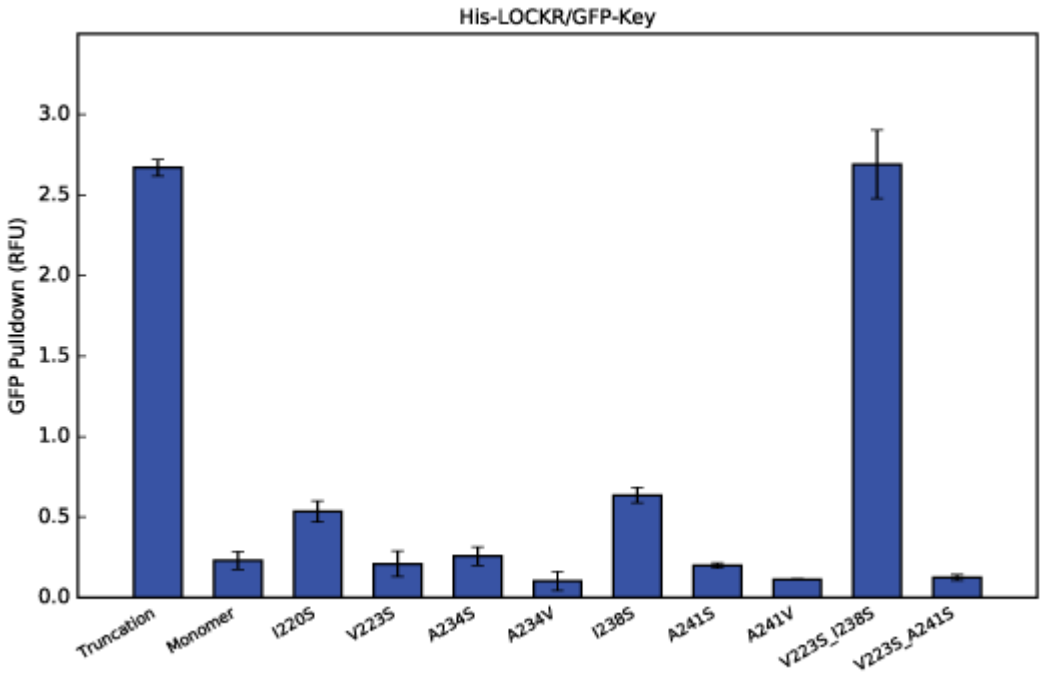

Extended Data Figure 2 – Mutation screening LOCKR candidates

GFP Plate assay to find mutations for LOCKR. Different putative LOCKR constructs were adhered via 6x-His tag to a Ni coated 96-well plate, Key-GFP was applied, and excess washed. Resulting fluorescence represents Key-GFP bound to LOCKR constructs. The truncation was used as a positive control, since the Key binds to the open interface. The monomer as a negative control since it does not bind the Key. Error bars represent the standard deviation of three replicates.

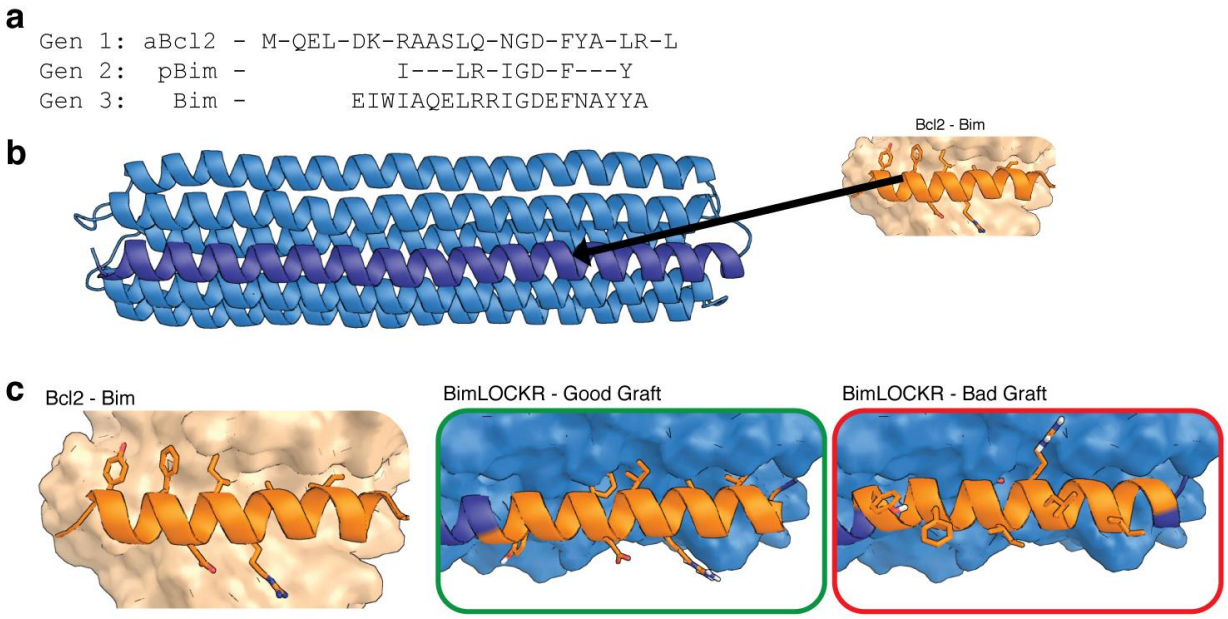

Extended Data Figure 3 - Caging Bim-related sequences.

a) Three Bcl2 binding sequences were grafted onto the Latch. aBcl2 is a single helix from a designed Bcl2 binder (pdb: 5JSN) where non Bcl2-interacting residues were reverted back to the standard LOCKR Latch sequence, shown as dashes. pBim is the partial Bim sequence where only Bcl2-interacting residues are grafted onto the Latch. Bim is the full consensus sequence of the BH3 domain. b) LOCKR (left) with the Latch in dark blue. The helical Bim sequence is taken from the Bim/Bcl2 interaction and grafted onto the Latch c) Left: Bcl2 (tan) binding to Bim (purple) from pdb:2MV6 with pBim residues shown as sticks. Center: a well caged graft where important binding residues are caged. Right: a poor graft where Bcl2 binding residues are exposed and polar surface residues are against the Cage interface.

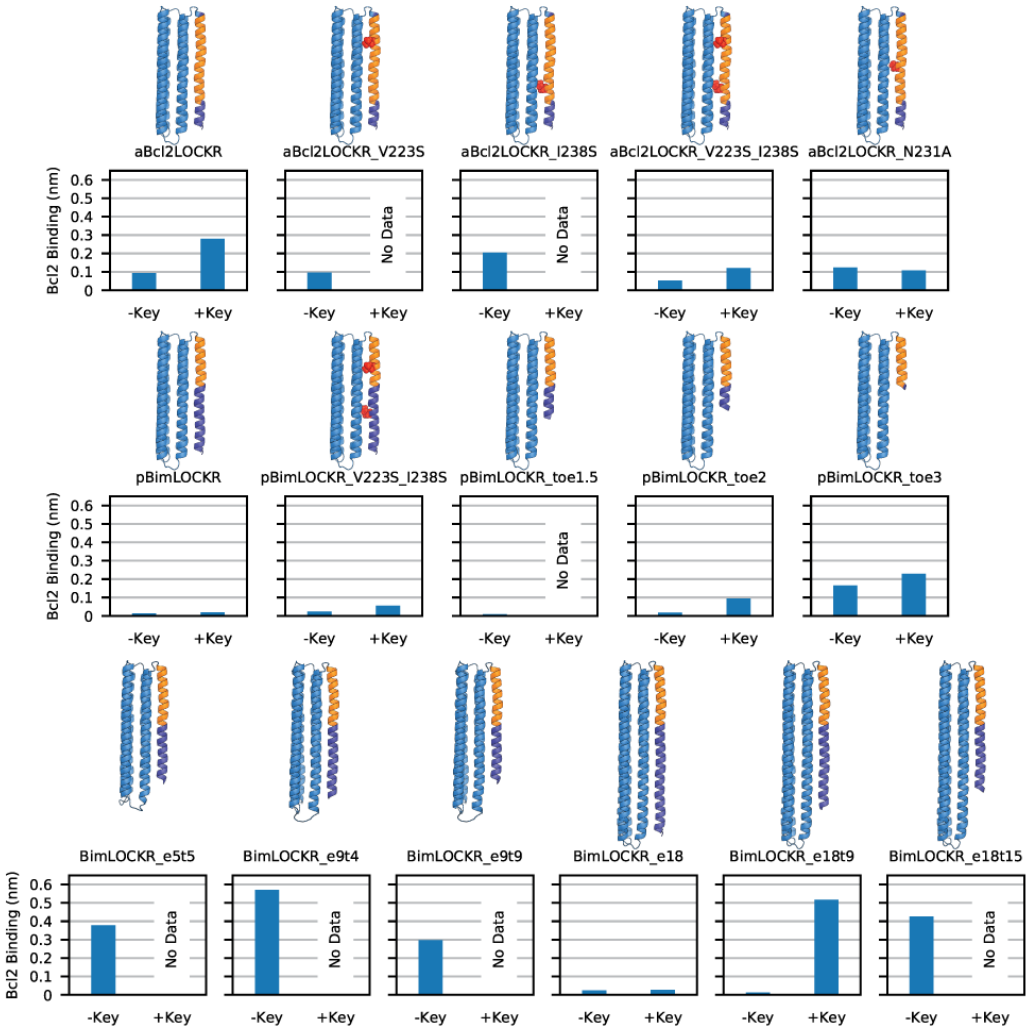

Extended Data Figure 4 – Tuning BimLOCKR

aBcl2, pBim, and Bim were caged to varying degrees of success. Early versions of the switch, with aBcl2 and pBim did not efficiently cage Bcl2 binding in the off state. They also only weakly bound the Key leading to small dynamic range. The Cage and Key was extended by 5, 9, and 18 residues in an attempt to provide a larger interface to tightly hold the Latch in the off state and provide a larger interface for Key binding to increase the dynamic range of activation. Mutations on the Latch, identified in Extended Data 2, and providing toeholds for Key binding were the two strategies employed to tune the switch. In graphs, "off" refers to 250-310 nM switch an absence of Key while "on" refers to excess Key added. The height of the bar graph shows the R_{eq} as measured by Bio-layer interferometry.

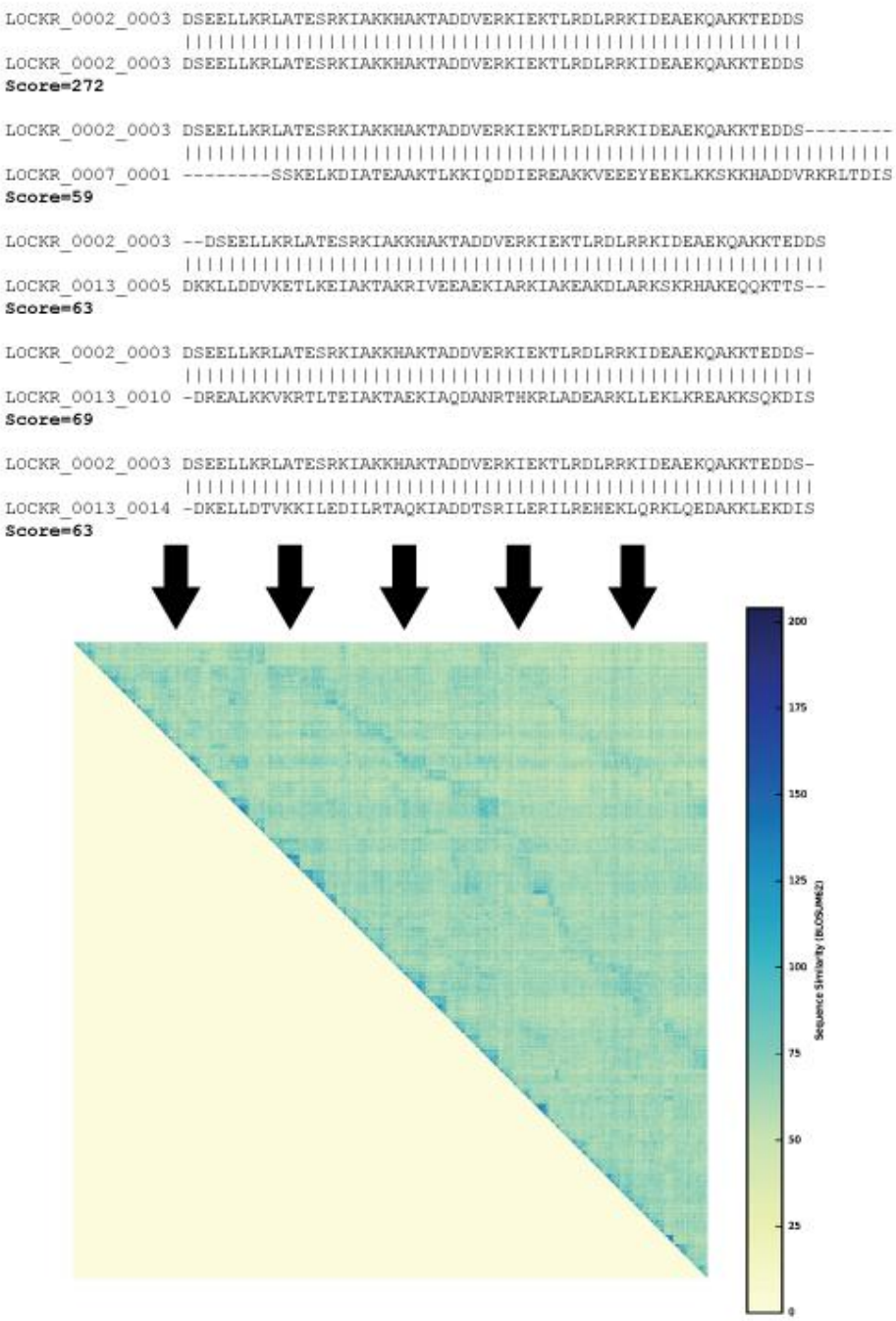

Extended Data Figure 5 – Sequence Alignment for Filtering Orthogonality

Sequence alignment of 1504 Keys for filtering for orthogonality. Every pairwise alignment was scored using BLOSUM62 scoring, disallowing gaps while not penalizing end-gaps. This algorithm finds the BLOSUM62 score of the most similar superposition of each pair of Keys taking into account amino acid identity.

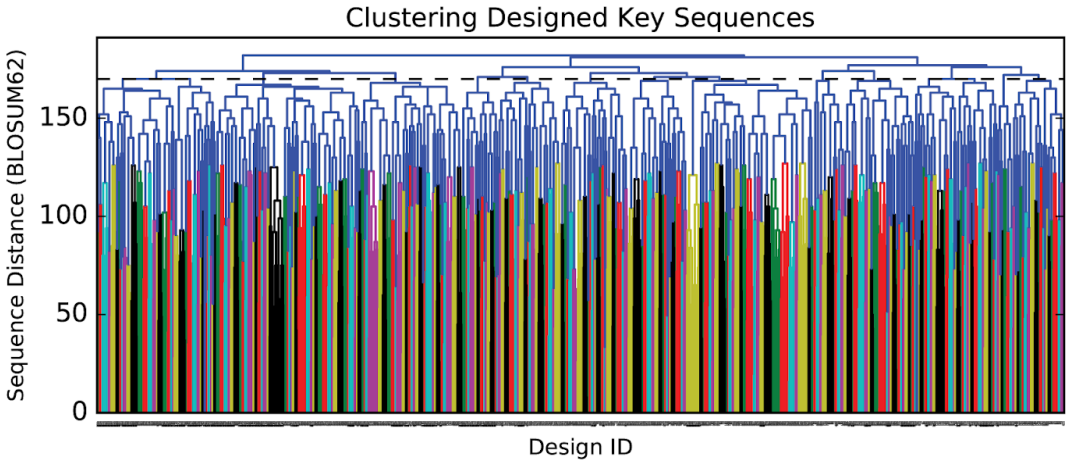

Extended Data Figure 6 – Clustering for Determining Orthogonality

Clustering sequences aligned in Extended Data Figure 5. Each sequence along the y-axis was clustered using a hierarchical clustering algorithm. The cutoff at 170 (horizontal, black dotted line) selects 13 clusters from which the centers were chosen as designs to order.

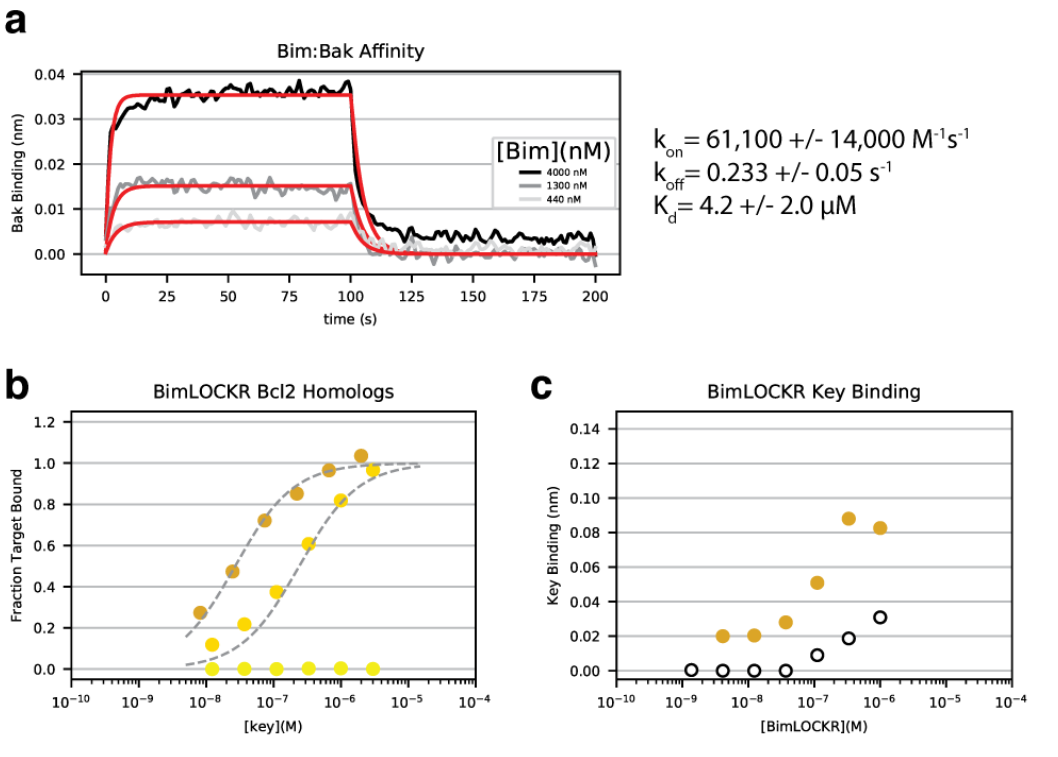

Extended Data Figure 7 - Validation of model in Figure 1a

a) Measurement of Bim:Bak affinity. Biolayer interferometry (BLI) at three concentrations gives on and off rates for Bim:Bak binding, yielding the constants shown on right. Mean shown with standard deviation of four replicates. b) BLI measurement of $BimLOCKR_a$ (400 nM) binding to Bcl2 (gold), BclB (yellow), and Bak (lighter yellow - BimLOCKR at 1 µM) as Key is added to solution. Normalized due to differences in R_{max} for Bcl2 and BclB on the tip. c) BLI measurement of $BimLOCKR_a$ binding to Key_a immobilized on the tip. Open circles are with no Bcl2 present, gold points are with Bcl2 present at 500 nM.

a

```
cODC Full:     LPMSCAQES
cODC noPro:    L-MSCAQES
cODC CA_only:  ----CA---
```

b

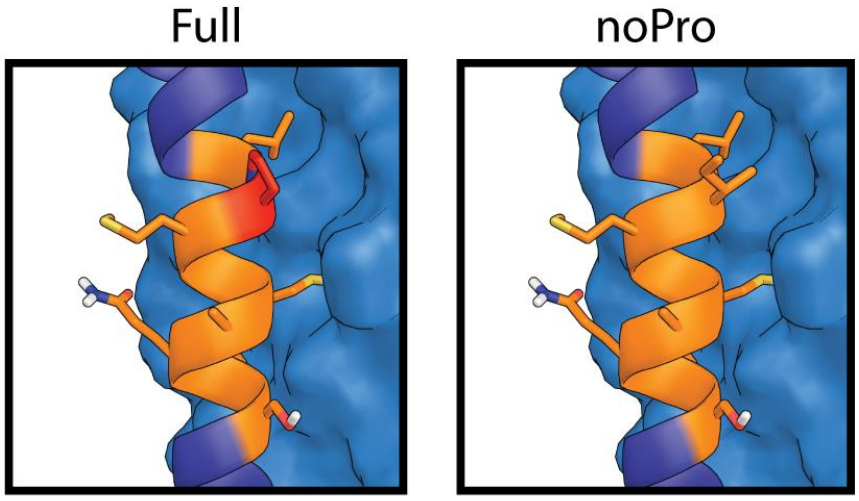

Extended Data Figure 8 - Caging cODC sequences

a) Three variations of the cODC degron to Cage. Variations meant to tune K_{open} by removing the destabilizing proline (noPro) and minimizing mutations to the Latch (CA only). b) Predicted models of the full and noPro cODC sequences (orange) threaded onto the Latch (dark blue). Thread position chosen such that the cysteine residue needed for degradation is sequestered against the Cage (light blue). Proline highlighted in red in the full cODC mutated to an isoleucine in the noPro variant.

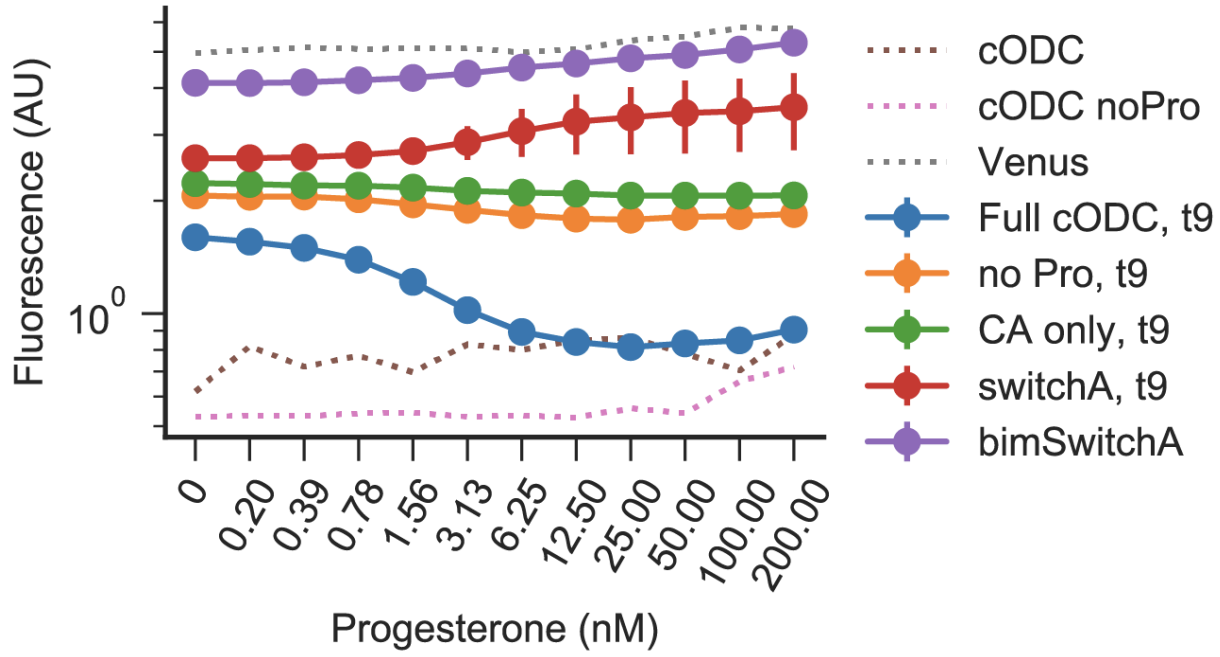

Extended Data Figure 9 – Comparing the Stability of cODC Variants

YFP fused to cODC variants caged in $Switch_a$ to an empty $Switch_a$ and to $bimSwitch_a$. The dual inducible system from Fig 4a was used to express the various YFP-$Switch_a$ fusions (solid lines and dots) via pGal1 and E2, and Key_a-BFP via pZ3 and Pg. YFP (Venus) alone, YFP fused to the WT cODC (cODC) or YFP fused to the proline removed cODC (cODC noPro), were also expressed using pGal1 and E2 (dashed lines). Cells were induced with a saturating dose of E2 (50 nM) and Pg was titrated in from 0-200 nM. Fluorescence was measured at steady-state using a flow cytometer and error bars represent s.d. of biological replicates. A moderate decrease in YFP fluorescence was observed as a function of Pg for the full cODC variant, whereas only a small decrease was observed for the proline removed and CA only. No decrease in fluorescence was observed as a function of Key induction for YFP alone, empty $Switch_a$, or $bimSwitch_a$.

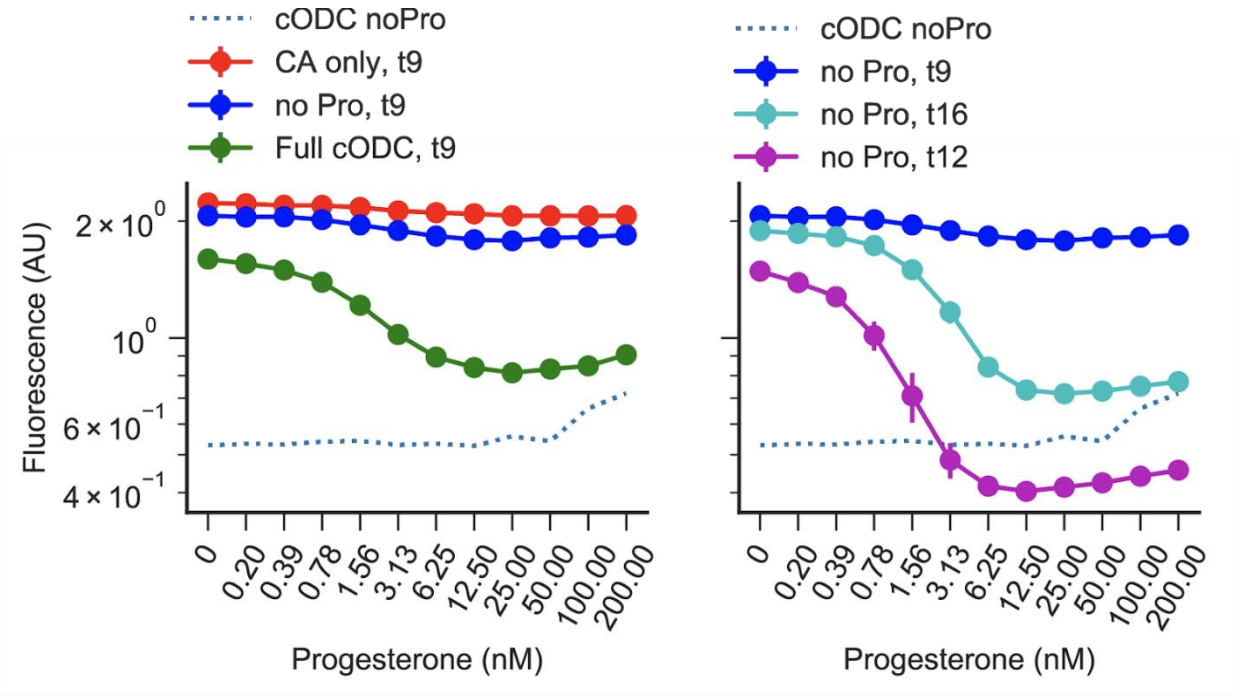

Extended Data Figure 10 - Tuning toehold lengths of degronLOCKR$_a$

The dual inducible system from Fig 4a was used to express the various YFP-Switch$_a$ fusions via pGal1 and E2, and Key$_a$-BFP via pZ3 and Pg. YFP fused to the proline removed cODC (cODC no Pro) was also expressed using pGal1 and E2 (dashed line). Cells were induced with a saturating dose of E2 (50 nM) and Pg was titrated in from 0-200 nM. Fluorescence was measured at steady-state using a flow cytometer and error bars represent s.d. of biological replicates. (Left) cODC variants from Extended Data Figure 8 alone to show dynamic range of Full cODC. (Right) Extending toehold on proline removed version from 9 to 12 and 16aa. Proline removed with 12aa toehold shows the greatest dynamic range of all the switches tested.

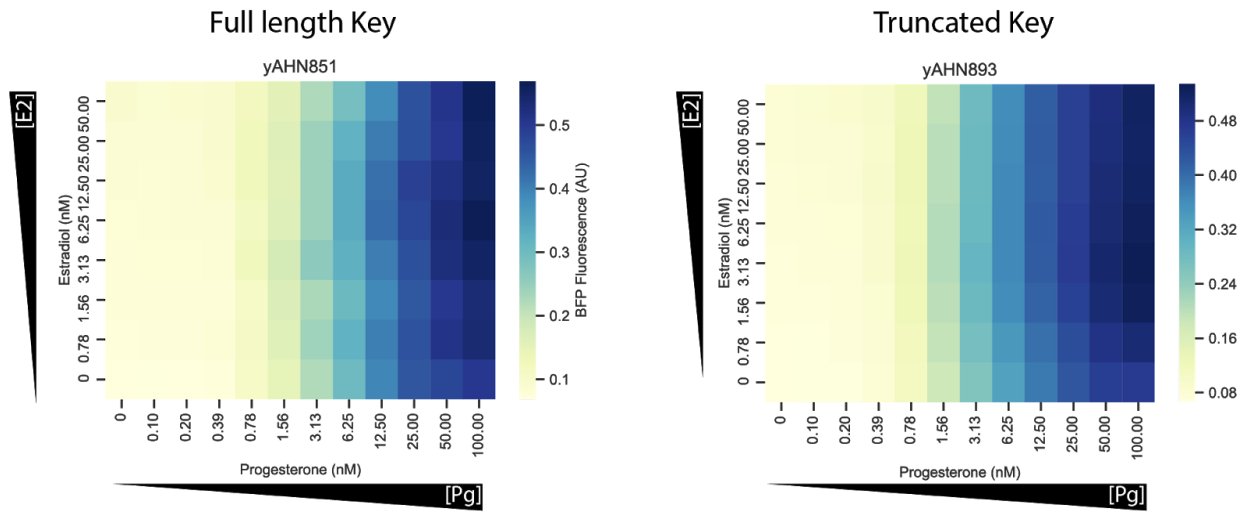

Extended Data Figure 11 - BFP expression corresponding to Figure 4b

E2 and Pg were used to induce expression of YFP-degronSwitch$_a$ and Key$_a$ (Full length or truncated)-BFP, respectively. Fluorescence was measured at steady-state using a flow cytometer. BFP expression was not dependent on expression of the Switch, suggesting the Key does not co-degrade with the Switch.

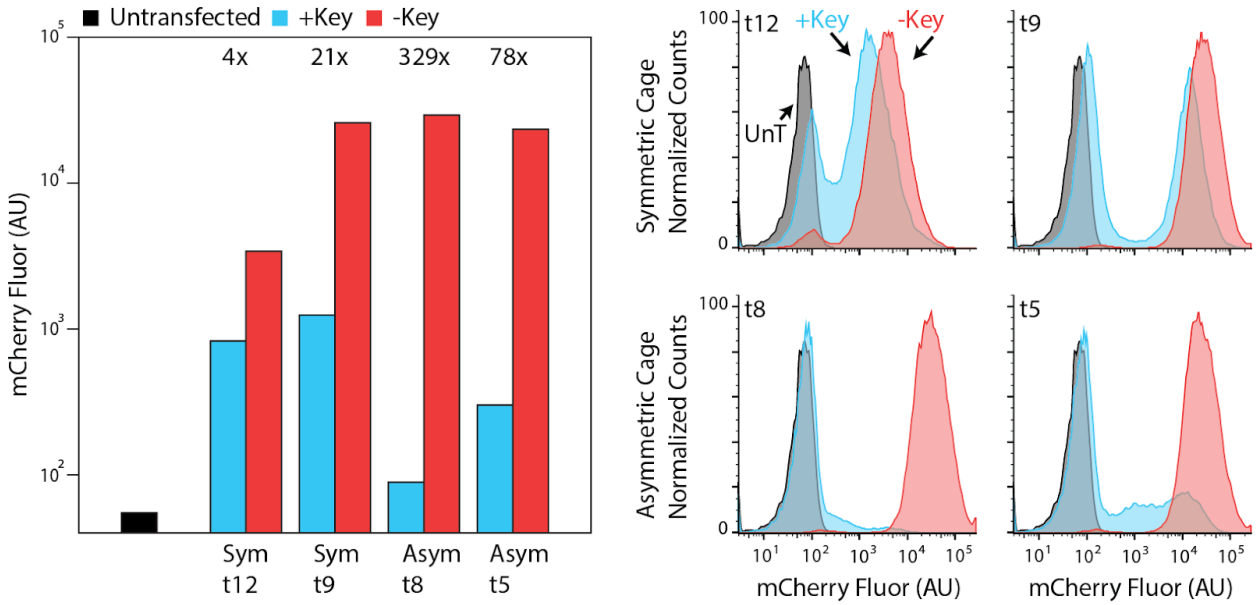

Extended Data Figure 12 - degronSwitch expression in HEK 293T cells

HEK 293T cells expressing BFP-Key or just BFP. Fluorescence was measured using flow cytometry. Histograms and the geometric means are presented for cells expressing the symmetric (Sym) and asymmetric (Asym) degronSwitches with and without Key. Two toehold lengths (t12, t9, t8, t5) are shown for each degronSwitch variant.

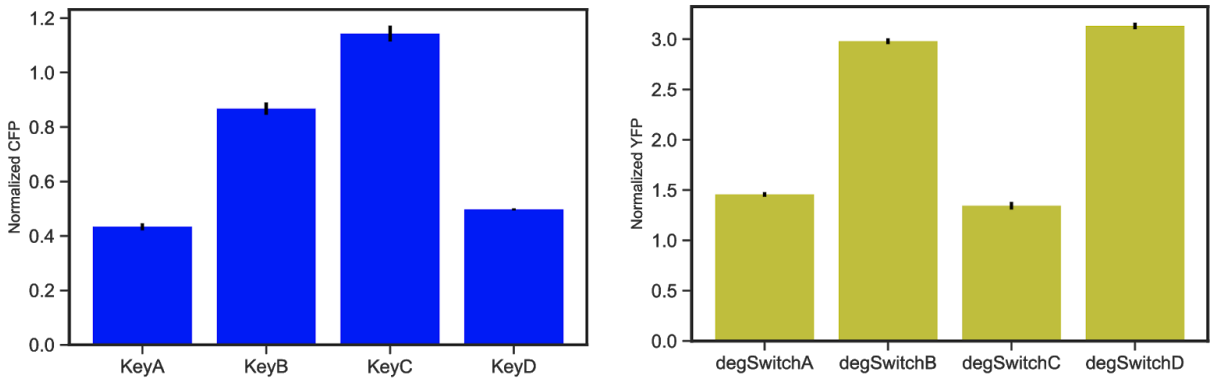

Extended Data Figure 13 - Orthogonal degronLOCKR Expression

Expression of orthogonal YFP-degronSwitch and Key-CFP. Four different switches and Keys (A, B, C, D) were expressed using the strong pTDH3 promoter. Fluorescence was measured at steady-state using a flow cytometer and error bars represent s.d. of biological replicates.

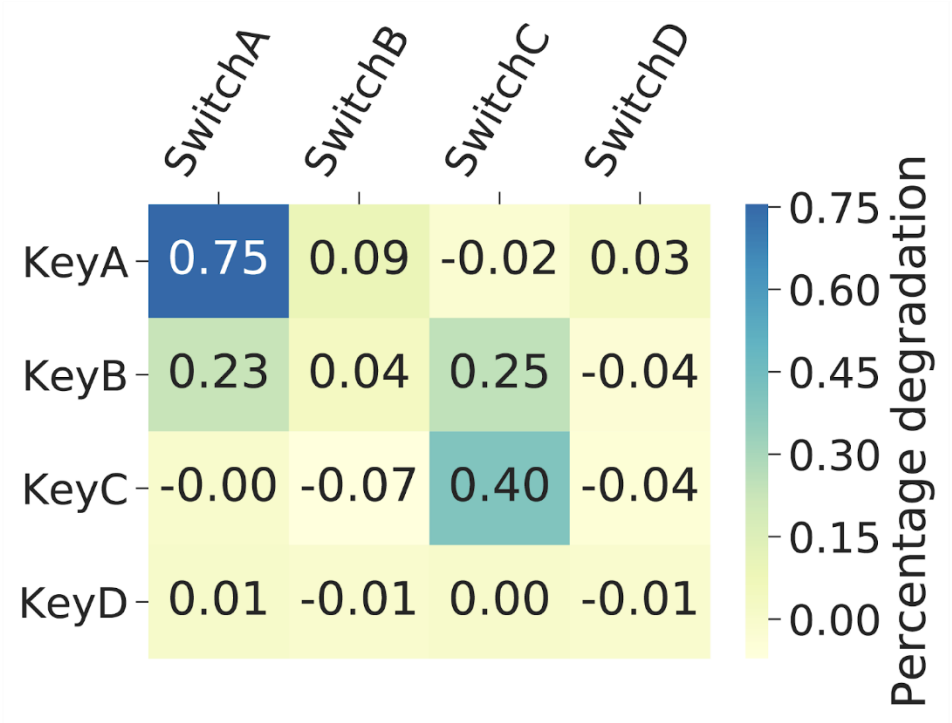

Extended Data Figure 14 - degronLOCKR$_{a-d}$ orthogonality

All combinations of pTDH3-YFP-degronSwitch and pTDH3-Key-CFP were tested. Fluorescence was measured at steady-state using a flow cytometer. Percentage degradation was calculated by subtracting the YFP-degronSwitch fluorescence with the given Key-CFP coexpressed from the YFP-degronSwitch fluorescence without any Key expressed and normalizing by the YFP-degronSwitch fluorescence without any Key expressed. degronSwitch$_a$ is activated strongly by Key$_a$ and weakly by Key$_b$. degronSwitch$_c$ is activated strongly by Key$_c$ and weakly by Key$_b$. Because degronSwitch$_a$ and degronSwitch$_c$ are not activated by Key$_c$ and Key$_a$ respectively, we consider these two to be an orthogonal pair.

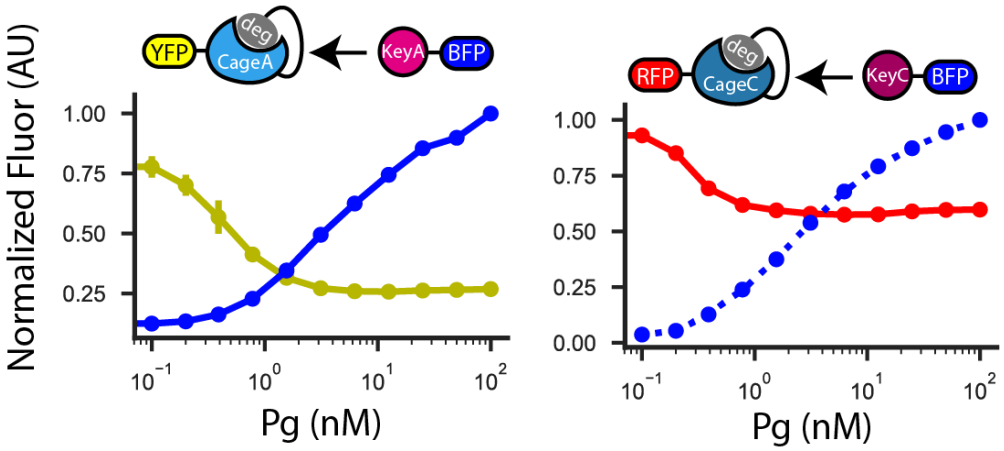

Extended Data Figure 15 - degronLOCKR controls for Figure 4d.

YFP-degronSwitch$_a$ was expressed using the pTEF1 constitutive promoter and RFP-degronSwitch$_c$ was expressed using the pTEF1 constitutive promoter. The respective Keys fused to BFP were expressed using pZ3 and Pg. Fluorescence was measured at steady-state using a flow cytometer and error bars represent s.d. of biological replicates.

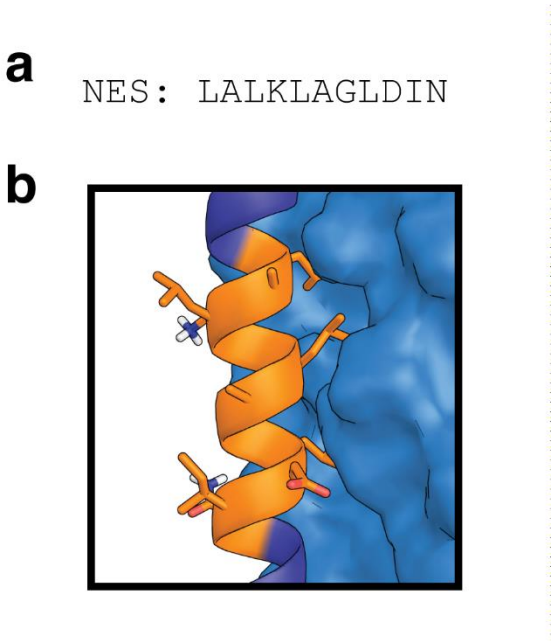

Extended Data Figure 16 - Threading a nuclear export sequence

a) NES used in this report. b) The NES (orange) caged on the helical Latch (dark blue, cartoon) with hydrophobic residues sequestered against the Cage (light blue, surface)

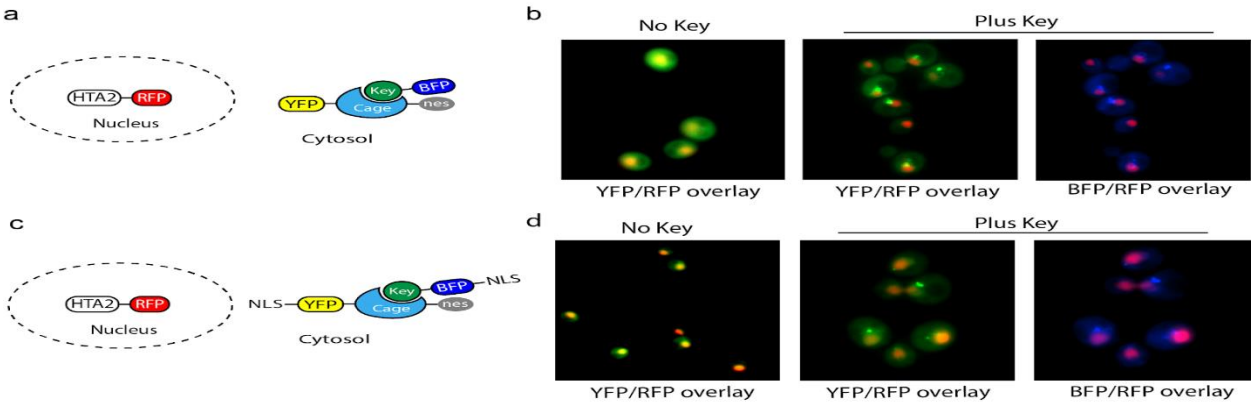

Extended Data Figure 17 - Cytosolic aggregation of nesLOCKR

a) Schematic of cytosolic YFP-nesSwitch$_a$ and Key-BFP with nuclear marker HTA2-RFP. b) YFP fluorescence shows the expected cytosolic distribution when YFP-nesSwitch$_a$ is expressed with no NLS (left) but punctae of YFP fluorescence is observed when both YFP-nesSwitch$_a$ and Key-BFP are expressed in the cytosol, which we assume is due to aggregation of the nesSwitch$_a$. Key-BFP fluorescence is co-localized to YFP-nesSwitch$_a$ fluorescence (right). c) Schematic of NLS-YFP-nesSwitch$_a$ with Key-BFP-NLS with nuclear marker HTA2-RFP. d) YFP-nesSwitch$_a$ is localized to the nucleus when expressed with the strong (SV40) NLS (left). When Key-BFP is expressed with a moderately strong NLS, the same pattern of YFP localization is observed as when Key-BFP is expressed without a NLS (Figure 6b), indicating that uncaging of the NES is independent of Key-BFP localization. Key-BFP-NLS fluorescence is co-localized to NLS-YFP-nesSwitch$_a$ fluorescence (right)

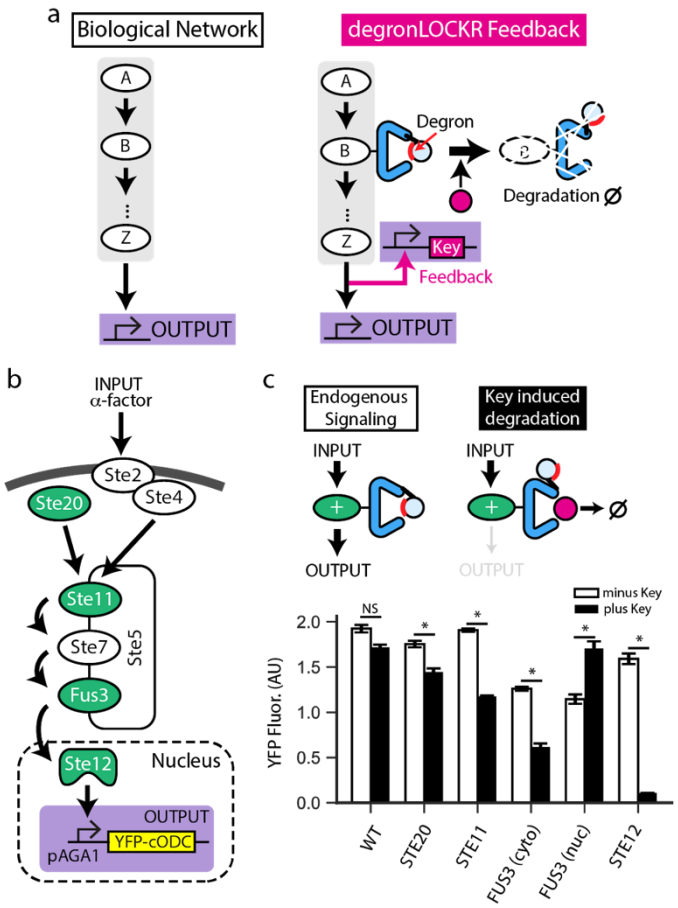

Extended Data Figure 18 - degronLOCKR is a tool for controlling biological pathways.

a) Schematic of degronLOCKR as a modular tool to implement synthetic feedback control on an endogenous or synthetic biological network by fusing the degronSwitch to an effector molecule and driving the expression of the key from the output of the network. b) Simplified schematic of the yeast mating pathway not showing complex endogenous feedback. Pathway is activated by addition of α-factor and signaling activity is measured using a pAGA1-YFP-cODC reporter. c) degronLOCKR induced degradation of positive effector molecules to control mating pathway activity. The endogenous copy of indicated molecule was fused to degronSwitch and key was expressed using a progesterone inducible system. Cells were induced with a saturating dose of α-factor and pathway activity with and without key was compared. pAGA1-YFP-cODC was measured on a flow cytometer after four hours of growth. Data represent mean ± s.d. of three biological replicates. *P<0.005; two-sided student's t-test.

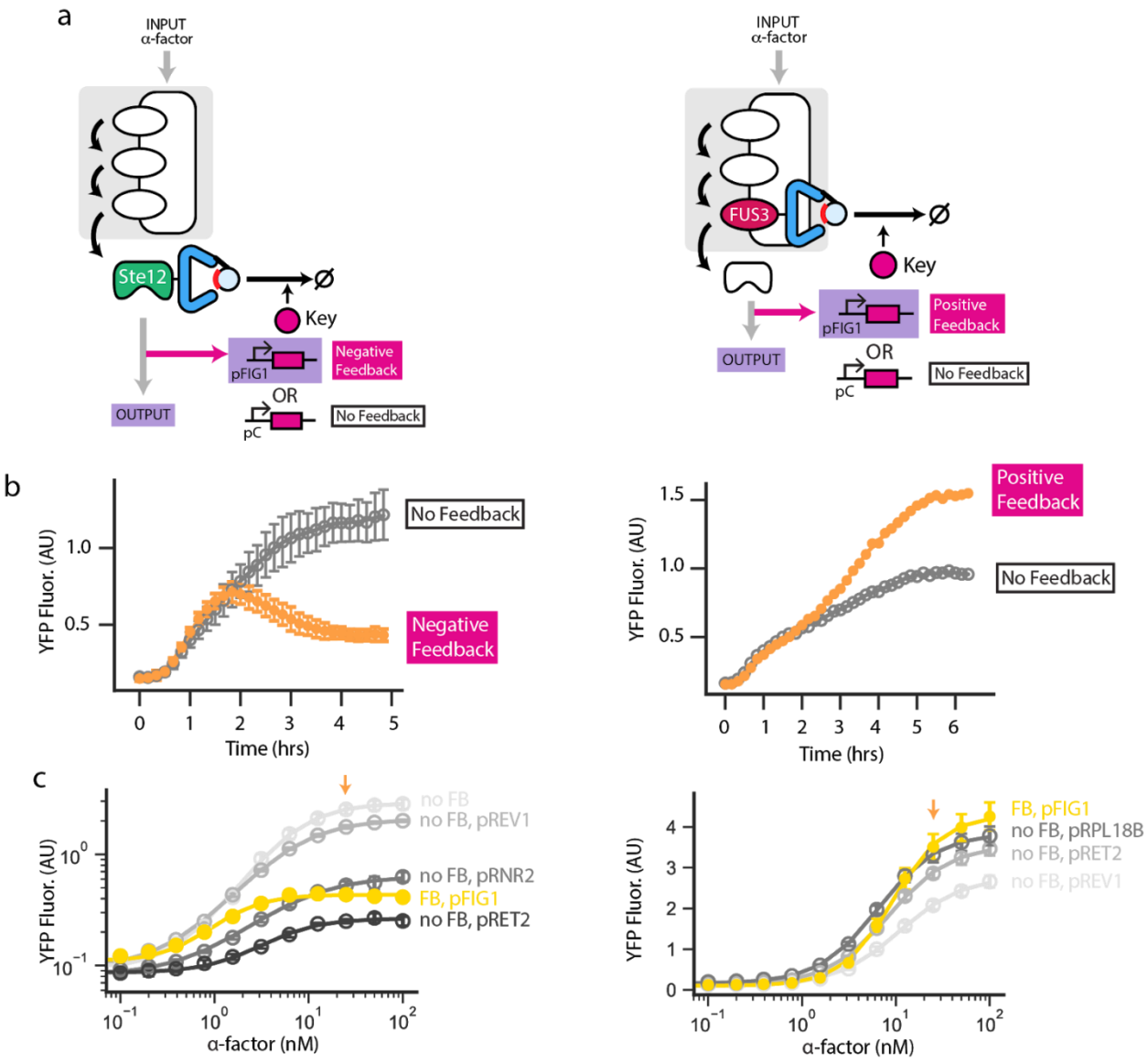

Extended Data Figure 19 - degronLOCKR implements feedback of the mating pathway

a) Schematic of synthetic negative and positive feedback where the endogenous copy of STE12 (left) or FUS3 (right) is fused to the degronSwitch and either the pathway reporter pFIG1 (synthetic feedback) or a constitutive promoter (no feedback) is used to express key-CFP-NLS. All output measurements are for pAGA1-YFP-cODC. b) Measurements of pAGA1-YFP-cODC dynamics for synthetic negative (left) and positive (right) feedback. Synthetic feedback and no feedback (pREV1) strains were induced with 25nM α-factor at time t=0hr and flow cytometry measurements (points) were performed every 10 minutes. Points represent the mean ± s.d. of three biological replicates. Lines represent a moving average taken over three data points. c) Comparison of α-factor dose response of synthetic negative (left) and positive (right) feedback.

Feedback implemented using pFIG1 was compared to no feedback strains with different levels of constitutive key expression. pAGA1-YFP-cODC fluorescence was measured using flow cytometry four hours after α-factor induction. Points represent the mean ± s.d. of three biological replicates. Solid lines are a hill function fit to the data. Doses of α-factor from the experiment in (b) are indicated on the graph.

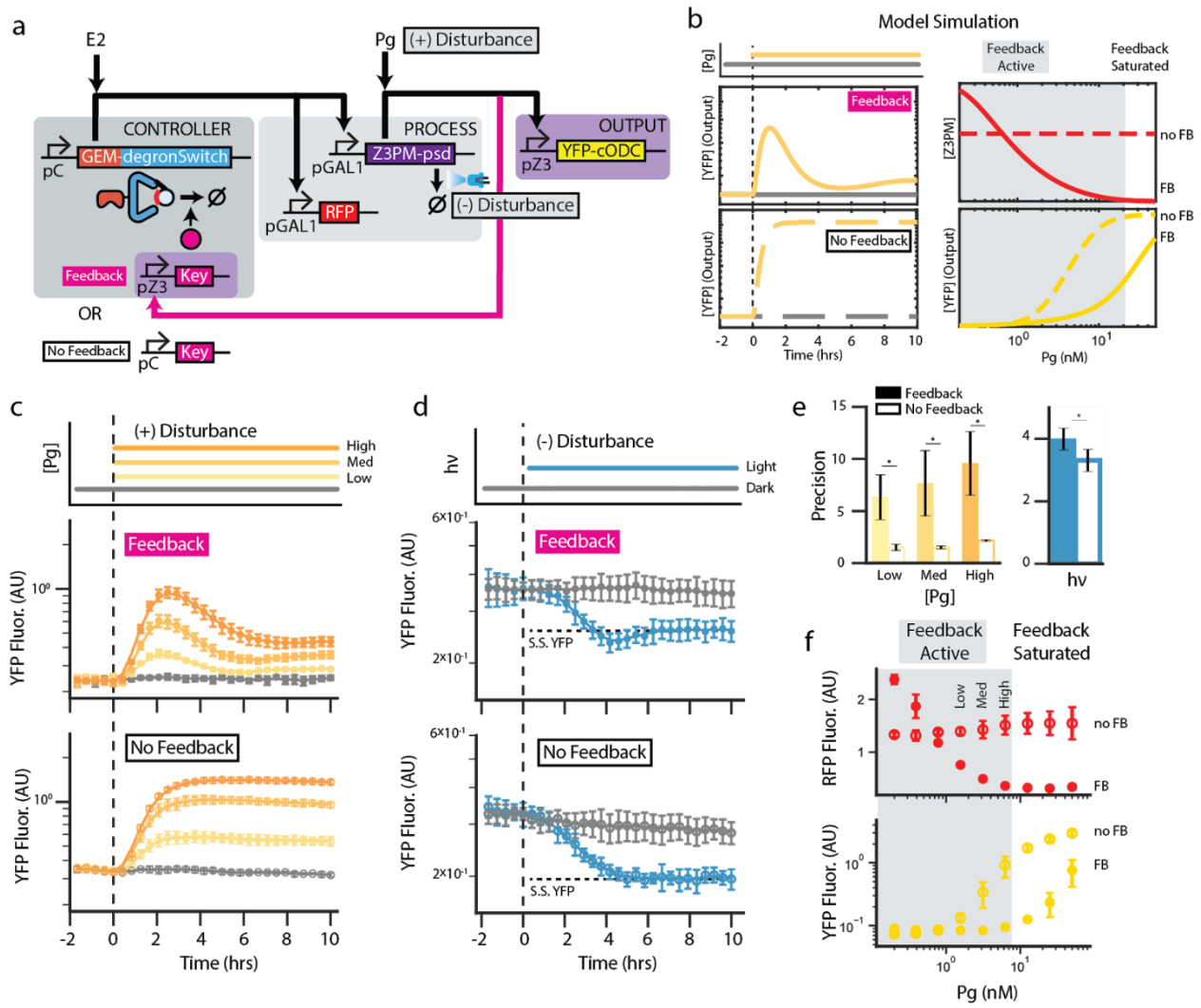

Extended Data Figure 20 - Operational properties of degronLOCKR feedback module

a) Schematic of synthetic feedback circuit. GEM-degronSwitch is expressed constitutively and is activated by estradiol (E2) to drive expression of pGAL1-Z3PM-psd. Z3PM is activated by progesterone (Pg) to drive expression from pZ3. Blue light can be used to induce degradation of Z3PM-psd. pZ3-YFP-cODC is the measured output of the circuit, and pZ3-key-CFP-NLS drives feedback (synthetic feedback) in the circuit by activating degradation of GEM-degronSwitch. In the circuit with no feedback a constitutive promoter is used to express key-CFP-NLS. b) Model simulation (see supplementary information) of the feedback and no feedback circuits. The simulated dynamics (left) and change of steady-state (right) of output following a Pg disturbance indicate that feedback buffers against increasing Pg concentration by degrading GEM and reducing Z3PM concentration. c) Dynamic measurements of pZ3-Venus-cODC using automated flow cytometry for the synthetic feedback and no feedback strains (pRNR2-key-CFP-NLS)

following a positive disturbance. Cells were grown to steady-state expression in 0.78nM Pg and 7.5nM E2. At time 0 hrs cells were either kept at the same Pg concentration or induced to a new final concentration of 1.56 nM (low), 3.13 nM (med), or 6.25 nM (high) Pg. Dynamics were measured for another ten hours. Solid line represents a moving average taken over three data points and points represent the mean ± s.d. of three biological replicates. d) Dynamic measurements of pZ3-Venus-cODC using automated flow cytometry for the synthetic feedback and no feedback strains (pRPL18B-key-CFP-NLS driving key) following a negative disturbance. Cells were grown to steady-state expression in 1.57nM Pg and 30nM E2 then subjected to blue-light at time 0 hrs to activate the psd. Dynamics were measured for ten hours post-disturbance. Solid line represents a moving average taken over three data points and points represent the mean ± s.d. of three biological replicates. e) Precision of the synthetic feedback versus no feedback circuits to each of the disturbances. Data are the mean ± s.d. of three biological replicates. *P<0.05; two-sided student's t-test. f) Comparison of steady-state circuit behavior (ten hours after stimulation) with and without feedback (pRNR2-key-CFP-NLS) as a function of Pg at a fixed concentration of 7.5nM E2. RFP fluorescence is a proxy for Z3PM concentration and YFP fluorescence is the output of the circuit. Pg doses used for positive disturbance in c) are indicated. Points represent mean ± s.d. of three biological replicates.

APPENDIX C – EXTENDED DATA TABLES

Table 1- SAXS Statistics

Design Name	Concentration	q range	I(0) (from P(r))	Rg (from P(r))	I(0) (from Gunier)	Rg (from Gunier)	Dmax	Parod Volume	Px
Trimer	6.6	0.02-0.3	1700	24.9	1740	24.84	71	66743	3.6
Monomer	6	0.01-0.39	241	25.9	246	25	86	54706	4
Truncation	6	0.01-0.39	192	26.5	211	26.2	85	59086	3.8
LOCKR	6	0.01-0.39	195	26.2	213	26.3	85	62293	3.6

Table 2 – Functional peptides designed into LOCKR Switches

Name	Sequence
aBcl2 – Designed Bcl2 binder	M-QEL-DK-RAASLQ-NGD-FYA-LR-L
pBim	I--LR-IGD-F--Y
Bim	EIWIAQELRRIGDEFNAYYA
cODC	LPMSCAQES
cODC_noPro	L-MSCAQES
cODC_CA_only	CA
Nuclear Export Sequence	LALKLAGLDIN
StrepTagII	NWSHPQFEK
SpyTag	AHIVMVDAYK
TEV Protease Site	ENLYFQGS
NanoBit Split Luciferase	VSGWRLFKKIS

Table 3 – Protein Sequences Used

Name	Sequence
SB76L	SKEAVTKLQALNIKLAEKLLEALARLQELNIALVYLAVELTDPKRIADEIKKVKDKSKEIVERAEEEIAR AAAESKKILDEGSGSGSDAVAELQALNLKLAELLLEAIAKLQELNIKLVELLTKLTDPATIREAIRKVKE DSERIVAEAERLIAAAKAESERIIREGSGSGDPDVARLQELNIELARELLRAAAELQELNIKLVELASEL TDP[DEARKAIARVKRESKRIVEDAERLIREAAAASEKISRE]
SB76L_truncation	SKEAVTKLQALNIKLAEKLLEALARLQELNIALVYLAVELTDPKRIADEIKKVKDKSKEIVERAEEEIAR AAAESKKILDEGSGSGSDAVAELQALNLKLAELLLEAIAKLQELNIKLVELLTKLTDPATIREAIRKVKE DSERIVAEAERLIAAAKAESERIIREGSGSGDPDVARLQELNIELARELLRAAAELQELNIKLVELASE
Switch_a	SKEAVTKLQALNIKLAEKLLEALARLQELNIALVYLAVELTDPKRIADEIKKVKDKSKEIVERAEEEIAR AAAESKKILDEGSGSGSDAVAELQALNLKLAELLLEAIAKLQELNIKLVELLTKLTDPATIREAIRKVKE DSERIVAEAERLIAAAKAESERIIREGSGSGDPDVARLQELNIELARELLRAAAELQELNIKLVELASEL TDP[DEARKAIARSKRESKRIVEDAERLSREAAAASEKISRE]
aBcl2Switch_1	SKEAVTKLQALNIKLAEKLLEALARLQELNIALVYLAVELTDPKRIADEIKKVKDKSKEIVERAEEEIAR AAAESKKILDEGSGSGSDAVAELQALNLKLAELLLEAIAKLQELNIKLVELLTKLTDPATIREAIRKVKE DSERIVAEAERLIAAAKAESERIIREGSGSGDPDVARLQELNIELARELLRAAAELQELNIKLVELASEL TDP[KMAQELIDKVRAASLQINGDAFYAILRALAASEKLSKE]
aBcl2Swit	SKEAVTKLQALNIKLAEKLLEALARLQELNIALVYLAVELTDPKRIADEIKKVKDKSKEIVERAEEEIAR

ch_2	AAAESKKILDEGSGSGSDAVAELQALNLKLAELLLEAIAKLQELNIKLVELLTKLTDPATIREAIRKVKE DSERIVAEAERLIAAAKAESERIIREGSGSGDPDVARLQELNIELARELLRAAAELQELNIKLVELASEL TDP[KMAQELSDKVRAASLQINGDAFYAILRALAASEKLSKE]
aBcl2Switch_3	SKEAVTKLQALNIKLAEKLLEALARLQELNIALVYLAVELTDPKRIADEIKKVKDKSKEIVERAEEEIAR AAAESKKILDEGSGSGSDAVAELQALNLKLAELLLEAIAKLQELNIKLVELLTKLTDPATIREAIRKVKE DSERIVAEAERLIAAAKAESERIIREGSGSGDPDVARLQELNIELARELLRAAAELQELNIKLVELASEL TDP[KMAQELIDKSRAASLQINGDAFYAILRALAASEKLSKE]
aBcl2Switch_4	SKEAVTKLQALNIKLAEKLLEALARLQELNIALVYLAVELTDPKRIADEIKKVKDKSKEIVERAEEEIAR AAAESKKILDEGSGSGSDAVAELQALNLKLAELLLEAIAKLQELNIKLVELLTKLTDPATIREAIRKVKE DSERIVAEAERLIAAAKAESERIIREGSGSGDPDVARLQELNIELARELLRAAAELQELNIKLVELASEL TDP[KMAQELIDKVRAASLQINGDAFYASLRALAASEKLSKE]
aBcl2Switch_5	SKEAVTKLQALNIKLAEKLLEALARLQELNIALVYLAVELTDPKRIADEIKKVKDKSKEIVERAEEEIAR AAAESKKILDEGSGSGSDAVAELQALNLKLAELLLEAIAKLQELNIKLVELLTKLTDPATIREAIRKVKE DSERIVAEAERLIAAAKAESERIIREGSGSGDPDVARLQELNIELARELLRAAAELQELNIKLVELASEL TDP[KMAQELSDKVRAASLQINGDAFYASLRALAASEKLSKE]
aBcl2Switch_6	SKEAVTKLQALNIKLAEKLLEALARLQELNIALVYLAVELTDPKRIADEIKKVKDKSKEIVERAEEEIAR AAAESKKILDEGSGSGSDAVAELQALNLKLAELLLEAIAKLQELNIKLVELLTKLTDPATIREAIRKVKE DSERIVAEAERLIAAAKAESERIIREGSGSGDPDVARLQELNIELARELLRAAAELQELNIKLVELASEL TDP[KMAQELIDKSRAASLQINGDAFYASLRALAASEKLSKE]
aBcl2Switch_7	SKEAVTKLQALNIKLAEKLLEALARLQELNIALVYLAVELTDPKRIADEIKKVKDKSKEIVERAEEEIAR AAAESKKILDEGSGSGSDAVAELQALNLKLAELLLEAIAKLQELNIKLVELLTKLTDPATIREAIRKVKE DSERIVAEAERLIAAAKAESERIIREGSGSGDPDVARLQELNIELARELLRAAAELQELNIKLVELASEL TDP[KMAQELIDKVRAASLQIAGDAFYAILRALAASEKLSKE]
aBcl2Switch_8	SKEAVTKLQALNIKLAEKLLEALARLQELNIALVYLAVELTDPKRIADEIKKVKDKSKEIVERAEEEIAR AAAESKKILDEGSGSGSDAVAELQALNLKLAELLLEAIAKLQELNIKLVELLTKLTDPATIREAIRKVKE DSERIVAEAERLIAAAKAESERIIREGSGSGDPDVARLQELNIELARELLRAAAELQELNIKLVELASEL GSGSGSGDP[KMAQELIDKVRAASLQINGDAFYASLRALAASEKLSKE]
pBimSwitch	SKEAVTKLQALNIKLAEKLLEALARLQELNIALVYLAVELTDPKRIADEIKKVKDKSKEIVERAEEEIAR AAAESKKILDEGSGSGSDAVAELQALNLKLAELLLEAIAKLQELNIKLVELLTKLTDPATIREAIRKVKE DSERIVAEAERLIAAAKAESERIIREGSGSGDPDVARLQELNIELARELLRAAAELQELNIKLVELASEG SGSGS[EIAEALRAIGDVFNESYRIVEDAERLIREAAAASEKISRE]
pBimSwitch_toe1.5	SKEAVTKLQALNIKLAEKLLEALARLQELNIALVYLAVELTDPKRIADEIKKVKDKSKEIVERAEEEIAR AAAESKKILDEGSGSGSDAVAELQALNLKLAELLLEAIAKLQELNIKLVELLTKLTDPATIREAIRKVKE DSERIVAEAERLIAAAKAESERIIREGSGSGDPDVARLQELNIELARELLRAAAELQELNIKLVELASEG SGSGS[EIAEALRAIGDVFNESYRIVEDAERLIR]
pBimSwitch_toe2	SKEAVTKLQALNIKLAEKLLEALARLQELNIALVYLAVELTDPKRIADEIKKVKDKSKEIVERAEEEIAR AAAESKKILDEGSGSGSDAVAELQALNLKLAELLLEAIAKLQELNIKLVELLTKLTDPATIREAIRKVKE DSERIVAEAERLIAAAKAESERIIREGSGSGDPDVARLQELNIELARELLRAAAELQELNIKLVELASEG SGSGS[EIAEALRAIGDVFNESYRIVEDAER]
pBimSwitch_toe3	SKEAVTKLQALNIKLAEKLLEALARLQELNIALVYLAVELTDPKRIADEIKKVKDKSKEIVERAEEEIAR AAAESKKILDEGSGSGSDAVAELQALNLKLAELLLEAIAKLQELNIKLVELLTKLTDPATIREAIRKVKE DSERIVAEAERLIAAAKAESERIIREGSGSGDPDVARLQELNIELARELLRAAAELQELNIKLVELASEG SGSGS[EIAEALRAIGDVFNESYR]
pBimSwitch_mut	SKEAVTKLQALNIKLAEKLLEALARLQELNIALVYLAVELTDPKRIADEIKKVKDKSKEIVERAEEEIAR AAAESKKILDEGSGSGSDAVAELQALNLKLAELLLEAIAKLQELNIKLVELLTKLTDPATIREAIRKVKE DSERIVAEAERLIAAAKAESERIIREGSGSGDPDVARLQELNIELARELLRAAAELQELNIKLVELASEG SGSGS[EIAEALRAIGDSFNESYRIVEDAERLSREAAAASEKISRE]
Switch_e5	KLLEAVTKLQALNIKLAEKLLEALARLQELNIALVYLAVELTDPKRIADEIKKVKDKSKEIVERAEEEIA RAAAESKKILDEAEEEGSGSGSELLLEAVAELQALNLKLAELLLEAIAKLQELNIKLVELLTKLTDPATI REAIRKVKEDSERIVAEAERLIAAAKAESERIIREAERLAGSGSGSRELLRDVARLQELNIELARELLRA AAELQELNIKLVELASELTDP[DEARKAIARVKRESKRIVEDAERLIREAAAASEKISREAERLI]
BimSwitc	KLLEAVTKLQALNIKLAEKLLEALARLQELNIALVYLAVELTDPKRIADEIKKVKDKSKEIVERAEEEIA

h_e5	RAAAESKKILDEAEEEGSGSGSELLLEAVAELQALNLKLAELLLEAIAKLQELNIKLVELLTKLTDPATI REAIRKVKEDSERIVAEAERLIAAAKAESERIIREAERLAGSGSGSRELLRDVARLQELNIELARELLRA AAELQELNIKLVELASELTDE[IWIAQELRRIGDEFNAYYADAERLIREAAAASEKISREAERLI]
BimSwitch_e5t5	KLLEAVTKLQALNIKLAEKLLEALARLQELNIALVYLAVELTDPKRIADEIKKVKDKSKEIVERAEEEIA RAAAESKKILDEAEEEGSGSGSELLLEAVAELQALNLKLAELLLEAIAKLQELNIKLVELLTKLTDPATI REAIRKVKEDSERIVAEAERLIAAAKAESERIIREAERLAGSGSGSRELLRDVARLQELNIELARELLRA AAELQELNIKLVELASELTDE[IWIAQELRRIGDEFNAYYADAERLIREAAAASEKISRE]
Switch_e9	KLAEKLLEAVTKLQALNIKLAEKLLEALARLQELNIALVYLAVELTDPKRIADEIKKVKDKSKEIVERAE EEIARAAAESKKILDEAEEEIARAGSGSGSLKLAELLLEAVAELQALNLKLAELLLEAIAKLQELNIKLV ELLTKLTDPATIREAIRKVKEDSERIVAEAERLIAAAKAESERIIREAERLIAAAAGSGSGSIELARELL RDVARLQELNIELARELLRAAAELQELNIKLVELASELTDP[DEARKAIARVKRESKRIVEDAERLIREA AAASEKISREAERLIREAA]
BimSwitch_e9	KLAEKLLEAVTKLQALNIKLAEKLLEALARLQELNIALVYLAVELTDPKRIADEIKKVKDKSKEIVERAE EEIARAAAESKKILDEAEEEIARAGSGSGSLKLAELLLEAVAELQALNLKLAELLLEAIAKLQELNIKLV ELLTKLTDPATIREAIRKVKEDSERIVAEAERLIAAAKAESERIIREAERLIAAAAGSGSGSIELARELL RDVARLQELNIELARELLRAAAELQELNIKLVELASELTDE[IWIAQELRRIGDEFNAYYADAERLIREA AAASEKISREAERLIREAA]
BimSwitch_e9t4	KLAEKLLEAVTKLQALNIKLAEKLLEALARLQELNIALVYLAVELTDPKRIADEIKKVKDKSKEIVERAE EEIARAAAESKKILDEAEEEIARAGSGSGSLKLAELLLEAVAELQALNLKLAELLLEAIAKLQELNIKLV ELLTKLTDPATIREAIRKVKEDSERIVAEAERLIAAAKAESERIIREAERLIAAAAGSGSGSIELARELL RDVARLQELNIELARELLRAAAELQELNIKLVELASELTDE[IWIAQELRRIGDEFNAYYADAERLIREA AAASEKISREAERLI]
BimSwitch_e9t9	KLAEKLLEAVTKLQALNIKLAEKLLEALARLQELNIALVYLAVELTDPKRIADEIKKVKDKSKEIVERAE EEIARAAAESKKILDEAEEEIARAGSGSGSLKLAELLLEAVAELQALNLKLAELLLEAIAKLQELNIKLV ELLTKLTDPATIREAIRKVKEDSERIVAEAERLIAAAKAESERIIREAERLIAAAAGSGSGSIELARELL RDVARLQELNIELARELLRAAAELQELNIKLVELASELTDE[IWIAQELRRIGDEFNAYYADAERLIREA AAASEKISRE]
Switch_e18	SKEAVTKLQALNIKLAEKLLEAVTKLQALNIKLAEKLLEALARLQELNIALVYLAVELTDPKRIADEIKK VKDKSKEIVERAEEEIARAAAESKKILDEAEEEIARAAAESKKILDEGSGSGSDAVAELQALNLKLAELL LEAVAELQALNLKLAELLLEAIAKLQELNIKLVELLTKLTDPATIREAIRKVKEDSERIVAEAERLIAAA KAESERIIREAERLIAAAKAESERIIREGSGSGSDPDVARLQELNIELARELLRDVARLQELNIELARELL RAAAELQELNIKLVELASELTDP[DEARKAIARVKRESKRIVEDAERLIREAAAASEKISREAERLIREA AAASEKISRE]
BimSwitch_e18	SKEAVTKLQALNIKLAEKLLEAVTKLQALNIKLAEKLLEALARLQELNIALVYLAVELTDPKRIADEIKK VKDKSKEIVERAEEEIARAAAESKKILDEAEEEIARAAAESKKILDEGSGSGSDAVAELQALNLKLAELL LEAVAELQALNLKLAELLLEAIAKLQELNIKLVELLTKLTDPATIREAIRKVKEDSERIVAEAERLIAAA KAESERIIREAERLIAAAKAESERIIREGSGSGSDPDVARLQELNIELARELLRDVARLQELNIELARELL RAAAELQELNIKLVELASELTDE[IWIAQELRRIGDEFNAYYADAERLIREAAAASEKISREAERLIREA AAASEKISRE]
BimSwitch_e18t9	SKEAVTKLQALNIKLAEKLLEAVTKLQALNIKLAEKLLEALARLQELNIALVYLAVELTDPKRIADEIKK VKDKSKEIVERAEEEIARAAAESKKILDEAEEEIARAAAESKKILDEGSGSGSDAVAELQALNLKLAELL LEAVAELQALNLKLAELLLEAIAKLQELNIKLVELLTKLTDPATIREAIRKVKEDSERIVAEAERLIAAA KAESERIIREAERLIAAAKAESERIIREGSGSGSDPDVARLQELNIELARELLRDVARLQELNIELARELL RAAAELQELNIKLVELASELTDE[IWIAQELRRIGDEFNAYYADAERLIREAAAASEKISREAERLIREA A]
BimSwitch_e18t15	SKEAVTKLQALNIKLAEKLLEAVTKLQALNIKLAEKLLEALARLQELNIALVYLAVELTDPKRIADEIKK VKDKSKEIVERAEEEIARAAAESKKILDEAEEEIARAAAESKKILDEGSGSGSDAVAELQALNLKLAELL LEAVAELQALNLKLAELLLEAIAKLQELNIKLVELLTKLTDPATIREAIRKVKEDSERIVAEAERLIAAA KAESERIIREAERLIAAAKAESERIIREGSGSGSDPDVARLQELNIELARELLRDVARLQELNIELARELL RAAAELQELNIKLVELASELTDE[IWIAQELRRIGDEFNAYYADAERLIREAAAASEKISREAER]
Switch_b	SHAAVIKLSDLNIRLLDKLLQAVIKLTELNAELNRKLIEALQRLFDLNVALVHLAAELTDPKRIADEIKK VKDKSKEIVERAEEEIARAAAESKKILDEAEEEIARAAAESKKILDEGSGSGSDAVAELQALNLKLAELL LEAVAELQALNLKLAELLLEAIAKLQELNIKLVELLTKLTDPATIREAIRKVKEDSERIVAEAERLIAAA

	KAESERIIREAERLIAAAKAESERIIREGSGSNDPQVAQNQETFIELARDALRLVAENQEAFIEVARLTL RAAALAQEVAIKAVEAASEGGSGSGP[NKEEIEKLAKEAREKLKKAEKEHKEIHDKLRKKNKKAREDLKK KADELRETNKRVN]
BimSwitch_b_t9	SHAAVIKLSDLNIRLLDKLLQAVIKLTELNAELNRKLIEALQRLFDLNVALVHLAAELTDPKRIADEIKK VKDKSKEIVERAEEEIARAAAESKKILDEAEEEIARAAAESKKILDEGSGSGSDAVAELQALNLKLAELL LEAVAELQALNLKLAELLLEAIAKLQELNIKLVELLTKLTDPATIREAIRKVKEDSERIVAEAERLIAAA KAESERIIREAERLIAAAKAESERIIREGSGSNDPQVAQNQETFIELARDALRLVAENQEAFIEVARLTL RAAALAQEVAIKAVEAASEGGSGSGP[NEIWIAQELRRIGDEFNAYYAEHKEIHDKLRKKNKKAREDLKK KADE]
Switch_c	SLEAVLKLAELNLKLSDKLAEAVQKLAALLNKLLEKLSEALQRLFELNVALVTLAIELTDPKRIADEIKK VKDKSKEIVERAEEEIARAAAESKKILDEAEEEIARAAAESKKILDEGSGSGSDAVAELQALNLKLAELL LEAVAELQALNLKLAELLLEAIAKLQELNIKLVELLTKLTDPATIREAIRKVKEDSERIVAEAERLIAAA KAESERIIREAERLIAAAKAESERIIREGSGSNDPLVARLQELLIEHARELLRLVATSQEIFIELARAFL ANAAQLQEAAIKAVEAASENGSGSGP[SSEKVRRELKESLKENHKQNQKLLKDHKRAQEKLNRELEELKK KHKKTLDDIRRES]
BimSwitch_c_t9	SLEAVLKLAELNLKLSDKLAEAVQKLAALLNKLLEKLSEALQRLFELNVALVTLAIELTDPKRIADEIKK VKDKSKEIVERAEEEIARAAAESKKILDEAEEEIARAAAESKKILDEGSGSGSDAVAELQALNLKLAELL LEAVAELQALNLKLAELLLEAIAKLQELNIKLVELLTKLTDPATIREAIRKVKEDSERIVAEAERLIAAA KAESERIIREAERLIAAAKAESERIIREGSGSNDPLVARLQELLIEHARELLRLVATSQEIFIELARAFL ANAAQLQEAAIKAVEAASENGSG[EIWIAQELRRIGDEFNAYYAQNQKLLKDHKRAQEKLNRELEELKKK HKK]
Switch_d	SLEAVLKLFELNHKLSEKLLEAVLKLHALNQKLSQKLLEALARLLELNVALVELAIELTDPKRIADEIKK VKDKSKEIVERAEEEIARAAAESKKILDEAEEEIARAAAESKKILDEGSGSGSDAVAELQALNLKLAELL LEAVAELQALNLKLAELLLEAIAKLQELNIKLVELLTKLTDPATIREAIRKVKEDSERIVAEAERLIAAA KAESERIIREAERLIAAAKAESERIIREGSGSGDPEVARLQEAFIEQAREILRNVAAAQEALIEQARRLL ALAALAQEAAIKAVELASEHGSGSGP[DTVKRILEELRRRFEKLAKDLDDIARKLLEDHKKHNKELKDKQ RKIKKEADDAARS]
BimSwitch_d_t9	SLEAVLKLFELNHKLSEKLLEAVLKLHALNQKLSQKLLEALARLLELNVALVELAIELTDPKRIADEIKK VKDKSKEIVERAEEEIARAAAESKKILDEAEEEIARAAAESKKILDEGSGSGSDAVAELQALNLKLAELL LEAVAELQALNLKLAELLLEAIAKLQELNIKLVELLTKLTDPATIREAIRKVKEDSERIVAEAERLIAAA KAESERIIREAERLIAAAKAESERIIREGSGSGDPEVARLQEAFIEQAREILRNVAAAQEALIEQARRLL ALAALAQEAAIKAVELASEHGSGSE[IWIAQELRRIGDEFNAYYADLDDIARKLLEDHKKHNKELKDKQR KIK]
BimSwitch_d_t12	SLEAVLKLFELNHKLSEKLLEAVLKLHALNQKLSQKLLEALARLLELNVALVELAIELTDPKRIADEIKK VKDKSKEIVERAEEEIARAAAESKKILDEAEEEIARAAAESKKILDEGSGSGSDAVAELQALNLKLAELL LEAVAELQALNLKLAELLLEAIAKLQELNIKLVELLTKLTDPATIREAIRKVKEDSERIVAEAERLIAAA KAESERIIREAERLIAAAKAESERIIREGSGSGDPEVARLQEAFIEQAREILRNVAAAQEALIEQARRLL ALAALAQEAAIKAVELASEHGSGSE[IWIAQELRRIGDEFNAYYADLDDIARKLLEDHKKHNKELKDKQR]
BimSwitch_d_t15	SLEAVLKLFELNHKLSEKLLEAVLKLHALNQKLSQKLLEALARLLELNVALVELAIELTDPKRIADEIKK VKDKSKEIVERAEEEIARAAAESKKILDEAEEEIARAAAESKKILDEGSGSGSDAVAELQALNLKLAELL LEAVAELQALNLKLAELLLEAIAKLQELNIKLVELLTKLTDPATIREAIRKVKEDSERIVAEAERLIAAA KAESERIIREAERLIAAAKAESERIIREGSGSGDPEVARLQEAFIEQAREILRNVAAAQEALIEQARRLL ALAALAQEAAIKAVELASEHGSGSE[IWIAQELRRIGDEFNAYYADLDDIARKLLEDHKKHNKELKD]
Switch_e	SLEAVLKLQDLNSKLSEKLSEAQLKLQALNNKLLRKLLEALLRLQDLNQALVNLALQLTDPKRIADEIKK VKDKSKEIVERAEEEIARAAAESKKILDEAEEEIARAAAESKKILDEGSGSGSDAVAELQALNLKLAELL LEAVAELQALNLKLAELLLEAIAKLQELNIKLVELLTKLTDPATIREAIRKVKEDSERIVAEAERLIAAA KAESERIIREAERLIAAAKAESERIIREGSGSGDPDVAKSQEHLIEHARELLRQVAKSQELFIELARQLL RLAAKSQELAIKAVELASEAGSGSGP[DDVERRLRKANKESKKEAEELTEEAKKANEKTKEDSKELTKEN RKTNKTIKDEARS]
Switch_f	SREAVEKLAELNHKLSHKLQQAQQKLQALNLKLLQKLLEALDRLQDLNNALVKLAQRLTDPKRIADEIKK VKDKSKEIVERAEEEIARAAAESKKILDEAEEEIARAAAESKKILDEGSGSGSDAVAELQALNLKLAELL LEAVAELQALNLKLAELLLEAIAKLQELNIKLVELLTKLTDPATIREAIRKVKEDSERIVAEAERLIAAA

	KAESERIIREAERLIAAAKAESERIIREGSGSGDPDVARQQETLIEQARRLLRNVAESQELFIEAARTVL RLAAKLQEINIKQVELASEAGSGSGP[DDEERRSEKTVQDAKREIKKVEDDLQRLNEEQKKKVKKQEDEN QKTLKKHKDDARS]
degronSwitch_a_t9_full_cODC	SKEAVTKLQALNIKLAEKLLEAVTKLQALNIKLAEKLLEALARLQELNIALVYLAVELTDPKRIADEIKK VKDKSKEIVERAEEEIARAAAESKKILDEAEEEIARAAAESKKILDEGSGSGSDAVAELQALNLKLAELL LEAVAELQALNLKLAELLLEAIAKLQELNIKLVELLTKLTDPATIREAIRKVKEDSERIVAEAERLIAAA KAESERIIREAERLIAAAKAESERIIREGSGSGDPDVARLQELNIELARELLRDVARLQELNIELARELL RAAAELQELNIKLVELASELTDP[DEARKAIARVKRESKRIVEDAERLPMSCAQESEKISREAERLIREA A]
degronSwitch_a_t9_noPro	SKEAVTKLQALNIKLAEKLLEAVTKLQALNIKLAEKLLEALARLQELNIALVYLAVELTDPKRIADEIKK VKDKSKEIVERAEEEIARAAAESKKILDEAEEEIARAAAESKKILDEGSGSGSDAVAELQALNLKLAELL LEAVAELQALNLKLAELLLEAIAKLQELNIKLVELLTKLTDPATIREAIRKVKEDSERIVAEAERLIAAA KAESERIIREAERLIAAAKAESERIIREGSGSGDPDVARLQELNIELARELLRDVARLQELNIELARELL RAAAELQELNIKLVELASELTDP[DEARKAIARVKRESKRIVEDAERLAMSCAQESEKISREAERLIREA A]
degronSwitch_a_t9_CA	SKEAVTKLQALNIKLAEKLLEAVTKLQALNIKLAEKLLEALARLQELNIALVYLAVELTDPKRIADEIKK VKDKSKEIVERAEEEIARAAAESKKILDEAEEEIARAAAESKKILDEGSGSGSDAVAELQALNLKLAELL LEAVAELQALNLKLAELLLEAIAKLQELNIKLVELLTKLTDPATIREAIRKVKEDSERIVAEAERLIAAA KAESERIIREAERLIAAAKAESERIIREGSGSGDPDVARLQELNIELARELLRDVARLQELNIELARELL RAAAELQELNIKLVELASELTDP[DEARKAIARVKRESKRIVEDAERLIRECAAASEKISREAERLIREA A]
degronSwitch_a_t12	SKEAVTKLQALNIKLAEKLLEAVTKLQALNIKLAEKLLEALARLQELNIALVYLAVELTDPKRIADEIKK VKDKSKEIVERAEEEIARAAAESKKILDEAEEEIARAAAESKKILDEGSGSGSDAVAELQALNLKLAELL LEAVAELQALNLKLAELLLEAIAKLQELNIKLVELLTKLTDPATIREAIRKVKEDSERIVAEAERLIAAA KAESERIIREAERLIAAAKAESERIIREGSGSGDPDVARLQELNIELARELLRDVARLQELNIELARELL RAAAELQELNIKLVELASELTDP[DEARKAIARVKRESKRIVEDLIMSCAQESAASEKISREAERLIR]
degronSwitch_a_t16	SKEAVTKLQALNIKLAEKLLEAVTKLQALNIKLAEKLLEALARLQELNIALVYLAVELTDPKRIADEIKK VKDKSKEIVERAEEEIARAAAESKKILDEAEEEIARAAAESKKILDEGSGSGSDAVAELQALNLKLAELL LEAVAELQALNLKLAELLLEAIAKLQELNIKLVELLTKLTDPATIREAIRKVKEDSERIVAEAERLIAAA KAESERIIREAERLIAAAKAESERIIREGSGSGDPDVARLQELNIELARELLRDVARLQELNIELARELL RAAAELQELNIKLVELASELTDP[DEARKAIARVKRESKRLVMSCAQESREAAAASEKISREAE]
degronSwitch_b_t9	SHAAVIKLSDLNIRLLDKLLQAVIKLTELNAELNRKLIEALQRLFDLNVALVHLAAELTDPKRIADEIKK VKDKSKEIVERAEEEIARAAAESKKILDEAEEEIARAAAESKKILDEGSGSGSDAVAELQALNLKLAELL LEAVAELQALNLKLAELLLEAIAKLQELNIKLVELLTKLTDPATIREAIRKVKEDSERIVAEAERLIAAA KAESERIIREAERLIAAAKAESERIIREGSGSNDPQVAQNQETFIELARDALRLVAENQEAFIEVARLTL RAAALAQEVAIKAVEAASEGGSGSGP[NKEEIEKLAKEAREKLKKAEKEHKMSCAQERKKNKKAREDLKK KADK]
degronSwitch_b_t13	SHAAVIKLSDLNIRLLDKLLQAVIKLTELNAELNRKLIEALQRLFDLNVALVHLAAELTDPKRIADEIKK VKDKSKEIVERAEEEIARAAAESKKILDEAEEEIARAAAESKKILDEGSGSGSDAVAELQALNLKLAELL LEAVAELQALNLKLAELLLEAIAKLQELNIKLVELLTKLTDPATIREAIRKVKEDSERIVAEAERLIAAA KAESERIIREAERLIAAAKAESERIIREGSGSNDPQVAQNQETFIELARDALRLVAENQEAFIEVARLTL RAAALAQEVAIKAVEAASEGGSGSGP[NKEEIEKLAKEAREKLKKAEMSCAQEHDKLRKKNKKAREDLKK]
degronSwitch_c_t9	SLEAVLKLAELNLKLSDKLAEAVQKLAALLNKLLEKLSEALQRLFELNVALVTLAIELTDPKRIADEIKK VKDKSKEIVERAEEEIARAAAESKKILDEAEEEIARAAAESKKILDEGSGSGSDAVAELQALNLKLAELL LEAVAELQALNLKLAELLLEAIAKLQELNIKLVELLTKLTDPATIREAIRKVKEDSERIVAEAERLIAAA KAESERIIREAERLIAAAKAESERIIREGSGSNDPLVARLQELLIEHARELLRLVATSQEIFIELARAFL ANAAQLQEAAIKAVEAASENGSGSGP[SSEKVRRELKESLKENHKQNQKLLMSCAQEQEKLNRELEELKK KHKK]
degronSwitch_c_t13	SLEAVLKLAELNLKLSDKLAEAVQKLAALLNKLLEKLSEALQRLFELNVALVTLAIELTDPKRIADEIKK VKDKSKEIVERAEEEIARAAAESKKILDEAEEEIARAAAESKKILDEGSGSGSDAVAELQALNLKLAELL LEAVAELQALNLKLAELLLEAIAKLQELNIKLVELLTKLTDPATIREAIRKVKEDSERIVAEAERLIAAA KAESERIIREAERLIAAAKAESERIIREGSGSNDPLVARLQELLIEHARELLRLVATSQEIFIELARAFL

	ANAAQLQEAAIKAVEAASENGSGSGP[SSEKVRRELKESLKENHKQNMSCAQEHKRAQEKLNRELEELKK]
degronSwitch_d_t9	SLEAVLKLFELNHKLSEKLLEAVLKLHALNQKLSQKLLEALARLLELNVALVELAIELTDPKRIADEIKK VKDKSKEIVERAEEEIARAAAESKKILDEAEEEIARAAAESKKILDEGSGSGSDAVAELQALNLKLAELL LEAVAELQALNLKLAELLLEAIAKLQELNIKLVELLTKLTDPATIREAIRKVKEDSERIVAEAERLIAAA KAESERIIREAERLIAAAKAESERIIREGSGSGDPEVARLQEAFIEQAREILRNVAAAQEALIEQARRLL ALAALAQEAAIKAVELASEHGSGSGP[DTVKRILEELRRRFEKLAKDLDDIAMSCAQEHKKHNKELKDKQ RKIK]
degronSwitch_a_asymmetric_short_t5	SELARKLLEASTKLQRLNIRLAEALLEAIARLQELNLELVYLAVELTDPKRIRDEIKEVKDKSKEIIRRA EKEIDDAAKESEKILEEAREAISGSGSELAKLLLKAIAETQDLNLRAAKAFLEAAAKLQELNIRAVELLV KLTDPATIREALEHAKRRSKEIIDEAERAIRAAKRESERIIEEARRLIEKGSGSGSELARELLRAHAQLQ RLNLELLRELLRALAQLQELNLDLLRLASELTDPDEARKAIARVKRESKRLVMSCAQESREAAAASEKIS REA
degronSwitch_a_asymmetric_short_t8	SELARKLLEASTKLQRLNIRLAEALLEAIARLQELNLELVYLAVELTDPKRIRDEIKEVKDKSKEIIRRA EKEIDDAAKESEKILEEAREAISGSGSELAKLLLKAIAETQDLNLRAAKAFLEAAAKLQELNIRAVELLV KLTDPATIREALEHAKRRSKEIIDEAERAIRAAKRESERIIEEARRLIEKGSGSGSELARELLRAHAQLQ RLNLELLRELLRALAQLQELNLDLLRLASELTDPDEARKAIARVKRLSMSCAQESERLIREAAAASEKIK
nesSwitch_a_t9	SKEAVTKLQALNIKLAEKLLEAVTKLQALNIKLAEKLLEALARLQELNIALVYLAVELTDPKRIADEIKK VKDKSKEIVERAEEEIARAAAESKKILDEAEEEIARAAAESKKILDEGSGSGSDAVAELQALNLKLAELL LEAVAELQALNLKLAELLLEAIAKLQELNIKLVELLTKLTDPATIREAIRKVKEDSERIVAEAERLIAAA KAESERIIREAERLIAAAKAESERIIREGSGSGDPDVARLQELNIELARELLRDVARLQELNIELARELL RAAAELQELNIKLVELASELTDP[DEARKAIARVKRESKRIVEDLALKLAGLDINSEKISREAERLIREA A]
strepSwitch_299	SKEAVTKLQALNIKLAEKLLEAVTKLQALNIKLAEKLLEALARLQELNIALVYLAVELTDPKRIADEIKK VKDKSKEIVERAEEEIARAAAESKKILDEAEEEIARAAAESKKILDEGSGSGSDAVAELQALNLKLAELL LEAVAELQALNLKLAELLLEAIAKLQELNIKLVELLTKLTDPATIREAIRKVKEDSERIVAEAERLIAAA KAESERIIREAERLIAAAKAESERIIREGSGSGDPDVARLQELNIELARELLRDVARLQELNIELARELL RAAAELQELNIKLVELASGNWSHPQFEKKAIARVKRESKRIVEDAERLIREAAAASEKISREAERLIREA AAASEKISRE
strepSwitch_306	SKEAVTKLQALNIKLAEKLLEAVTKLQALNIKLAEKLLEALARLQELNIALVYLAVELTDPKRIADEIKK VKDKSKEIVERAEEEIARAAAESKKILDEAEEEIARAAAESKKILDEGSGSGSDAVAELQALNLKLAELL LEAVAELQALNLKLAELLLEAIAKLQELNIKLVELLTKLTDPATIREAIRKVKEDSERIVAEAERLIAAA KAESERIIREAERLIAAAKAESERIIREGSGSGDPDVARLQELNIELARELLRDVARLQELNIELARELL RAAAELQELNIKLVELASELTDPDENWSHPQFEKRESKRIVEDAERLIREAAAASEKISREAERLIREAA AASEKISRE
strepSwitch_312	SKEAVTKLQALNIKLAEKLLEAVTKLQALNIKLAEKLLEALARLQELNIALVYLAVELTDPKRIADEIKK VKDKSKEIVERAEEEIARAAAESKKILDEAEEEIARAAAESKKILDEGSGSGSDAVAELQALNLKLAELL LEAVAELQALNLKLAELLLEAIAKLQELNIKLVELLTKLTDPATIREAIRKVKEDSERIVAEAERLIAAA KAESERIIREAERLIAAAKAESERIIREGSGSGDPDVARLQELNIELARELLRDVARLQELNIELARELL RAAAELQELNIKLVELASELTDPDEARKAIANWSHPQFEKVEDAERLIREAAAASEKISREAERLIREAA AASEKISRE
strepSwitch_313	SKEAVTKLQALNIKLAEKLLEAVTKLQALNIKLAEKLLEALARLQELNIALVYLAVELTDPKRIADEIKK VKDKSKEIVERAEEEIARAAAESKKILDEAEEEIARAAAESKKILDEGSGSGSDAVAELQALNLKLAELL LEAVAELQALNLKLAELLLEAIAKLQELNIKLVELLTKLTDPATIREAIRKVKEDSERIVAEAERLIAAA KAESERIIREAERLIAAAKAESERIIREGSGSGDPDVARLQELNIELARELLRDVARLQELNIELARELL RAAAELQELNIKLVELASELTDPDEARKAIARNWSHPQFEKEDAERLIREAAAASEKISREAERLIREAA AASEKISRE
strepSwitch_320	SKEAVTKLQALNIKLAEKLLEAVTKLQALNIKLAEKLLEALARLQELNIALVYLAVELTDPKRIADEIKK VKDKSKEIVERAEEEIARAAAESKKILDEAEEEIARAAAESKKILDEGSGSGSDAVAELQALNLKLAELL LEAVAELQALNLKLAELLLEAIAKLQELNIKLVELLTKLTDPATIREAIRKVKEDSERIVAEAERLIAAA KAESERIIREAERLIAAAKAESERIIREGSGSGDPDVARLQELNIELARELLRDVARLQELNIELARELL RAAAELQELNIKLVELASELTDPDEARKAIARVKRESKRNWSHPQFEKREAAAASEKISREAERLIREAA AASEKISRE

strepSwitch_323	SKEAVTKLQALNIKLAEKLLEAVTKLQALNIKLAEKLLEALARLQELNIALVYLAVELTDPKRIADEIKK VKDKSKEIVERAEEEIARAAAESKKILDEAEEEIARAAAESKKILDEGSGSGSDAVAELQALNLKLAELL LEAVAELQALNLKLAELLLEAIAKLQELNIKLVELLTKLTDPATIREAIRKVKEDSERIVAEAERLIAAA KAESERIIREAERLIAAAKAESERIIREGSGSGDPDVARLQELNIELARELLRDVARLQELNIELARELL RAAAELQELNIKLVELASELTDPDEARKAIARVKRESKRIVENWSHPQFEKAAASEKISREAERLIREAA AASEKISRE
strepSwitch_329	SKEAVTKLQALNIKLAEKLLEAVTKLQALNIKLAEKLLEALARLQELNIALVYLAVELTDPKRIADEIKK VKDKSKEIVERAEEEIARAAAESKKILDEAEEEIARAAAESKKILDEGSGSGSDAVAELQALNLKLAELL LEAVAELQALNLKLAELLLEAIAKLQELNIKLVELLTKLTDPATIREAIRKVKEDSERIVAEAERLIAAA KAESERIIREAERLIAAAKAESERIIREGSGSGDPDVARLQELNIELARELLRDVARLQELNIELARELL RAAAELQELNIKLVELASELTDPDEARKAIARVKRESKRIVEDAERLINWSHPQFEKISREAERLIREAA AASEKISRE
spySwitch_2	SELARKLLEASTKLQRLNIRLAEALLEAIARLQELNLELVYLAVELTDPKRIRDEIKEVKDKSKEIIRRA EKEIDDAAKESEKILEEAREAISGSGSELAKLLLKAIAETQDLNLRAAKAFLEAAAKLQELNIRAVELLV KLTDPATIREALEHAKRRSKEIIDEAERAIRAAKRESERIIEEARRLIEKGSGSGSELARELLRAHAQLQ RLNLELLRELLRALAQLQELNLDLLRLASELTDPDEARAHIVMVDAYKKRIVEDAERLIREAAAASEKIS REAERLIR
spySwitch_8	SELARKLLEASTKLQRLNIRLAEALLEAIARLQELNLELVYLAVELTDPKRIRDEIKEVKDKSKEIIRRA EKEIDDAAKESEKILEEAREAISGSGSELAKLLLKAIAETQDLNLRAAKAFLEAAAKLQELNIRAVELLV KLTDPATIREALEHAKRRSKEIIDEAERAIRAAKRESERIIEEARRLIEKGSGSGSELARELLRAHAQLQ RLNLELLRELLRALAQLQELNLDLLRLASELTDPDEARKAIARVKRESKAHIVMVDAYKREAAAASEKIS REAERLIR
tevSwitch_2	SELARKLLEASTKLQRLNIRLAEALLEAIARLQELNLELVYLAVELTDPKRIRDEIKEVKDKSKEIIRRA EKEIDDAAKESEKILEEAREAISGSGSELAKLLLKAIAETQDLNLRAAKAFLEAAAKLQELNIRAVELLV KLTDPATIREALEHAKRRSKEIIDEAERAIRAAKRESERIIEEARRLIEKGSGSGSELARELLRAHAQLQ RLNLELLRELLRALAQLQELNLDLLRLASELTDPDEARENLYFQGSESKRIVEDAERLIREAAAASEKIS REAERLIR
tevSwitch_6	SELARKLLEASTKLQRLNIRLAEALLEAIARLQELNLELVYLAVELTDPKRIRDEIKEVKDKSKEIIRRA EKEIDDAAKESEKILEEAREAISGSGSELAKLLLKAIAETQDLNLRAAKAFLEAAAKLQELNIRAVELLV KLTDPATIREALEHAKRRSKEIIDEAERAIRAAKRESERIIEEARRLIEKGSGSGSELARELLRAHAQLQ RLNLELLRELLRALAQLQELNLDLLRLASELTDPDEARKAIARVKRESKRIVENLYFQGSEAAAASEKIS REAERLIR
tev-spySwitch_short_40	SELARKLLEASTKLQRLNIRLAEALLEAIARLQELNLELVYLAVELTDPKRIRDEIKEVKDKSKEIIRRA EKEIDDAAKESEKILEEAREAISGSGSELAKLLLKAIAETQDLNLRAAKAFLEAAAKLQELNIRAVELLV KLTDPATIREALEHAKRRSKEIIDEAERAIRAAKRESERIIEEARRLIEKGSGSGSELARELLRAHAQLQ RLNLELLRELLRALAQLQELNLDLLRLASELTDPDEARKAIENLYFQGSRIVEDAEAHIVMVDAYKEKIS REAERLIR
tev-spySwitch_short_57	SELARKLLEASTKLQRLNIRLAEALLEAIARLQELNLELVYLAVELTDPKRIRDEIKEVKDKSKEIIRRA EKEIDDAAKESEKILEEAREAISGSGSELAKLLLKAIAETQDLNLRAAKAFLEAAAKLQELNIRAVELLV KLTDPATIREALEHAKRRSKEIIDEAERAIRAAKRESERIIEEARRLIEKGSGSGSELARELLRAHAQLQ RLNLELLRELLRALAQLQELNLDLLRLASELTDPDEARKAIARVENLYFQGSEDAERLIREAAHIVMVDA YKAERLIR
tev-spySwitch_short_63	SELARKLLEASTKLQRLNIRLAEALLEAIARLQELNLELVYLAVELTDPKRIRDEIKEVKDKSKEIIRRA EKEIDDAAKESEKILEEAREAISGSGSELAKLLLKAIAETQDLNLRAAKAFLEAAAKLQELNIRAVELLV KLTDPATIREALEHAKRRSKEIIDEAERAIRAAKRESERIIEEARRLIEKGSGSGSELARELLRAHAQLQ RLNLELLRELLRALAQLQELNLDLLRLASELTDPDEARKAIARVKENLYFQGSDAERLIREAAHIVMVDA YKAERLIR*
tev-spySwitch_29	SKEAAKKLQDLNIELARKLLEASTKLQRLNIRLAEALLEAIARLQELNLELVYLAVELTDPKRIRDEIKE VKDKSKEIIRRAEKEIDDAAKESKKILEEARKAIRDAAEESRKILEEGSGSGSDALDELQKLNLELAKLL LKAIAETQDLNLRAAKAFLEAAAKLQELNIRAVELLVKLTDPATIRRALEHAKRRSKEIIDEAERAIRAA KRESERIIEEARRLIEKAKEESERIIREGSGSGDPDIKKLQDLNIELARELLRAHAQLQRLNLELLRELL RALAQLQELNLDLLRLASELTDPDEARKAIARVKENLYFQGSDAERLIREAAAASEAHIVMVDAYKREAA AASEKISRE

tev-spySwitch_32	SKEAAKKLQDLNIELARKLLEASTKLQRLNIRLAEALLEAIARLQELNLELVYLAVELTDPKRIRDEIKE VKDKSKEIIRRAEKEIDDAAKESKKILEEARKAIRDAAEESRKILEEGSGSGSDALDELQKLNLELAKLL LKAIAETQDLNLRAAKAFLEAAAKLQELNIRAVELLVKLTDPATIRRALEHAKRRSKEIIDEAERAIRAA KRESERIIEEARRLIEKAKEESERIIREGSGSGDPDIKKLQDLNIELARELLRAHAQLQRLNLELLRELL RALAQLQELNLDLLRLASELTDPDEARKAIARVKENLYFQGSDAERLIREAAAASEKISREAEAHIVMVD AYKEKISRE
lucSwitch_1	SELARKLLEASTKLQRLNIRLAEALLEAIARLQELNLELVYLAVELTDPKRIRDEIKEVKDKSKEIIRRA EKEIDDAAKESEKILEEAREAISGSGSELAKLLLKAIAETQDLNLRAAKAFLEAAAKLQELNIRAVELLV KLTDPATIREALEHAKRRSKEIIDEAERAIRAAKRESERIIEEARRLIEKGSGSGSELARELLRAHAQLQ RLNLELLRELLRALAQLQELNLDLLRLASELTDPDEARVSGWRLFKKISRIVEDAERLIREAAAASEKIS REAERLIR*
lucSwitch_3	SELARKLLEASTKLQRLNIRLAEALLEAIARLQELNLELVYLAVELTDPKRIRDEIKEVKDKSKEIIRRA EKEIDDAAKESEKILEEAREAISGSGSELAKLLLKAIAETQDLNLRAAKAFLEAAAKLQELNIRAVELLV KLTDPATIREALEHAKRRSKEIIDEAERAIRAAKRESERIIEEARRLIEKGSGSGSELARELLRAHAQLQ RLNLELLRELLRALAQLQELNLDLLRLASELTDPDEARKAIARVKRESKVSGWRLFKKISEAAAASEKIS REAERLIR
fretSwitch	VSKGEELFTGVVPILVELDGDVNGHKFSVSGEGEGDATYGKLTLKFICTTGKLPVPWPTLVTTLSWGVQC FARYPDHMKQHDFFKSAMPEGYVQERTIFFKDDGNYKTRAEVKFEGDTLVNRIELKGIDFKEDGNILGHK LEYNYFSDNVYITADKQKNGIKANFKIRHNIEDGGVQLADHYQQNTPIGDGPVLLPDNHYLSTQSKLSKD PNEKRDHMVLLEFVTAAGITLELARKLLEASTKLQRLNIRLAEALLEAIARLQELNLELVYLAVELTDPK RIRDEIKEVKDKSKEIIRRAEKEIDDAAKESEKILEEAREAISGSGSELAKLLLKAIAETQDLNLRAAKA FLEAAAKLQELNIRAVELLVKLTDPATIREALEHAKRRSKEIIDEAERAIRAAKRESERIIEEARRLIEK GSGSGSELARELLRAHAQLQRLNLELLRELLRALAQLQELNLDLLRLASELTDPDEARKAIARVKRESNA YYADAERLIREAAAASEKVSKGEELFTGVVPILVELDGDVNGHKFSVSGEGEGDATYGKLTLKLICTTGK LPVPWPTLVTTLGYGVQCFARYPDHMKQHDFFKSAMPEGYVQERTIFFKDDGNYKTRAEVKFEGDTLVNR IELKGIDFKEDGNILGHKLEYNYNSHNVYITADKQKNGIKANFKIRHNIEDGGVQLADHYQQNTPIGDGP VLLPDNHYLSYQSKLSKDPNEKRDHMVLLEFVTAAGITLGMDELYKGSGC
fretSwitch_V254S	VSKGEELFTGVVPILVELDGDVNGHKFSVSGEGEGDATYGKLTLKFICTTGKLPVPWPTLVTTLSWGVQC FARYPDHMKQHDFFKSAMPEGYVQERTIFFKDDGNYKTRAEVKFEGDTLVNRIELKGIDFKEDGNILGHK LEYNYFSDNVYITADKQKNGIKANFKIRHNIEDGGVQLADHYQQNTPIGDGPVLLPDNHYLSTQSKLSKD PNEKRDHMVLLEFVTAAGITLELARKLLEASTKLQRLNIRLAEALLEAIARLQELNLELVYLAVELTDPK RIRDEIKEVKDKSKEIIRRAEKEIDDAAKESEKILEEAREAISGSGSELAKLLLKAIAETQDLNLRAAKA FLEAAAKLQELNIRAVELLVKLTDPATIREALEHAKRRSKEIIDEAERAIRAAKRESERIIEEARRLIEK GSGSGSELARELLRAHAQLQRLNLELLRELLRALAQLQELNLDLLRLASELTDPDEARKAIARSKRESNA YYADAERLIREAAAASEKVSKGEELFTGVVPILVELDGDVNGHKFSVSGEGEGDATYGKLTLKLICTTGK LPVPWPTLVTTLGYGVQCFARYPDHMKQHDFFKSAMPEGYVQERTIFFKDDGNYKTRAEVKFEGDTLVNR IELKGIDFKEDGNILGHKLEYNYNSHNVYITADKQKNGIKANFKIRHNIEDGGVQLADHYQQNTPIGDGP VLLPDNHYLSYQSKLSKDPNEKRDHMVLLEFVTAAGITLGMDELYKGSGC
fretSwitch_I269S	VSKGEELFTGVVPILVELDGDVNGHKFSVSGEGEGDATYGKLTLKFICTTGKLPVPWPTLVTTLSWGVQC FARYPDHMKQHDFFKSAMPEGYVQERTIFFKDDGNYKTRAEVKFEGDTLVNRIELKGIDFKEDGNILGHK LEYNYFSDNVYITADKQKNGIKANFKIRHNIEDGGVQLADHYQQNTPIGDGPVLLPDNHYLSTQSKLSKD PNEKRDHMVLLEFVTAAGITLELARKLLEASTKLQRLNIRLAEALLEAIARLQELNLELVYLAVELTDPK RIRDEIKEVKDKSKEIIRRAEKEIDDAAKESEKILEEAREAISGSGSELAKLLLKAIAETQDLNLRAAKA FLEAAAKLQELNIRAVELLVKLTDPATIREALEHAKRRSKEIIDEAERAIRAAKRESERIIEEARRLIEK GSGSGSELARELLRAHAQLQRLNLELLRELLRALAQLQELNLDLLRLASELTDPDEARKAIARVKRESNA YYADAERLSREAAAASEKVSKGEELFTGVVPILVELDGDVNGHKFSVSGEGEGDATYGKLTLKLICTTGK LPVPWPTLVTTLGYGVQCFARYPDHMKQHDFFKSAMPEGYVQERTIFFKDDGNYKTRAEVKFEGDTLVNR IELKGIDFKEDGNILGHKLEYNYNSHNVYITADKQKNGIKANFKIRHNIEDGGVQLADHYQQNTPIGDGP VLLPDNHYLSYQSKLSKDPNEKRDHMVLLEFVTAAGITLGMDELYKGSGC
fretSwitch_V254S_I269S	VSKGEELFTGVVPILVELDGDVNGHKFSVSGEGEGDATYGKLTLKFICTTGKLPVPWPTLVTTLSWGVQC FARYPDHMKQHDFFKSAMPEGYVQERTIFFKDDGNYKTRAEVKFEGDTLVNRIELKGIDFKEDGNILGHK LEYNYFSDNVYITADKQKNGIKANFKIRHNIEDGGVQLADHYQQNTPIGDGPVLLPDNHYLSTQSKLSKD PNEKRDHMVLLEFVTAAGITLELARKLLEASTKLQRLNIRLAEALLEAIARLQELNLELVYLAVELTDPK RIRDEIKEVKDKSKEIIRRAEKEIDDAAKESEKILEEAREAISGSGSELAKLLLKAIAETQDLNLRAAKA

	FLEAAAKLQELNIRAVELLVKLTDPATIREALEHAKRRSKEIIDEAERAIRAAKRESERIIEEARRLIEK GSGSGSELARELLRAHAQLQRLNLELLRELLRALAQLQELNLDLLRLASELTDPDEARKAIARSKRESNA YYADAERLSREAAAASEKVSKGEELFTGVVPILVELDGDVNGHKFSVSGEGEGDATYGKLTLKLICTTGK LPVPWPTLVTTLGYGVQCFARYPDHMKQHDFFKSAMPEGYVQERTIFFKDDGNYKTRAEVKFEGDTLVNR IELKGIDFKEDGNILGHKLEYNYNSHNVYITADKQKNGIKANFKIRHNIEDGGVQLADHYQQNTPIGDGP VLLPDNHYLSYQSKLSKDPNEKRDHMVLLEFVTAAGITLGMDELYKGSGC
Bim-fretSwitch	VSKGEELFTGVVPILVELDGDVNGHKFSVSGEGEGDATYGKLTLKFICTTGKLPVPWPTLVTTLSWGVQC FARYPDHMKQHDFFKSAMPEGYVQERTIFFKDDGNYKTRAEVKFEGDTLVNRIELKGIDFKEDGNILGHK LEYNYFSDNVYITADKQKNGIKANFKIRHNIEDGGVQLADHYQQNTPIGDGPVLLPDNHYLSTQSKLSKD PNEKRDHMVLLEFVTAAGITLELARKLLEASTKLQRLNIRLAEALLEAIARLQELNLELVYLAVELTDPK RIRDEIKEVKDKSKEIIRRAEKEIDDAAKESEKILEEAREAISGSGSELAKLLLKAIAETQDLNLRAAKA FLEAAAKLQELNIRAVELLVKLTDPATIREALEHAKRRSKEIIDEAERAIRAAKRESERIIEEARRLIEK GSGSGSELARELLRAHAQLQRLNLELLRELLRALAQLQELNLDLLRLASELTDEIWIAQELRRIGDEFNA YYADAERLIREAAAASEKISREAERLIRVSKGEELFTGVVPILVELDGDVNGHKFSVSGEGEGDATYGKL TLKLICTTGKLPVPWPTLVTTLGYGVQCFARYPDHMKQHDFFKSAMPEGYVQERTIFFKDDGNYKTRAEV KFEGDTLVNRIELKGIDFKEDGNILGHKLEYNYNSHNVYITADKQKNGIKANFKIRHNIEDGGVQLADHY QQNTPIGDGPVLLPDNHYLSYQSKLSKDPNEKRDHMVLLEFVTAAGITLGMDELYKGSGC
Bim-fretSwitch_I269S	VSKGEELFTGVVPILVELDGDVNGHKFSVSGEGEGDATYGKLTLKFICTTGKLPVPWPTLVTTLSWGVQC FARYPDHMKQHDFFKSAMPEGYVQERTIFFKDDGNYKTRAEVKFEGDTLVNRIELKGIDFKEDGNILGHK LEYNYFSDNVYITADKQKNGIKANFKIRHNIEDGGVQLADHYQQNTPIGDGPVLLPDNHYLSTQSKLSKD PNEKRDHMVLLEFVTAAGITLELARKLLEASTKLQRLNIRLAEALLEAIARLQELNLELVYLAVELTDPK RIRDEIKEVKDKSKEIIRRAEKEIDDAAKESEKILEEAREAISGSGSELAKLLLKAIAETQDLNLRAAKA FLEAAAKLQELNIRAVELLVKLTDPATIREALEHAKRRSKEIIDEAERAIRAAKRESERIIEEARRLIEK GSGSGSELARELLRAHAQLQRLNLELLRELLRALAQLQELNLDLLRLASELTDEIWIAQELRRIGDEFNA YYADAERLSREAAAASEKISREAERLIRVSKGEELFTGVVPILVELDGDVNGHKFSVSGEGEGDATYGKL TLKLICTTGKLPVPWPTLVTTLGYGVQCFARYPDHMKQHDFFKSAMPEGYVQERTIFFKDDGNYKTRAEV KFEGDTLVNRIELKGIDFKEDGNILGHKLEYNYNSHNVYITADKQKNGIKANFKIRHNIEDGGVQLADHY QQNTPIGDGPVLLPDNHYLSYQSKLSKDPNEKRDHMVLLEFVTAAGITLGMDELYKGSGC
Bim-fretSwitch_I269S_I287S	VSKGEELFTGVVPILVELDGDVNGHKFSVSGEGEGDATYGKLTLKFICTTGKLPVPWPTLVTTLSWGVQC FARYPDHMKQHDFFKSAMPEGYVQERTIFFKDDGNYKTRAEVKFEGDTLVNRIELKGIDFKEDGNILGHK LEYNYFSDNVYITADKQKNGIKANFKIRHNIEDGGVQLADHYQQNTPIGDGPVLLPDNHYLSTQSKLSKD PNEKRDHMVLLEFVTAAGITLELARKLLEASTKLQRLNIRLAEALLEAIARLQELNLELVYLAVELTDPK RIRDEIKEVKDKSKEIIRRAEKEIDDAAKESEKILEEAREAISGSGSELAKLLLKAIAETQDLNLRAAKA FLEAAAKLQELNIRAVELLVKLTDPATIREALEHAKRRSKEIIDEAERAIRAAKRESERIIEEARRLIEK GSGSGSELARELLRAHAQLQRLNLELLRELLRALAQLQELNLDLLRLASELTDEIWIAQELRRIGDEFNA YYADAERLSREAAAASEKISREAERLSRVSKGEELFTGVVPILVELDGDVNGHKFSVSGEGEGDATYGKL TLKLICTTGKLPVPWPTLVTTLGYGVQCFARYPDHMKQHDFFKSAMPEGYVQERTIFFKDDGNYKTRAEV KFEGDTLVNRIELKGIDFKEDGNILGHKLEYNYNSHNVYITADKQKNGIKANFKIRHNIEDGGVQLADHY QQNTPIGDGPVLLPDNHYLSYQSKLSKDPNEKRDHMVLLEFVTAAGITLGMDELYKGSGC
key_a	DEARKAIARVKRESKRIVEDAERLIREAAAASEKISRE
key_a_e5	DEARKAIARVKRESKRIVEDAERLIREAAAASEKISREAERLI
key_a_e9	DEARKAIARVKRESKRIVEDAERLIREAAAASEKISREAERLIREAA
key_a_e18	DEARKAIARVKRESKRIVEDAERLIREAAAASEKISREAERLIREAAAASEKISRE
key_b	NKEEIEKLAKEAREKLKKAEKEHKEIHDKLRKKNKKAREDLKKKADELRETNKRVN
key_c	SSEKVRRELKESLKENHKQNQKLLKDHKRAQEKLNRELEELKKKHKKTLDDIRRES
key_d	DTVKRILEELRRRFEKLAKDLDDIARKLLEDHKKHNKELKDKQRKIKKEADDAARS
key_e	DDVERRLRKANKESKKEAEELTEEAKKANEKTKEDSKELTKENRKTNKTIKDEARS
key_f	DDEERRSEKTVQDAKREIKKVEDDLQRLNEEQKKKVKKQEDENQKTLKKHKDDARS

VITA

Robert – known as Bobby to friends, family, and colleagues – was raised in East Lyme, CT and is an alumnus of East Lyme High School, Class of 2010. Bobby attended undergraduate at Rensselaer Polytechnic Institute where he received a Bachelor of Science in Biochemistry/Biophysics, and a Bachelor of Science in Bioinformatics and Molecular Biology, with a minor in Computer Science after graduating in 2014. At Rensselaer he worked with Chris Bystroff on protein biophysics by studying GFP chromophore dynamics and quenching mechanisms. There, he learned about the field of protein design and applied to University of Washington to work with David Baker for his PhD research. Upon matriculation into the graduate program for Biological Physics, Structure, and Design and completing his rotations, Bobby joined the lab in June of 2015.

He began work on designing helical heterodimers, but during several brainstorming sessions was tasked with designing a helical bundle protein capable of undergoing a conformational change. LOCKR was born out of these discussions in Autumn 2015. Throughout his graduate work, Bobby viewed his project as technology development in addition to pure scientific curiosity. From this perspective, LOCKR became a platform technology and has created a multitude of research projects in the Baker Lab and in industry. Bobby completed the Technology Entrepreneurship Certificate program from the Foster School of Business at University of Washington with an eye towards commercializing LOCKR technology. After discussions with his research partners (Scott Boyken and Marc Lajoie) and potential investors on potential opportunities, Bobby will be joining a startup in Seattle, Lyell Immunopharma Inc., after completion of the University of Washington PhD program as a Scientist to continue working with his research partners and LOCKR technology development.